"An investigation into the characteristics and potential therapeutic application of human bone marrow-derived mesenchymal stromal cells in experimental spinal cord injury"

Von der Fakultät für Mathematik, Informatik und Naturwissenschaften der RWTH Aachen University zur Erlangung des akademischen Grades einer Doktorin der Naturwissenschaften genehmigte Dissertation

vorgelegt von

Diplom-Bioingenieurin (FH)
Katrin Montzka

aus Düren

Berichter: Universitätsprofessor Dr. Hermann Wagner

PD Dr. Gary Brook

Tag der mündlichen Prüfung: 09.08.2011

“Every great scientific truth goes through three stages.

First, people say it conflicts with the Bible.

Next they say it has been discovered before.

Lastly they say they always believed it.”

Louis Agassiz (1807-1873)

Table of contents

PAGE

1. Summary

Transplanted mesenchymal stromal cells (MSC) have been reported to improve functional recovery after spinal cord injury (SCI). The mechanism(s) responsible for this effect are, however, largely unknown. The first studies about MSC transplantation into spinal cord lesions reported differentiation of the donor cells to a neural lineage. This so-called transdifferentiation capacity has aroused great excitement as well as great scepticism. Other studies suggested that the beneficial effects were due to a paracrine mechanism. This thesis was designed to provide insights into the properties of MSC as well as into their fate and function after transplantation into spinal cord lesions.

Human MSC (hMSC) were found to constitutively express several neural-related markers, a property which may have led other groups to conclude that they were capable of transdifferentitation to a neural lineage. Interestingly, these markers demonstrated a donor-dependent variability which may have influenced the widely differing opinions about hMSC transdifferentiation.

Clinical application of hMSC requires the expansion of isolated cells to relevant numbers without supplementation of animal- or donor-derived serum. Conventional expansion, however, includes the employment of 10% fetal bovine serum (FBS) which might transfer infectous agents or might lead to the immune rejection of transplanted cells. The isolation and expansion of hMSC in the absence of serum supplementation was attempted in the present thesis but could not be accomplished. However, significantly better proliferation could be achieved with supplementation of only 2% FBS and certain growth factors compared to the conventional medium. The multipotent capacity of hMSC was found to be unaffected by the employment of this serum-reduced medium.

Since the beneficial effects of hMSC transplantation into SCI were thought to be due to paracrine mechanisms, the expression patterns for several growth factors and cytokines were investigated. A donor-dependent variability of expression could be demonstrated in untreated hMSC as well as in hMSC that had been exposed to lipopolysaccharide (LPS). To investigate the possibility that hMSC could change their specific expression pattern when implanted into debris-laden spinal cord lesions, hMSC were co-cultivated with tissue homogenates from normal and injured rat spinal cords. To determine if this possibility might be tissue specific, homogenates from normal and infarcted rat heart were also applied. None of the above homogenates were found to change the individual donor-dependent patterns of growth factor- or cytokine expression suggesting that indivual hMSC expression patterns remained unaltered following implantation into the lesioned spinal cord. However, such donor-dependent variability might have a profound influence on the degree of subsequent

functional recovery and it has to be considered that some donor samples might not have the appropriate growth factor and cytokine expression profiles for optimal tissue repair.

A major aspect of the present thesis was the evaluation of an hMSC-based tissue engineering strategy to promote orientated axonal re-growth and functional tissue repair in an experimental animal model of acute SCI. Therefore, cooperation partners transduced hMSC to express green fluorescent protein (GFP) to enable identification of transplanted cells. These cells were seeded into oriented 3D collagen scaffolds and implanted into thoracic spinal cord hemisections. Already 1 week after implantation, animals which received hMSC-seeded scaffolds demonstrated better functional improvement than the control animals, which was even significant after four weeks. This difference, however, was no longer significant at 8 weeks. Immunohistochemistry revealed that only small numbers of transplanted hMSC had survived up to the termination date of 8 weeks after implantation. Nonetheless, animals receiving hMSC-seeded scaffolds demonstrated increased numbers of regenerating axons as well as reduced astrocytic and inflammatory responses. Interestingly, donor hMSC were found to express chondroitin sulphate proteoglycans (CSPG) and although few viable cells could be detected, CSPG deposits could be observed throughout the scaffold.

In conclusion, it is likely that hMSC exert their regenerative properties by the expression of growth factors, cytokines and extracellular matrix molecules which are capable of influencing resident and invading cells.

2. Zusammenfassung

Transplantierte mesenchymale Stromazellen (MSZ) sind in der Lage die funktionelle Regeneration nach Rückenmarksverletzungen zu verbessern. Die verantwortlichen Mechanismen für diesen Effekt sind jedoch weitgehend unbekannt. Die ersten Studien über die Transplantation von MSZ in Läsionen des Rückenmarks zeigten eine Differenzierung der Spenderzellen in eine neurale Linie. Dieses so genannte Transdifferenzierungsvermögen rief enorme Aufregung aber auch große Skepsis hervor. Andere Studien kamen zu dem Schluss, dass der postive Effekt durch einen parakrinen Mechanismus hervorgerufen wird. Diese Dissertation wurde erstellt, um Einblicke in die Eigenschaften von MSZ sowie deren Schicksal und Funktion nach der Transplantation in Rückenmarksverletzungen zu erhalten.

Es konnte festgestellt werden, dass humane MSZ (hMSZ) grundsätzlich einige neurale Marker exprimieren, eine Eigenschaft die andere Gruppen dazu verleitet haben mag zu folgern, dass hMSZ in eine neurale Linie transdifferenzieren können. Interessanterweise konnte nachgewiesen werden, dass diese Marker eine Spender-abhängige Variabilität aufweisen, die die weitgehend unterschiedlichen Meinungen über die Transdifferenzierung von hMSZ beeinflusst haben könnte.

Die klinische Anwendung von hMSZ erfordert die Expansion der isolierten Zellen in entsprechender Anzahl ohne die Ergänzung von tierischem oder humanem Serum. Die konventionelle Expansion beinhaltet jedoch die Verwendung von 10% fötalem Kälberserum (FKS), welches infektiöse Erreger übertragen oder zu einer immunologischen Abstoßungsreaktion der transplantierten Zellen führen könnte. In der vorliegenden Dissertation wurde die Isolation und Expansion von hMSZ ohne Ergänzung von Serum angestrebt, konnte jedoch nicht erzielt werden. Allerdings konnte im Vergleich zum konventionellen Medium eine signifikant bessere Proliferation mit der Ergänzung von nur 2% FKS und bestimmten Wachstumsfaktoren erreicht werden. Die Multipotenz der hMSZ wurde durch die Verwendung dieses Serum-reduzierten Mediums nicht beeinflusst.

Da die förderlichen Eigenschaften der hMSZ Transplantation in Rückenmarksverletzungen die Folge von parakrinen Mechanismen zu sein scheinen, wurde das Expressionsmuster verschiedener Wachstumsfaktoren und Zytokine untersucht. Unbehandelte hMSZ als auch hMSZ die mit Lipopolysacchariden (LPS) behandelt wurden, wiesen eine Spender-abhängige Variabilität auf. Um die Möglichkeit zu untersuchen, ob hMSZ ihr spezifisches Expressionsmuster nach Implantation in zerstörtes Rückenmarksgewebe ändern können, wurden hMSZ mit Homogenaten von gesundem sowie verletztem Rückenmark von Ratten ko-kultiviert. Um weiterhin feststellen zu können, ob eine solche Änderung gewebsspezifisch ist, wurden zusätzlich Homogenate von gesundem und geschädigtem Herzgewebe von Ratten verwendet. Keines der genannten Homogenate war in der Lage die individuellen

Muster der Wachstumsfaktor- und Zytokin-Expression zu verändern, was darauf schließen lässt, dass die individuellen Expressionsmuster der hMSZ nach Implantation in geschädigtes Rückenmark unverändert bleibt. Eine solche spenderabhängige Variabilität kann jedoch den Grad einer folgenden funktionellen Regeneration weitreichend beeinflussen und es muss in Betracht gezogen werden, dass manche Spenderproben nicht die geeigneten Wachstumsfaktor- und Zytokin-Expressionsmuster für eine optimale Geweberegeneration aufweisen.

Ein Hauptaspekt der vorliegenden Dissertation war die Evaluation einer auf hMSZ-basierenden *Tissue Engineering* Strategie, die orientiertes axonales Wachstum und funktionelle Geweberegeneration in einem experimentellen Tiermodell der akuten Rückenmarksverletzung fördert. Hierfür wurden von einem Kooperationspartner hMSZ mit grün fluoreszierendem Protein (GFP) transduziert, um eine Identifikation der transplantierten Zellen zu ermöglichen. Diese Zellen wurden in orientierten Kollagen-Trägermatierialien ausgesät und in Hemisektionen des thorakalen Rückenmarks implantiert. Schon nach 1 Woche zeigten Tiere, die hMSZ-besiedelte Trägermaterialien implantiert bekamen, eine deutliche funktionelle Verbesserung im Vergleich zu den Kontrolltieren. Des Weiteren zeigten die Verhaltensanalysen eine signifikante funktionelle Verbesserung im Vergleich zu den Kontrolltieren 4 Wochen nach Implantation, aber ohne Signifikanz nach 8 Wochen. Immunhistochemische Untersuchungen belegten, dass nur eine geringe Anzahl der transplantierten hMSZ bis zum Ende von 8 Wochen nach Implantation überlebt hatten. Dennoch wiesen die Tiere, die hMSZ besiedelte Trägermaterialien erhalten hatten, eine erhöhte Anzahl regenerierter Axone sowie eine reduzierte astrozytische und inflammatorische Reaktion auf. Interessanterweise exprimierten die Spender-hMSZ Chondroitinsulfat-Proteoglycane (CSPG) und obwohl nur wenige lebende Zellen detektiert wurden, konnten CSPG Ablagerungen im gesamten Trägermaterial nachgewiesen werden.

Folglich ist es sehr wahrscheinlich, dass die regenerativen Eigenschaften der hMSZ von der Expression von Wachstumsfaktoren, Zytokinen und extrazellulären Matrixmolekülen herrühren, die ihrerseits in der Lage sind ansässige und eindringende Zellen zu beeinflussen.

3. Introduction

3.1 Definition and types of stem cells

In recent years, interest in understanding the differentiation capabilities of stem cells and their potential use in the treatment of diseases and injuries has become a major focus in regenerative medicine. Stem cells are defined by two cardinal features: (i) they are capable of renewing themselves continuously and (ii) they have the ability to differentiate into a range of different cell types (1). These two criteria are fulfilled by cells derived from both embryonic and adult sources (Figure 3.1). Embryonic stem cells (ESC) are derived from the inner cell mass (ICM) of a blastocyst. These cells are capable of passing through progenitor and precursor stages to differentiate into all tissues of the three germ layers (i. e. mesoderm, endoderm, ectoderm), and have therefore been classified as **pluripotent**. Adult (or somatic) stem cells can be found in a variety of tissues, including bone marrow (2, 3), liver (4), skin (5), brain (6) and intestine (7). Such adult derived stem cells are more restricted in their differentiation potential and have been classified as **multipotent**. A well studied population of such multipotent stem cells is that of the haematopoietic stem cells (8). In addition to pluripotent and multipotent stem cells, a population of **unipotent** stem cells (differentiation capacity only towards a single cell type) also exists, for example the spermatogonial stem cells that can only differentiate into a single sperm cell lineage (9).

The differentiation potential depends on the turnover of cells in a certain tissue, as well as the ability for repair following injury or disease (10, 11). Cell lineages with a high turnover are mostly generated from pluripotent or multipotent stem cells, while cells with a long lifespan are differentiated from more restricted stem cells. For example, fully differentiated blood cells have a relatively short lifespan and therefore need to be replenished continuously, whereas neurons of the central nervous system have a much longer lifespan (12). For this purpose, stem cells are located in environmental niches of a given tissue, where intrinsic and extrinsic mechanisms regulate self-renewal and differentiation (13, 14). The concept of a stem cell niche was first suggested by Schofield in 1978 and further supported by a variety of experiments (15, 16).

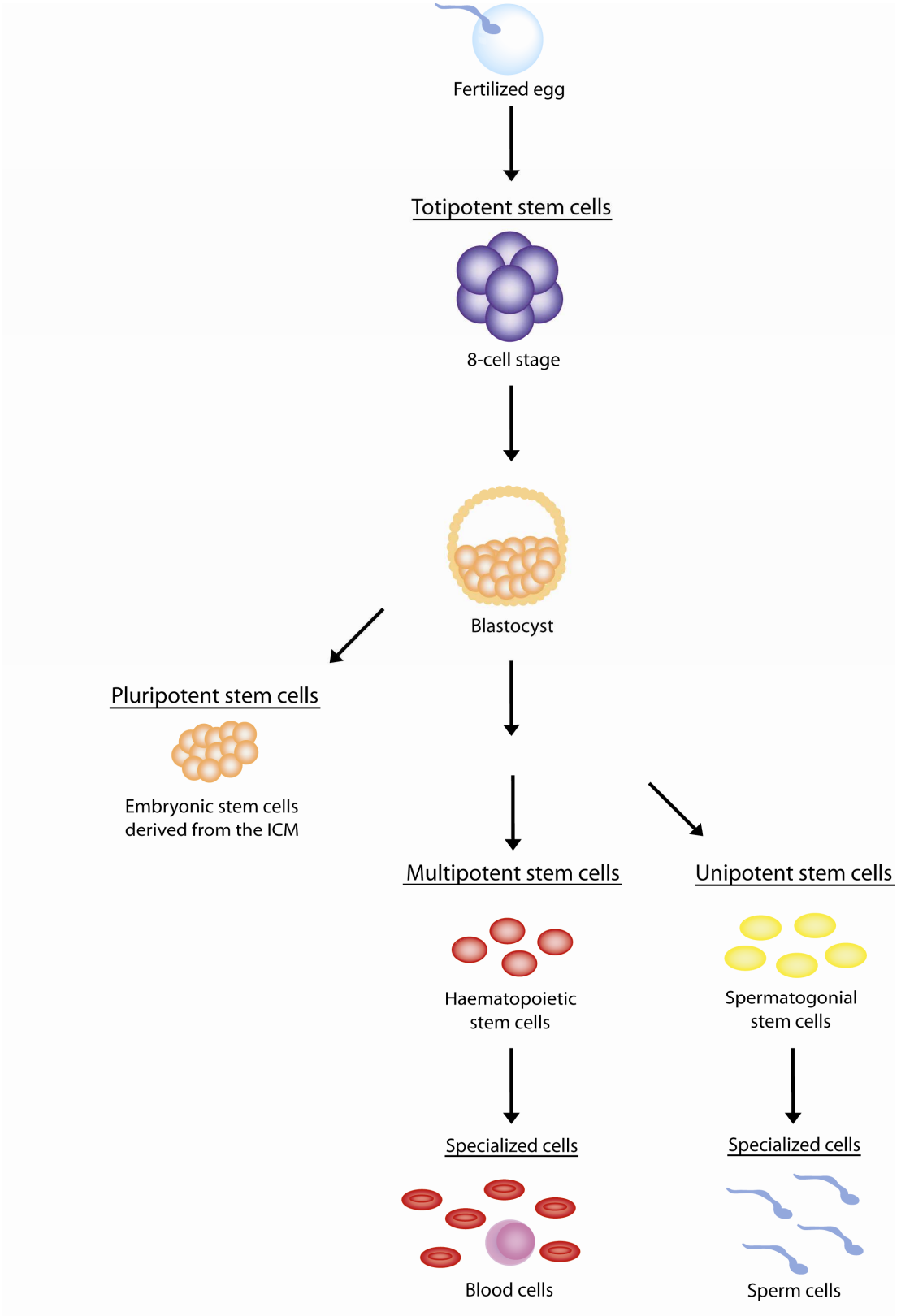

Figure 3.1: Genesis of stem cells and their plasticity. Totipotent stem cells are generated by the first three divisions of the fertilized egg. Further cell divisions form the blastocyst which contains pluripotent embryonic stem cells. Adult or somatic stem cells are more restricted in their differentiation potential and are classified as multipotent (i.e. haematopoietic) or unipotent (i.e. spermatogonial) stem cells.

For many years it was thought that multipotent adult stem cells could only differentiate into cell lineages relevant for the tissue in which they resided. However, more recent investigations have suggested that some populations of adult stem cells have the capacity to differentiate into lineages of cell types completely different from their tissue of origin. This ability has been termed **transdifferentiation** (or plasticity) and implies that such cells are capable of undergoing immense genetic reprogramming (17, 18). Although this phenomenon has aroused substantial excitement, many researchers remain sceptical about the issue and have proposed that such plasticity is merely the result of cell fusion. Clear evidence that such fusion events can indeed take place has been obtained from several *in vitro* co-culture experiments (19, 20). However, it has also become clear that these events occur at only low frequency. Therefore, three other explanations for plasticity are still in discussion: (1) multiple tissue-specific stem cells exist in different tissues, (2) veritable pluripotent stem cells exist in postnatal life, or (3) cells may undergo dedifferentiation and redifferentiation (21). Generally, it is assumed that the differentiation potential of a stem cell is dependent on its developmental stage, and that development is a unidirectional process (i.e. stem cells progressing through progenitor and precursor stages to fully differentiated and mature cell types (22)). During such unidirectional differentiation, it was believed that a switch from one lineage pathway to another could not be accomplished. However, some reports have suggested that this process may not be just unidirectional. It has been reported that some niches are capable of reverting progenitor cells back to a stem cell phenotype (23, 24). Such reversibility had previously been identified in amphibians (25, 26). Although stem cell research is no longer in its infancy, there are still many issues concerning the function of stem cells in health and disease that remain to be clarified. Nonetheless, their potential for application in future cell-based intervention strategies in regenerative medicine remains enormous.

3.2 Mesenchymal stromal cells

Mesenchymal stromal cells (MSC) were first described by Friedenstein *et al.* as a stromal support system for haematopoietic stem cells in the bone marrow (27). These cells can be readily isolated from bone marrow, due to their propensity to adhere to tissue culture plastic as compared to the other cell types present within the bone marrow aspirates. Through repeated media replacement, it is possible to remove non-adherent (i. e. non-MSC) cells. Alternatively, it is possible to isolate MSC by centrifugation through a Ficoll or Percoll density gradient solution (28). Nevertheless, MSC constitute only a very small fraction of cells obtained from the bone marrow aspirate (approximately one MSC per 10^5 cells) but their numbers can be expanded easily (28). Apart from bone marrow, MSC can also be isolated from other sources, such as adipose tissue (29), skeletal muscle (30), peripheral- (31) and

umbilical cord blood (32), as well as from amniotic fluid (33). MSC express a range of markers such as CD73, CD90 and CD105, but lack haematopoietic surface markers such as CD11b, CD14, CD19, CD34, CD45, CD79α, and HLA-DR, (34). Characteristically, MSC can readily differentiate into adipocytes, chondrocytes and osteocytes (3). However, in the last few years it has been suggested that, under certain culture conditions, MSC might be able to cross lineage boundaries which were until recently thought to be uncrossable. (Trans-) differentiation into ectodermal cell types, such as neural cells (35-37), as well as endodermal cell types, for example hepatocytes (38, 39), has been reported (Figure 3.2).

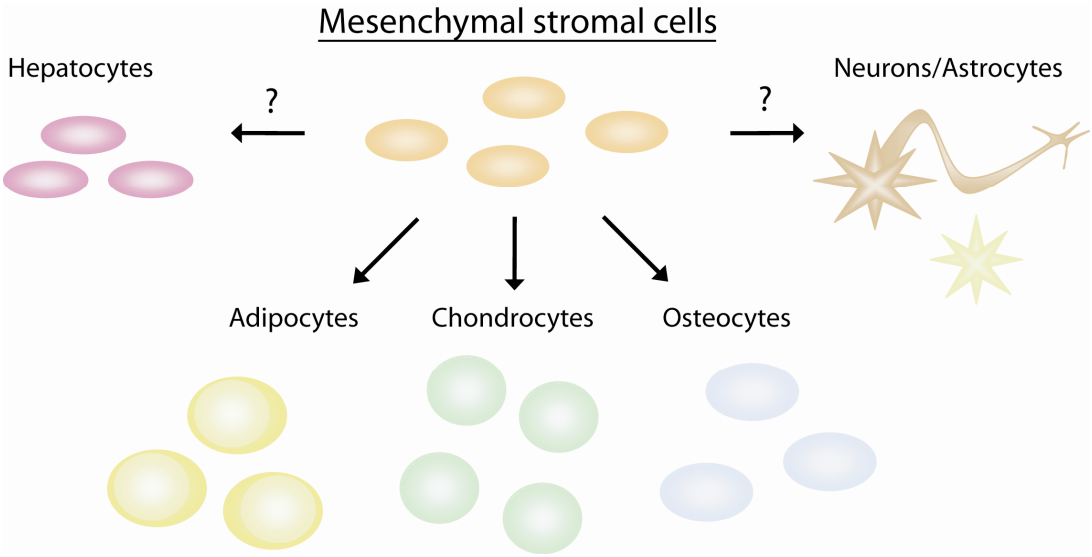

Figure 3.2: Differentiation capacity of mesenchymal stromal cells. Mesenchymal stromal cells can differentiate into adipocytes, chondrocytes and osteocytes. Additionally, studies suggest the transdifferentiation potential of mesenchymal stromal cells into ectodermal (i.e. neurons and astrocytes) as wells as endodermal cell types (i.e. hepatocytes).

Although the multipotent differentiation capacity of MSC has been well established, the incontravertible proof of their stem cell character is still lacking, since MSC are not a homogenous population of cells and only a few of these cells are able to generate fibroblast colonies (40). The term mesenchymal *stem* cell, may thus no longer be valid (41).

3.3 Therapeutic potential of mesenchymal stromal cells in spinal cord injury

Several therapeutic goals have been targeted by the cell transplantation approach to repair spinal cord injury (SCI): (i) bridging of cystic cavitation, (ii) replacement of dead cells, and (iii)

establishment of an environment which promotes axonal regeneration. A wide range of different strategies have been investigated, including transplantation of whole tissue pieces such as peripheral nerves (42), embryonic spinal cord tissue (43) or the transplantation of cell suspensions (as either purified- or mixed cell populations). Populations of cells chosen for promoting tissue repair following experimental SCI have included purified Schwann cells (44), olfactory ensheathing cells (OEC, (45)) and embryonic stem or progenitor cells (46, 47). Adult stem or progenitor cells have also been investigated for their ability to promote tissue repair after SCI, amongst which MSC were suggested to be a promising candidates (48). Transplantation of adult stem- or progenitor cells should diminish ethical concerns in contrast to embryonic stem- or progenitor cells. Furthermore, the possibility of generating autologous cells avoids any complications due to rejection.

In preclinical studies it was demonstrated that a delayed transplantation of rat MSC promotes functional improvement after injury to the spinal cord (49, 50). However, the mechanism for this improvement was not identified. Histological analysis displayed the survival of transplanted, BrdU-labelled cells, as well as an overall distribution of the MSC throughout the damaged tissue, indicating high migratory activity. Furthermore, some neural antigens, such as nestin, NeuN and the oligodendrocyte marker Rip have been identified in the transplanted cells (50). However, it has been reported that only NeuN was detectable in donor MSC (e. g. Hofstetter et al. (49)). Such (negative) findings regarding the transdifferentiation capacity of MSC *in vitro* and *in vivo* have also been described by others (51, 52). Interestingly, in the report of Hofstetter and colleagues, donor MSC were found to form longitudinally orientated columns within the lesion. Such columns were associated with nestin-postive host cells (that were suggested but not proven to be immature astrocytes), mature GFAP-positive astrocytes as well as 5HT- and neurofilament (NF)-positive axons. It was suggested that the most likely mechanism of improved function was by donor cell expression of a range of growth factors, cytokines and cell surface adhesion molecules that supported axon regeneration rather than by replacing lost glia or neurons (49).

An indirect (or neuroprotective) mechanism of improved function was also later suggested following MSC transplantation into rat spinal cord contusion injuries (53). The donor MSC occupied the lesion cavity and contributed to the preservation of host tissue, in particular of host myelin. Similar to the reports of Hofstetter and colleagues (49), donor MSC were observed to form longitudinally orientated guidance structures which supported host axonal growth. This effect was presumably being supported by the release of growth factors (i.e. NGF, BDNF, vascular endothelial growth factor (VEGF) and hepatocyte growth factor (HGF)) from the donor cells (54, 55).

In contrast, Parr and colleagues could not detect any functional recovery after transplantation of eGFP-positive rat MSC into a model of mid-thoracic (T8-T9) spinal cord compression injury (56). Furthermore, immunohistochemistry revealed no detection of any neural-related markers within the transplanted cells, demonstrating that no neural differentiation had taken place. However, transplantation of MSC did result in a significant reduction in the maximal area of cavitation compared to the control group.

As an alternative approach to the direct transplantation of donor cells into or close to the lesion site, MSC have been intravenously injected to assess their ability to "home" to pathological tissues following spinal cord compression injuries (57). Rat donor MSC were labelled with iron-oxide nanoparticles, enabling their migration to be tracked *in vivo* by magnetic resonance imaging. MSC injected one week after SCI migrated to the lesion site and induced a significant improvement of locomotor function by 35 days. Transplanted cells also induced a significant reduction of secondary tissue degeneration and a following increase in spared white and grey matter. A similar approach was applied to chronic compression injuries of the spinal cord (rats having been lesioned 4 months earlier). Although transplanted MSC had no effect on locomotor function in the chronic lesion model, a significant improvement of hindlimb sensitivity was detected (57). Histological analysis of the lesioned spinal cord tissue revealed no differences in the volume of white- and grey matter compared to the control animals.

The potential of human donor MSC to induce functional recovery in SCI models of varying severity demonstrated a most pronounced effect in *moderate* contusion injuries (58). MSC-transplantation directly into the lesion epicentre one week after injury resulted in a significant histological and behavioural improvement. No significant differences could be detected between the non-grafted, *mildly* contused animals and those that received MSC transplants. The *severely* contused animals were distinguished by a high mortality due to a poor health and complicating issues like infections and autophagia (58).

Although the mechanism of improved function following MSC transplantation in rodent models of SCI is far from clear, the procedure has been proven to be safe. Transplantation of rhesus monkey MSC into spinal cord injured rhesus monkeys was therefore performed in an attempt to move the technology closer to the clinical domain (59). A T9-T10 contusion injury was induced and half of the animals received a delayed (2 week) implantation of "neurally pre-differentiated" MSC, the remaining control animals received vehicle injections. By 3 months after cell transplantation, the grafted animals demonstrated almost normal sensory responses and improved locomotion. Identification of donor cells revealed that approximately 10% expressed some neural-related antigens (e.g. NF, neuron-specific enolase (NSE) and glial fibrillary acidic protein (GFAP)). However, the nuclear marker

(Hoechst 33342) that was chosen for pre-labelling cells prior to transplantation is notoriously prone to leakage and transfer to host cells (60). Once again, the data concerning transdifferentiation remained uncertain. The functional improvement, however, was clear.

Despite the uncertainties surrounding the mechanism(s) of functional improvement, other groups have moved the technology directly to clinical investigations and have reported case studies and even phase I clinical trials (61, 62). A case report was used to highlight the electrophysiological and functional improvement of two patients with established, chronic SCI (61). Autologous MSC were obtained through needle aspiration of iliac crest bone marrow. Co-cultivation of MSC with the patients' autoimmune T (AT) cells was reported to induce transdifferentiation towards a neural stem cell-like phenotype (NSC) (63). Forty eight hours prior to the transplantation of the newly generated NSC, the patients received an intravenous infusion of AT cells to generate a controlled inflammatory micro-environment for the transdifferentiated NSC. The injection of NSC was subsequently performed by an infusion via the artery feeding the lesion site and the patients underwent physiotherapy. Both patients (one paraplegic, the other quadriplegic) in the study demonstrated an apparent improvement of sensory and motor function.

Transplantation of autologous bone marrow mononuclear cells containing MSC into patients suffering from traumatic SCI and complete loss of motor and sensory function was investigated in a phase I clinical trial (62). In this trial, 20 patients received cell transplants between 10 days and 18 months post injury, either via trans-femoral catheterization of the arteria vertebralis or intravenously. Both application strategies were investigated in acute (10 - 30 days post injury) and chronic patients (2 -17 months after SCI). Although phase I clinical trials are performed to evaluate clinical safety, investigations of motor and sensory function was also assessed in the grafted patients. An improvement of function was noted in 5/7 of the acute patients and 1/13 of the chronic patients. Most importantly, the progress of 11 of the patients could be followed up for more than two years, revealing no complications and allowing the confirmation of the safety of this intervention strategy.

3.4 Hypothesis and goals of the thesis

The hypothesis to be tested in the present thesis is that the reported beneficial effect of MSC transplantation into spinal cord lesions is due to a paracrine mechanism rather than the doubtful transdifferentiation of MSC to neural phenotypes.

Since transdifferentiation of MSC into cells of the neural lineage has been controversially discussed, the origin of these different opinions will be investigated. Therefore, the basal expression of neural-related markers in untreated hMSC from different donors will be determined.

MSC are of substantial importance in several clinical applications and a defined cultivation protocol for clinical use is needed. Conventially, laboratory MSC expansion has been performed in culture medium supplemented with 10% serum. Since animal- or donor-derived sera might transfer infectious agents or might lead to a host immune response, a standardized serum-free cultivation protocol for the expansion of MSC will be developed.

Increasing evidence suggests that the regenerative properties of MSC are due to paracrine effects. Indeed, MSC are capable of secreting a variety of growth factors and cytokines which may enhance the re-growth of axons. One question that will be addressed in the present thesis is the possibility that MSC might change their growth factor and cytokine expression patterns when implanted into the injured spinal cord. Therefore, hMSC will be co-cultivated with tissue extracts of normal or injured rat spinal cord. To evaluate the possibility that such an expression change may be due to tissue-specific effects, extracts of normal or injured rat heart will also be used as tissue controls.

Although MSC have been demonstrated to have beneficial effects in promoting spinal cord repair, the majority of the studies have performed compression/contusion injuries followed by direct or delayed injection of MSC. The main aim of the present thesis is to investigate the regenerative properties of hMSC in an experimental model of acute penetrating spinal cord injuries followed by direct implantation of an hMSC-seeded, orientated microporous 3D scaffold. For quantitative evaluation of the functional improvements, a number of behavioural and histological methods will be applied and correlated.

4. Neural differentiation potential of human bone marrow-derived mesenchymal stromal cells: misleading marker gene expression

4.1 Abstract

In contrast to pluripotent embryonic stem cells, adult stem cells have been considered to be multipotent, being somewhat more restricted in their differentiation capacity and only giving rise to cell types related to their tissue of origin. Several studies, however, have reported that bone marrow-derived MSC are capable of transdifferentiating to neural cell types, effectively crossing normal lineage restriction boundaries. Such reports have been based on the detection of neural-related proteins by the differentiated MSC. In order to assess the potential of human adult MSC to undergo true differentiation to a neural lineage and to determine the degree of homogeneity between donor samples, we have used RT-PCR and immunocytochemistry to investigate the basal expression of a range of neural related mRNAs and proteins in populations of non-differentiated MSC obtained from 4 donors.

The expression analysis revealed that several of the commonly used marker genes from other studies like nestin, Enolase2 and microtubule associated protein 1b (MAP1b) are already expressed by undifferentiated human MSC. Furthermore, mRNA for some of the neural-related transcription factors, e.g. Engrailed-1 and Nurr1 were also strongly expressed. However, several other neural-related mRNAs (e.g. DRD2, enolase2, NFL and MBP) could be identified, but not in all donor samples. Similarly, synaptic vesicle-related mRNA, STX1A could only be detected in 2 of the 4 undifferentiated donor hMSC samples. More significantly, each donor sample revealed a unique expression pattern, demonstrating a significant variation of marker expression.

The present study highlights the existence of an inter-donor variability of expression of neural-related markers in human MSC samples that has not previously been described. This donor-related heterogeneity might influence the reproducibility of transdifferentiation protocols as well as contributing to the ongoing controversy about differentiation capacities of MSC. Therefore, further studies need to consider the differences between donor samples prior to any treatment as well as the possibility of harvesting donor cells that may be inappropriate for transplantation strategies.

4.2 Introduction

MSC, often termed mesenchymal stem cells, may be isolated from bone marrow, adipose and other tissues. They adhere strongly to tissue culture plastic and are capable of multipotent differentiation that can be demonstrated *in vitro*. MSC can differentiate into

osteoblasts, chondroblasts, adipocytes and myoblasts (reviewed in (3)). Since the survival and migration of human MSC (hMSC) grafted into rat brains was demonstrated (64), the possibility that such cells might act as suitable tools for promoting central nervous system (CNS) repair has been raised. This notion was further strengthened by the report that murine MSC may differentiate into mature astrocytes after implantation into neonatal mouse brains (65). Donor MSC have also been reported to give rise to neuronal phenotypes in adult mice brains after transplantation (66, 67). During the last six years, there have been many reports describing *in vitro* neural transdifferentiation of MSC derived from a range of different species (e.g. human, mouse, rat). All protocols that have been used for such investigations can be divided into three broad categories: i.e. those using (i) chemical compounds (37, 68-71), (ii) growth factors (72-75), or (iii) neurosphere-like cultivation (76-81). Furthermore, combinations of these different protocols have also been reported to induce neural differentiation (82, 83). Such reports of *in vitro* neural transdifferentiation by MSC derived from experimental animal- or human sources have been based on the detection of neural-related mRNA as well as proteins by the treated cells. In the present investigation, RT-PCR and immunocytochemistry were used to demonstrate the basal expression of several of the commonly used marker genes or proteins by undifferentiated human MSC. The data obtained by this study revealed a substantial degree of heterogeneity of the basal expression of neural-related genes that had not previously been described.

4.3 Materials and methods

4.3.1 Sampling of human MSC

Bone marrow was aspirated from patients during hip joint replacement following informed consent, according to local ethical board approval of the University Hospital, Aachen.

4.3.2 Isolation and cultivation of human MSC

Bone marrow aspirates were diluted 1:5 in mesenchymal stem cell growth medium (MSCGM, Lonza, Vervieres, Belgium) and immediately seeded into polystyrene plastic 75 cm^2 tissue culture flasks at 37°C in 5% humidified CO_2. After seven days, non-adherent cells were removed by media replacement and adherent cells were expanded in MSCGM. Media exchange was performed every 3-4 days until cells reached 80% confluence. For passaging, the cells were detached with trypsin/EDTA solution (Lonza, Vervieres, Belgium) and re-seeded with a density of 4000 cells/cm^2.

4.3.3 Characterization of isolated human MSC

For characterization of human MSC, three criteria were used: i) adherence to tissue culture plastic, ii) specific surface antigen expression, and iii) multipotent differentiation potential (34). The morphology of plastic adherent cells was monitored using an inverse microscope (DM IL Invers, Leica, Wetzlar, Germany). To detect specific surface antigens, cells were detached and fixed with 4% paraformaldehyde for 20 min. After washing with 0.1 M phosphate-buffered saline (PBS), cells were incubated in blocking solution (20% FBS in PBS, Biowest, Nuaille, France) for 20 min. After washing with PBS, the cell pellets (250,000 per antibody) were resuspended in 100 µl PBS, 2 µl primary antibody was added and incubated for 30 min. Monoclonal primary antibodies recognizing surface markers CD11b (Invitrogen, Carlsbad, USA), CD19, CD34, CD45, CD73, CD90 (Becton Dickinson, San Jose, USA), CD105 (Invitrogen) and HLA-DR (Abcam, Cambridge, UK) were used. After three washing steps with PBS, 2 µl of the secondary antibody (Alexa-488 conjugated goat anti-mouse, Invitrogen) was incubated in 100 µl PBS for 30 min in the dark. After two final washing steps, the cells were re-suspended in 400 µl PBS and analyzed using a FACSCalibur and FACSCalibur software (Becton Dickinson).

Multipotency was monitored by *in vitro* differentiation of MSC to adipogenic, chondrogenic and osteogenic lineages according to Pittenger et al. (28). To induce adipogenesis, cells were cultivated in adipogenic induction medium (DMEM (Lonza, Vervieres, Belgium) with 10% FCS, 0.5 µM dexamethasone, 0.5 µM indomethacin, and 0.5 mM isobutyl-methyl-xanthine (all Sigma, Steinheim, Germany)). Medium was changed every 3 days for 3 weeks. To visualise lipid droplets, Oil Red O staining (Sigma) was used as a histologic stain.

Osteogenic differentiation was induced by cultivation of MSC in osteogenic induction medium (DMEM with 10% FCS , 20 nM sodium β-glycerophosphate, 1 nM dexamethasone, and 50 µg/ml 1-ascorbic acid 2-phosphate, all purchased form Sigma). Medium was changed every 3 days for 3 weeks. Osteogenic differentiation was visualised by Alizarin-Red-S staining (Sigma) of matrix mineralization associated with osteoblasts (according to the method of (84)).

For chondrogenic differentiation, 2.5 x 10^5 cells were centrifuged to obtain cell pellets. These pellets were induced with serum free induction media (DMEM) containing 100 nM dexamethasone, 0.17 mM 1-ascorbic acid 2-phosphate, 100 µg/ml sodium pyruvate, 40 µg/ml proline (all Sigma), and 1 % ITS-Plus (Becton Dickinson). TGF-β3 (CellSystems, Sankt Katharinen, Germany) was added in a concentration of 10 ng/ml at each medium exchange. After 21 days, pellets were fixed with PFA and paraffin embedded. Thin sections were stained with Toluidine blue (Sigma) to show metachromatic staining which is characteristic of cartilage (84, 85).

4.3.4 Gene expression analysis

RNA was isolated using the RNeasy Mini Kit (Qiagen, Hilden, Germany) according the manufacturers protocol. The integrity of isolated RNA was evaluated using the 2100 bioanalyzer (Agilent Technologies, Palo Alto, USA). For PCR analysis 2 µg RNA was reverse transcribed using Omniscript Reverse Transcriptase (Qiagen, Hilden, Germany) according the manufacturers protocol using oligo-d(T) primers and random hexamers. Commercially available samples of human adult and fetal brain total RNA were used as positive controls (Ambion, Austin, USA and Clontech-Takara Bio Europe, Saint-Germain-en-Laye, France). For amplification of target genes, 0.2 units Taq polymerase (Amersham Biosciences, New York, USA) were used with a standard PCR program (denaturation: 10 sec at 96°C; primer hybridisation: 2 min at various target specifc temperatures, see table 1; elongation: 2 min at 72°C).

Table 4.1: Primer sequences and PCR conditions

Primer	Forward (5´- 3´)	Reverse (5´- 3´)	Hybridization temperature (°C)	Cycles	Amplicon size (bp)
ASCL1	aag caa gtc aag cga cag cg	agtcgt tgg agt agt tgg gg	62	35	352
Bag1	tca ccc aca gca at gaga ag	cag aaa acc ctg ctg gat tc	66	30	344
DRD2	tca tcg ctg tca tcg tct tcg	gat gga gat cat gac ggt gac	65	40	344
Engrailed-1	agc cac agg cat caa gaa cg	cac ctg tcc gag tct ttc tc	65	40	303
Enolase2	ggc aaa ggt gtc ctg aa gg c	gtg ccg gcc ttc aac gtg at	67	30	284
GAPDH	tga agg tcg gag tca acg gat ttg gt	cat gtg ggc cat gag gtc cac cac	62	30	983
GFAP	gtg gta ccg ctc caa gtt tgc ag	aat ggt gat ccg gtt ctc ctc	59	40	373
MAP1B	act gca gga cca gga act ac	cag tgt cac ctg cat gtt gc	67	25	255
MAPT	agc tct ggt gaa cct cca aaa tc	cat cca tca taa acc agg agg tg	58	40	361, 454
MBP	cct ggc cac agc aag tac	ggg agc cgt agt gag cag t	61	35	251
Nestin	gcg ttg gaa cag agg ttg gag	gca cag gtg tct caa ggg tag	65	30	385
NEUROD6	ctg aga atc ggc aag aga cc	ctg cac agt aat gca tgc cg	62	35	433
NFH	tga aca cag acg cta tgc gct cag	cac ctt tat gtg agt gga cac aga g	58	35	398
NFL	acc aac gag aag caa gcg ctc	cat cag cgc tat gca gga cac	59	35	590
NFM	aaa gac atc gag gag gcg tc	cgc tgc gta cag aaa act cc	61	35	592
Nurr1	aag gct tct tta agc gca cag	cga tta gca tac agg tcc aac	55	25	518
S100ß	gga gac aag cac aag ctg aag	agc tac aac acg gct gga aag	63	30	322
STX1A	atc gca gag aac gtg gag gag	agc gtg gag tgc tgt gtc ttc	67	30	230
SYP	ggt gct gca atg ggt ctt cgc	aag ccg aac acc acc gag gtg	59	35	537
TH	atc cac cat cta gag acc cg	tcc ccg ttc tgc tta cac ag	63	40	824

PCR products were analyzed by electrophoresis on a 1.7% agarose gel and visualized with 0.5 µg/ml ethidium bromide. PCR conditions were established using adult and fetal brain

cDNA and best results from at least two independent experiments were chosen for expression analysis of hMSC. Expression of each marker was monitored by testing cDNA of all four donors using the same master mix, PCR condition and gel electrophoresis.

4.3.5 Immunocytochemistry

The hMSC were seeded at a relatively low density to allow the clear identification of individual cells for quantification. After removal of the media and washing in 0.1 M PBS, cells were fixed with 4 % paraformaldehyde in PBS for 30 min. Afterwards, the samples were washed three times with PBS and non-specific binding sites blocked by a 1 hour incubation in PBS containing 3 % normal goat serum (Sigma), 1 % bovine serum albumin (BSA, fraction 5, Serva, Heidelberg, Germany) and 1 % Triton X-100 (Sigma). The primary antibodies anti-enolase2 (monoclonal, Dako M0873; 1:500), anti-MAP1b (monoclonal, Sigma M4528; 1:500), anti-Nurr1 (monoclonal, Abnova H00004929-M07; 1:200) and anti-nestin (polyclonal, Chemicon AB5922; 1:200) were diluted in PBS containing 1% BSA and incubated at room temperature overnight. The secondary antibodies, goat-anti-mouse Alexa 594 (1:500, Invitrogen) and goat-anti-rabbit Alexa 488 (1:500, Invitrogen), were also diluted PBS containing 1% BSA and incubated for 2.5 hours at room temperature. Finally, nuclei were stained with diamidinophenylindole (DAPI, 1:1000, Roche), cover-slipped with Fluoroprep (bioMerieux, Marcy l'Etoile, France) and observed using a Leica DM RX microscope (Leica, Wetzlar, Germany) with 20x objective. Omission of primary antibodies served as negative control and resulted in no detectable staining. Immunocytochemistry of cells obtained from three different donors was performed on 2 separate occasions. The proportion of cells immunoreactive for a particular antigen was quantified by counting 100 cells per donor sample. To achieve this, 10 randomly chosen, non-overlapping microscopic fields (each 577 µm x 465 µm) distributed evenly across the whole sample were photographed to provide representative images of the stained and non-stained cells. The 10 fields were believed to be representative of whole donor samples because the immunocytochemistry revealed that there was no heterogeneity of the distributions of the stained and non-stained cells - i.e. there were no clusters of stained cells or non-stained cells.

4.4 Results

4.4.1 Characterization of human MSC

Isolated hMSC were characterized by three criteria: (i) adherence to tissue culture plastic, (ii) specific surface antigen expression, and (iii) multipotent differentiation as defined by the

Mesenchymal and Tissue Stem Cell Committee of the International Society for Cellular Therapy (34).

Fluorescent activated cell sorting (FACS) analysis demonstrated that the expanded, plastic adherent cells used in the present investigation were positive for the surface markers CD73, CD90 and CD105, but negative for CD11b, CD19, CD34, CD45 and HLA-DR (Figure 4.1).

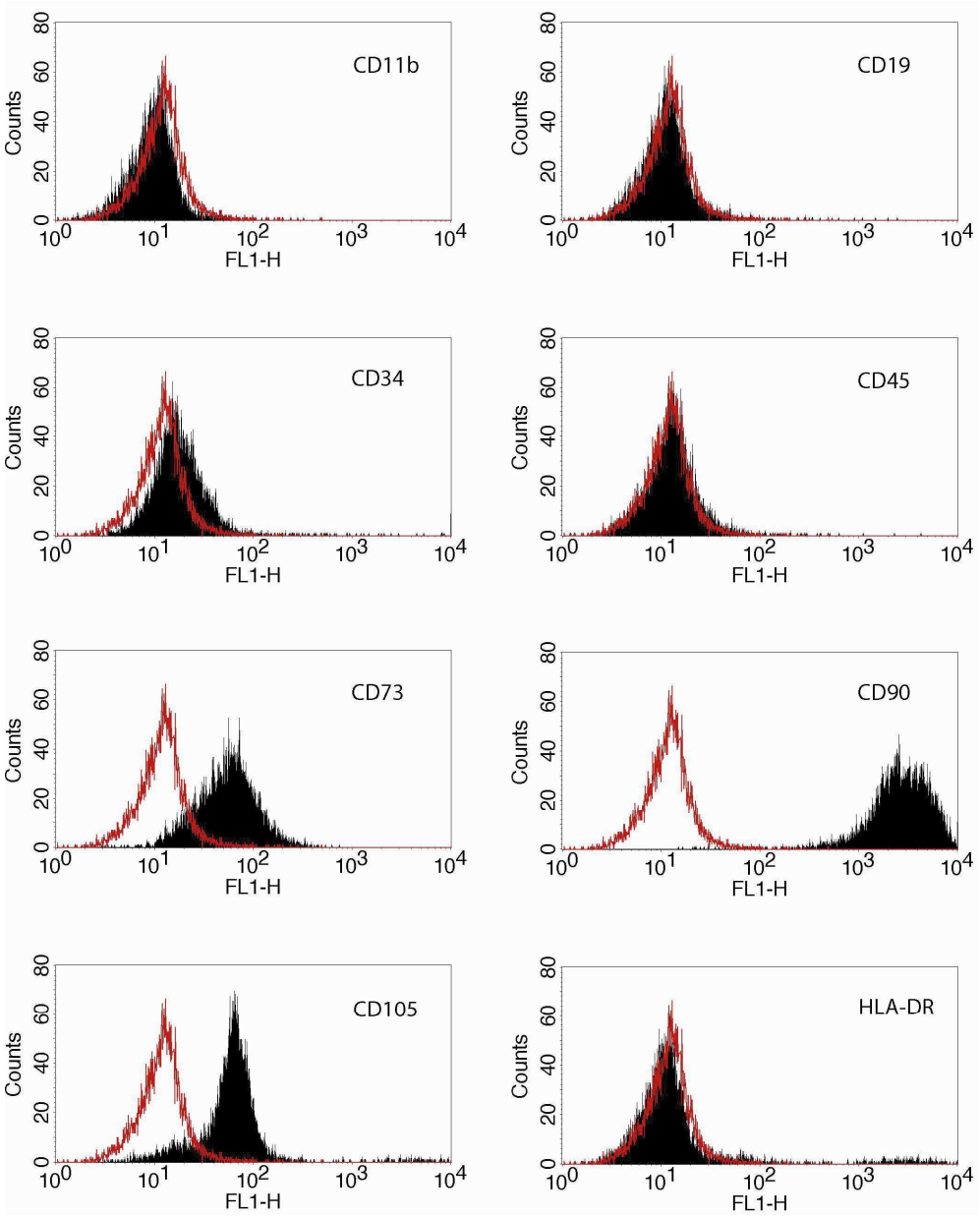

Figure 4.1: Surface marker expression of human MSC. FACS analysis of the immunophenotypic surface profile for CD11b, CD19, CD34, CD45, CD73, CD90, CD105 and HLA-DR of isolated hMSC. Red histograms represent the fluorescence from negative-control cells incubated with only secondary antibody; black histograms represent the counts of cells incubated with the relevant primary antibody. The logarithm on the X-axis (FL1-H channel) represents the intensity of the fluorescent signal and the number of cells is given on the Y-axis. HMSC isolated in this study were positive for the markers CD73, CD90 and CD105, but negative for CD11b, CD19, CD34, CD45 and HLA-DR according to the criteria for MSC.

To demonstrate their multipotent potential, MSC were differentiated to adipocytes, chondrocytes and osteocytes according to published protocols (28). Lipid vacuoles in differentiated adipocytes were visualized with Oil Red O (Figure 4.2A). However, not all cells demonstrated the same degree of staining. Induction of chondrogenic differentiation was performed in cell pellets which developed a proteoglycan-rich extracellular matrix. Thin sections of these pellets were stained with Toluidine Blue (Figure 4.2B), demonstrating a metachromatic staining that was characteristic of cartilage matrix (85). Osteogenic differentiation resulted in an immense production of mineral deposits that were stained with Alizarin-Red-S (Figure 4.2C). Thus, the cells used in this study fulfilled all criteria to be defined as MSC.

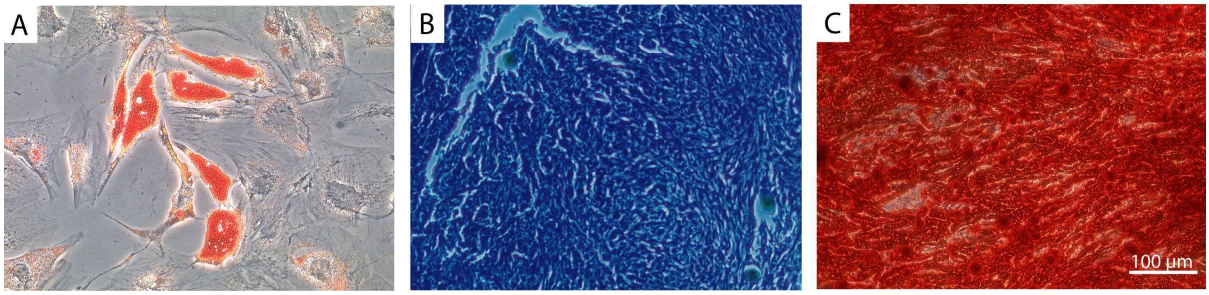

Figure 4.2: Differentiation capacity of hMSC. The hMSC were cultivated for 21 days in differentiation media to show multi-potentiality. (A) Adipogenic differentiation resulted in the formation of lipid vacuoles which were stained with Oil Red O; (B) Thin sections of chondrogenic differentiated hMSC-derived cell pellets were stained with Toluidine Blue, demonstrating a highly enriched extracellular matrix; (C) Alician Red staining of hMSC induced to osteocytes revealed an immense mineral deposition.

4.4.2 Neural marker expression by undifferentiated human MSC

The neural specific RNA transcripts, obtained from hMSC of four different donors, were categorized into four sub-groups: (i) neuronal markers, (ii) glial markers, (iii) neural related transcription factors and (iv) others (Figure 4.3, table 4.2). For every marker, both adult and fetal human brain extracts were used as positive controls.

Neuronal markers: One of the neuronal markers investigated was dopamine receptor D2 (DRD2), a marker for dopaminergic neurons (86), which was moderately expressed by three donors (donors 1, 2 and 4). Transcripts for enolase2 (or neuron-specific enolase, NSE), normally found in mature neurons and in cells of neuronal origin (87), were also found in human MSC (donor 2 moderate, donors 3 and 4 weak). Microtubule-associated protein 1b (MAP1b), that is suggested to play an important cytoskeletal role in development and function of the nervous system (88), was strongly detected in donors 2 to 4 as well as moderately in donor 1. Other widely used markers for neurons are the neurofilaments (NF).

The expression of NFH (heavy), NFM (medium) and NFL (light) in human MSC was analyzed in the present study. Low levels of transcripts for NFL could only be detected in donors 1 and 4, but moderate levels were found in donor 2. The syntaxin (STX1A) functions in the fusion of synaptic vesicles with the synaptic membrane of neurons (89). However, a moderate amount of STX1A was also detected in the undifferentiated MSC of donor 3 and 4. Another synaptic vesicle-related protein, synaptophysin (SYP) (90), was only slightly detectable in donors 2 to 4. The expression of tyrosine hydroxylase (TH), a neurotransmitter-related enzyme in catecholaminergic neurons, was also only weakly detectable in donor 2. No expression of mRNA for the axonal microtubule-associated protein tau (MAPT, (91)) could be observed (for an overview of the case-by-case expression of the markers genes, see Table 4.1).

Glial markers analyzed in this study were glial fibrillary acidic protein (GFAP) (92), myelin basic protein (MBP) (93) and the calcium binding protein, S100β (94). None of the hMSC were found to express S100β or GFAP, an intermediate filament protein that is normally expressed by astrocytes and Schwann cells. However, 3 of the hMSC population (donors 2-4) were found to express low levels of mRNA for MBP, a major myelin associated protein.

Neural-related transcription factors. Transcripts for achaete-scute complex homolog 1 (ASCL1, also known as Mash1), a transcription factor that plays a role in neuronal commitment and differentiation and in the generation of olfactory and autonomic neurons (95), could not be detected in any of the donor cells. Furthermore, none of the donor cells expressed mRNA for neurogenic differentiation 6 (NEUROD6), a factor suggested to be involved in the development and maintenance of the mammalian nervous system (96). However, the expression of the homeobox protein Engrailed-1 (important in the formation of interneurons (97) as well as in the regionalization of the developing brain (98)) and Nurr1 (involved in the function of dopaminergic neurons (99)), were detected at moderate (donor 3) and strong levels (donors 1, 2 and 4).

Others: The transcripts investigated in this category were Bag1, nestin and also GAPDH (which served as an internal control). Bag1, which has anti-apoptotic functions in a variety of cell types and plays an essential role in the survival of differentiated neurons (100), was highly expressed in all donor samples. The intermediate filament protein nestin, was initially identified as a marker for neural stem cells (101), but has since been found to have a much broader expression in a range of cell types and tissues (102-107). Transcripts for nestin were also detected in all human donor MSC samples, however, there were clear differences in the intensity of the signal; MSC derived from donor 2 being much stronger than that from donors 1, 3 and 4.

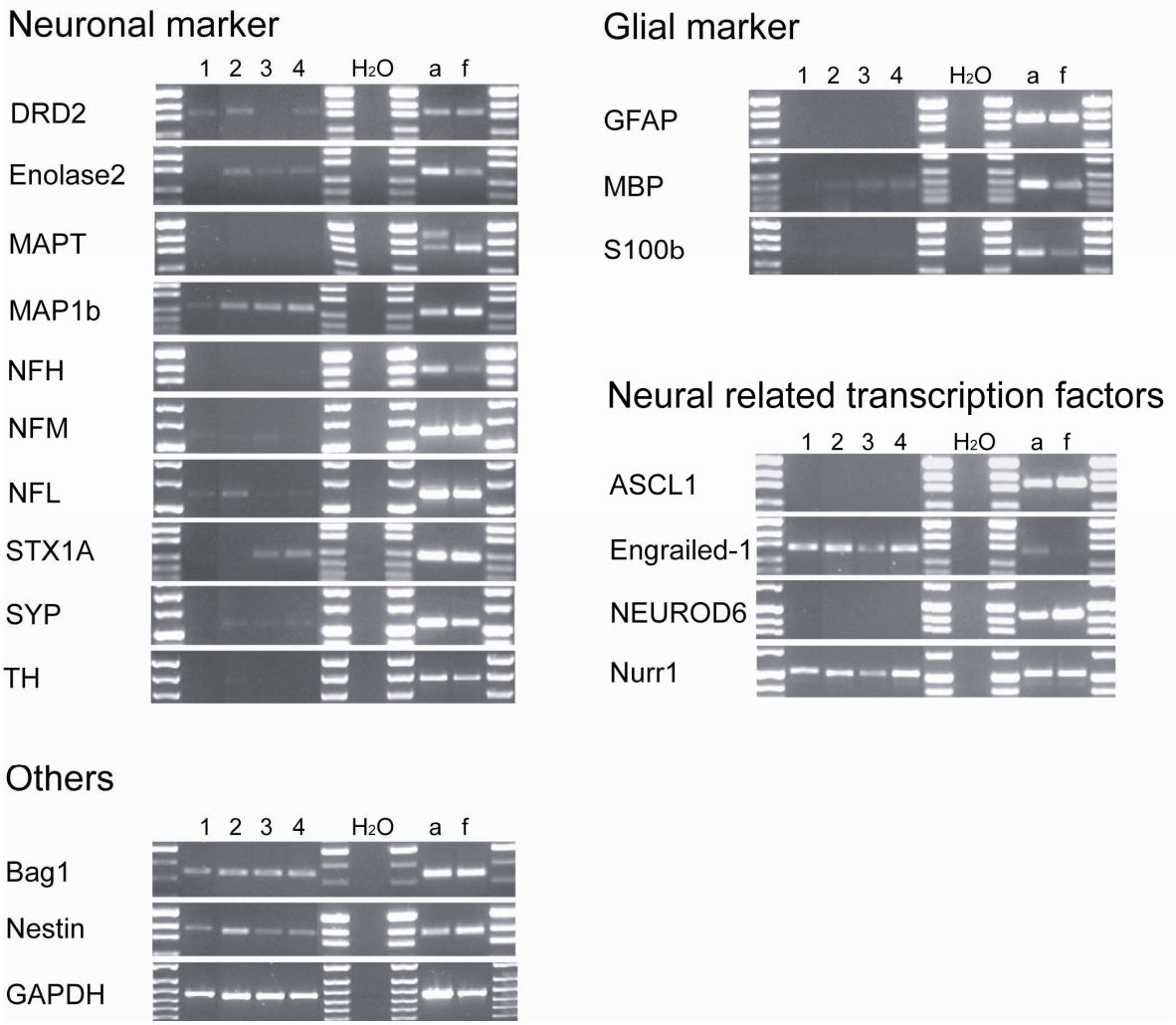

Figure 4.3: Neural marker expression of human MSCs. Neural marker transcripts of four different donors were amplified by RT-PCR. Water served as negative control and commercially obtained adult (a) or fetal (f) brain cDNA was used as positive control. GAPDH was used as standard.

The commercially available samples of total RNA that had been generated from adult and fetal human brain samples showed developmentally related changes in the intensity of expression for certain mRNAs, e.g. stronger bands for the neuronal markers Enolase2, NFH, SYP, the glial markers MBP and S100β, and the transcription factor Engrailed-1 were fall elevated in control adult samples. However, weaker bands for MAP1b, nestin and the transcription factors ASCL1 and NEUROD6 were found in adult control samples. No major differences in the intensity of bands between control adult and fetal brain samples could be found for the other transcripts (i.e. DRD2, NFM, NFL, STX1A, TH, GFAP, Nurr1 and Bag1). The differences in mRNA transcripts resemble the expected shifts in the intensity of expression during the development of the nervous system. The transcription factors of the basic helix-loop-helix family ASCL1 and NEUROD6 are expressed in neuronal progenitors (108, 109) and the cytoskeletal constituents nestin and MAP1b were expressed at higher

levels in the control fetal samples. On the contrary, Enolase2 (87), NFH (110), SYP (90), MBP (93) and S100β (111) are expressed by more mature cells, reflecting their higher level of expression in the control adult samples. Although the transcription factor Engrailed-1 plays a role in the formation of interneurons as well as in the regionalization of the developing brain (98), it is possible that the developmental stage from which the control fetal sample was obtained had already passed the time point for expression. Alternatively, expression of the transcript is only found in a fraction of cells and is diminished in total brain mRNA extraction. The faint Engrailed-1 band detected in the adult samples may have reflected its anti-apoptotic role in mature neurons (112).

Table 4.2: Summary of neural-related marker expression. PCR transcript expression was defined as strong (+++), moderate (++), weak (+) or not detectable (-).

Marker	Donor 1	Donor 2	Donor 3	Donor 4
DRD2	++	++	-	++
Enolase 2	-	++	+	+
MAPT	-	-	-	-
MAP1b	++	+++	+++	+++
NFH	-	-	-	-
NFM	-	-	-	-
NFL	+	++	-	+
STX1A	-	-	++	++
SYP	-	+	+	+
TH	-	+	-	-
GFAP	-	-	-	-
MBP	-	+	+	+
S100β	-	-	-	-
ASCL1	-	-	-	-
Engrailed-1	+++	+++	++	+++
NEUROD6	-	-	-	-
Nurr1	+++	+++	++	+++
Bag1	+++	+++	+++	+++
Nestin	++	+++	++	++
GAPDH	+++	+++	+++	+++

4.4.3 Immunocytochemical detection of neural marker proteins by undifferentiated human MSC

In addition to RT-PCR, a number of non-differentiated donor hMSC samples were chosen for immunocytochemical analysis. Staining of Enolase2 revealed a cytoplasmic distribution

(Figure 4.4A). A cytoskeletal staining was observed with antibodies against MAP1b (Figure 4.4B) and nestin (Figure 4.4D). However, staining for Nurr1 was detected at different intensities and revealed a cytoplasmic distribution (Figure 3.4C). Quantification of immunocytochemical staining from three donors (Figure 4.4E) revealed that Enolase2 expression was found in 59 ± 27.1% of all cells, Map1b expression was found in 66.7 ± 12.2% of all cells, and Nurr1 expression was found in 46.3 ± 10.8% of the cells expressed. Nestin expression was found to be present in all cells of the three donors analyzed. Thus, this data demonstrates that both protein and mRNAs of a range of neurally-related markers is already expressed by non-differentiated hMSC.

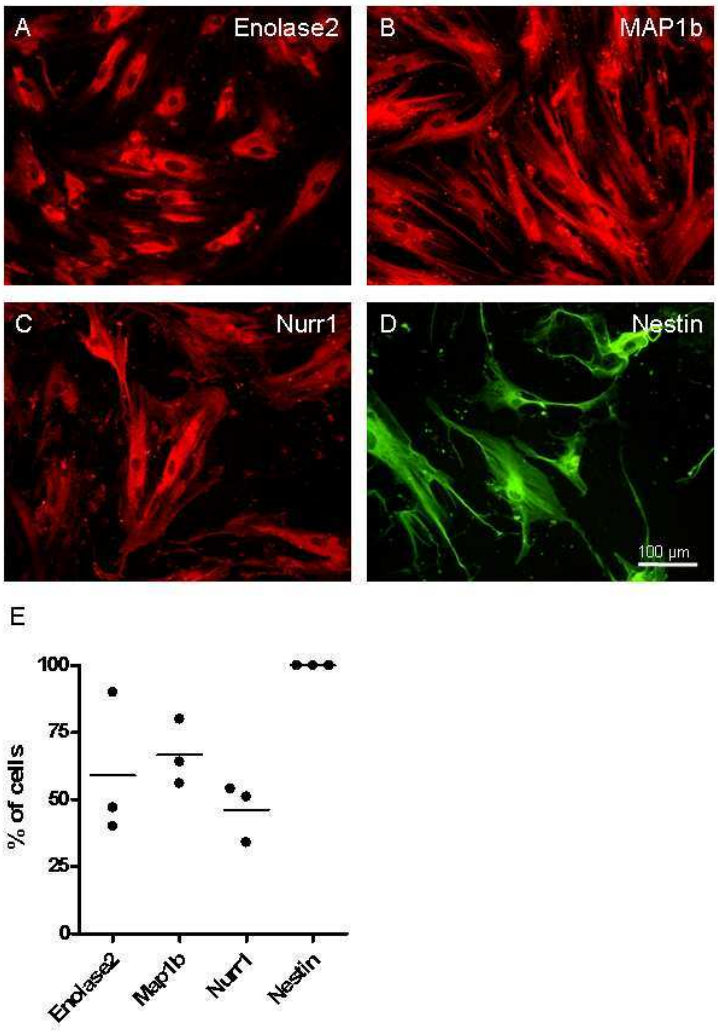

Figure 4.4: Expression of neural related proteins. Immunofluorescence for neural related proteins in undifferentiated hMSCs. (A) Enolase2, (B) MAP1b, (C) Nurr1 and (D) nestin. Staining revealed cytoplasmic distribution of Enolase2 and Nurr1, whereas the staining of MAP1b and nestin was cytoskeletal. Scale bar 100 µm. (E) Quantification of the percentage of stained cells from three different donors revealed following data: Enolase2 expression was found in 59% ± 27.1% of all cells, 66.7% ± 12.2% Map1b positive cells, and 46.3% ± 10.8% of the cells expressed Nurr1. Nestin expression was found to be present in all cells analyzed.

4.5 Discussion

The potential of adult MSC to transdifferentiate into neural cell types has aroused great interest in research. Such a capacity opens extensive possibilities for autologous therapeutic treatments in a variety of neurological disorders. However, clear and unequivocal data regarding differentiation needs to be generated to provide a solid foundation for further studies. In the present investigation, undifferentiated hMSC were found to express a number of neural-related genes (albeit at rather low levels for some mRNAs). Significantly, it became clear that there was considerable donor-related heterogeneity in the expression pattern of the hMSC populations, even though the criteria for isolation and identification (as set out by the *Mesenchymal and Tissue Stem Cell Committee of the International Society for Cellular Therapy* (34)) were followed. It is possible that such donor heterogeneity might be responsible for the variable degree of success reported by a number of research groups in their ability to transdifferentiate hMSC to a neural phenotype.

One of the first descriptions of neural differentiation by hMSC reported the detection of nestin and GFAP after differentiation, but importantly failed to report the pre-differentiated phenotype of the cells (72). This same oversight has also occurred in a most recent publication demonstrating the generation of neural cell types from human bone marrow-derived MSC (113). Neurospheres derived from human MSC were shown immunocytochemically to express nestin and Musashi-1, however, the basal expression profile of the MSC was not reported. Rapid morphological changes of rat MSC have also been reported to be associated with the detection of enolase2 and NFM (amongst other markers (37)). However, the non-treated, control cells were not analyzed and the rapid morphological changes aroused great skepticism because they did not reflect normal developmental processes (114). Such changes were later demonstrated to be due to the breakdown of the actin cytoskeleton (115).

Previous attempts to identify the basal expression pattern of undifferentiated human MSC using serial analysis of gene expression (SAGE) has revealed the presence of mRNA not only characteristic for mesenchymal cells but also endothelial, epithelial and neuronal lineages (116). Neural related mRNAs found to be amongst the 50 most abundant gene products expressed included high molecular weight neurofilament (NFH), the high affinity nerve growth factor receptor (TrkA) and glial derived nexin 1 alpha. However, in stark contrast, NFH was undetectable in all donor hMSC samples of the present investigation. This observation likely reflects the high degree of donor sample heterogeneity mentioned earlier.

Heterogeneity of gene expression by rat and human MSC has also reported following RT-PCR of cell populations and clonal cell lines, revealing mesodermal, germinal, endodermal

and ectodermal expression patterns (117, 118). Neurally related transcripts expressed by rat MSC included NMDA receptor sub-units, syntaxin, amyloid precursor protein, and both rat and human MSC were reported to express GFAP and NeuroD mRNA (117, 118). Both of these transcript were absent in all of the samples used in the present investigation. However, Syntaxin 1A was weakly expressed in 2 of the human samples but was negative in the remaining 2 donor samples, once again highlighting the substantial inter-donor variability.

In the present investigation, the expression of nestin mRNA could be found in all donor samples of undifferentiated hMSC. Nestin was originally identified as an intermediate filament protein expressed by neural stem cells (119). Recent reports using rat MSC have described undifferentiated MSC as being nestin-negative, but that expression increased progressively with increasingly higher passage numbers (76). The acquisition of nestin expression by the higher passage number MSC has been suggested to be an important stage in the ability of the cells to form spheres and subsequently undergo neural differentiation (76). It is possible that such progressive increase of nestin expression may reflect the culture conditions selecting for – and enhancing the proliferation of a sub-population of nestin-positive cells. The presence of such sub-populations of stem cells or progenitors within MSC may contribute to the high degree of heterogeneity reported by others (116-118, 120, 121). Indeed both intrinsic plasticity of MSC and contamination by stem cells from other sources (neural crest-derived stem cells) have been suggested to be contributory mechanism to the apparent switch to a neural phenotype by MSC (118, 122). Although recent publications have demonstrated the expression of a number of neural-related genes in non-differentiated population or clones of MSC, the degree of donor variability has, until now, remained unclear.

Transplantation of undifferentiated MSC into experimental models of CNS injury has clearly demonstrated improved motor and sensory function (49, 53, 57), and in a phase I clinical study, transplantation was proven to be safe (62, 123). Following engraftment, donor MSC were reported to be associated with a range of neuronal and glial markers suggesting the spontaneous differentiation of the grafted cells *in vivo* (67, 124-126). Since it was shown, that the spontaneous differentiation of grafted cells occurs only in few cells (124), other reasons for inducing a beneficial outcome should be considered. An on-going discussion revolves around the possible improvement in function being an outcome of cell fusion events between donor MSC with host cells (19, 20). However, cell fusion also occurs at only a very low frequency (19) and it has been described that neural differentiation can occur without this phenomenon (76, 80). An alternative, and possibly more likely, mechanism for improved function after implantation of MSC may be due to the local release of growth factors (55, 127). It has been shown that undifferentiated MSC express a range of growth factors

including neurotrophin-3 (NT-3), brain-derived neurotrophic factor (BDNF), glial-derived neurotrophic factor (GDNF), nerve growth factor (NGF), vascular endothelial growth factor (VEGF), hepatocyte growth factor (HGF) (128), ciliary neurotrophic factor (CNTF) and basic fibroblast growth factors (bFGF) (127, 129, 130). These factors could certainly play a role in several processes, including neurogenesis, neuroprotection, vascularisation and scar inhibition as it was already demonstrated for VEGF (131). Such donor heterogeneity was also reported by others for growth factor secretion by hMSC. Transplantation of cells was found to promote a variable, donor-dependent degree of axon growth and functional recovery (127). Furthermore, it is possible that donor MSC may also influence axonal or tissue regeneration in- and around the host lesion site by providing an array of growth-supporting extracellular matrix molecules, including fibronectin, collagens, laminin, hyaluronan and proteoglycans. These molecules are involved in migration, cell survival, cell proliferation and cell differentiation (reviewed in (132)) and a change in their local concentrations may influence endogenous neural stem cells (130).

4.6 Conclusion

The ability of MSC, in particular human MSC, to generate neural-related cell types for future transplantation-based intervention strategies has become a topic of considerable controversy. A number of possible mechanisms have been suggested to explain such cellular behaviour, including true transdifferentiation, the presence of multiply-primed stem cells capable of differentiating into a number of lineages, contamination by neural crest-derived stem cells and tissue culture artefacts. The present investigation supports the contention that MSC selected on the basis of plastic adherence, multipotency and FACS analysis are highly heterogeneous populations of cells. All donor samples investigated in the present demonstrated expression patterns that were different from each other. Such inter-donor variability regarding the expression of neural-related genes has not been previously described, but supports the heterogeneity of hMSC reported by others. It is possible that such inter-individual variability may affect the ability of donated cells to respond to particular tissue culture conditions. It should therefore be considered that not all donated MSC may be appropriate for future autograft cell transplantation strategies.

5. Expansion of human bone marrow-derived mesenchymal stromal cells: serum-reduced medium is better than conventional medium

5.1 Abstract

HMSC are of enormous interest for various clinical applications. For the expansion of isolated hMSC to relevant numbers for clinical applications, 10% FBS supplemented medium is commonly used. The main critical disadvantage of FBS is the possibility of the transmission of infectious agents as well as the possibility of immune rejection of the transplanted cells in response to the bovine serum. Therefore, we tested a commercially available medium, Panserin 401, which was specifically developed for serum-free cell cultivation. HMSC were isolated from bone marrow and expanded in either DMEM or Panserin 401 alone, or combined with FBS (2% or 10%), with or without supplementary growth factors. Cell proliferation and cytotoxicity were monitored twice a week for three weeks.

No proliferation was observed in any of the serum-free media. However, DMEM/10% FBS (the conventional culture medium for hMSC), and DMEM/2% FBS with growth factors revealed moderate proliferation. Interestingly, the best proliferation was obtained using Panserin 401 supplemented with 2% FBS and growth factors (as well as with 10% FBS). Analysis of cell growth in Panserin 401 supplemented with 2% FBS-only or with growth factors-only revealed no proliferation, demonstrating the necessity of the combination of 2% FBS and growth factors. Efficient isolation and expansion of hMSC from cancellous bone could also be performed using Panserin 401 with 2% FBS and growth factors. Furthermore, these isolated cultures maintained multipotency, as demonstrated by adipogenic and osteogenic differentiation.

5.2 Introduction

HMSC are of great interest in a variety of clinical applications. These multipotent cells are capable of differentiating into various mesenchymal cell-types, such as adipocytes, osteocytes, chondrocytes and myoblasts (3). Human MSC represent a small proportion (0.01-0.02%) of bone marrow cells (133) which can readily be isolated from the bone marrow and adipose tissue for expansion *in vitro* (28, 29). Cell-based transplantation strategies of autologous and allogenic hMSC have been assessed in clinical trials for a variety of diseases, including acute myocardial infarction (134), multiple sclerosis (135), graft-versus-host disease (136, 137), and osteogenesis imperfecta (138). For each clinical

application, adequate numbers of viable, transplantable donor cells need to be generated which retain their multipotency and are free of infectious agents. However, widely employed expansion protocols for hMSC still use animal serum in the culture medium (i.e. 10% FBS). FBS contains essential growth factors and nutrients needed for many cell cultures *in vitro,* however, the fact that it is of animal origin carries significant risks for the transmission of infectious agents and the potential for promoting or enhancing immune rejection. Therefore, the use of animal sera for cell-based therapies has come under scrutiny for the accreditation of clinical studies (139) and a number of alternative, human serum-based, media have been shown to be useful (140, 141). Since serum-free culture conditions may also be of great benefit, the growth promoting property of Panserin 401 (a commercially available medium, specifically developed for serum-free tissue cultures) on hMSC has been compared with that of the current standard medium (i.e. 10% FBS-containing medium).

5.3 Materials and methods

5.3.1 Cell culture

Cancellous bone fragments were obtained from patients during routine surgical procedures (with informed consent according to local ethical board approval of the University Hospital, Aachen) and the MSC were selected by their adherence to tissue culture plastic (34). Briefly, the bone fragments were washed with DMEM (Cambrex, East Rutherford, USA) and the collected media was centrifuged at 500 g for 5 min. The resulting cell pellet was re-suspended in 10 ml fresh DMEM supplemented with 10% fetal bovine serum (FBS; batch was selected by the capacity to support hMSC proliferation) (Biowest, Nuaille, France), transferred to a T75 flask (Greiner Bio-One, Frickenhausen, Germany) and maintained in a humidified cell culture incubator at 37°C and 5% CO_2. In some experiments the isolation, adhesion and proliferation of hMSC were conducted solely in Panserin 401 (Pan Biotech GmbH, Aidenbach, Germany) supplemented with 2% FBS and growth factors (Panserin 401/2% FBS+GF). Non-adherent cells were removed by medium exchange after one week. Subsequent medium exchange was performed every 3-4 days. When the cells reached near confluence, they were detached with trypsin/EDTA (PAA Laboratories GmbH, Pasching, Austria) and re-seeded at a density of 4000 cells/cm^2.

Multipotent differentiation capacity and surface marker profiles of the isolated hMSC were analyzed according to the guidelines set by the *Mesenchymal and Tissue Stem Cell Committee of the International Society for Cellular Therapy* (34) as demonstrated previously by our group (142). To analyse cell proliferation, hMSC from 4 human donors were seeded at 4000 cells/cm^2 in 12-well plates in DMEM/10% FBS. The following day, the cells were washed with 0.1 M phosphate-buffered saline (PBS) and grown in DMEM- or Panserin 401-

based media with or without FBS (2% or 10%) and growth factors (10 ng/ml epidermal growth factor (EGF), 1 ng/ml basic fibroblast growth factor (bFGF), 1 ng/ml platelet-derived growth factor BB (PDGF-BB) and 10 nM dexamathasone, all from Cell Concepts, Umkirch, Germany). For a detailed description of the various serum-free and serum-containing media, see Table 5.1.

Table 5.1: Media composition.

DMEM	**DMEM/2% FBS + GF**	**DMEM/10% FBS**
DMEM	DMEM 2% FBS 10 ng/ml EGF 1 ng/ml bFGF 1 ng/ml PDGF-BB 10 nM Dexamethasone	DMEM 10% FBS
Panserin 401	**Panserin 401/2% FBS + GF**	**Panserin 401/10% FBS**
Panserin 401	Panserin 401 2% FBS 10 ng/ml EGF 1 ng/ml bFGF 1 ng/ml PDGF-BB 10 nM Dexamethasone	Panserin 401 10% FBS

Panserin 401/2% FBS + GF	**Panserin 401/2% FBS**	**Panserin 401/GF**
Panserin 401 2% FBS 10 ng/ml EGF 1 ng/ml bFGF 1 ng/ml PDGF-BB 10 nM Dexamethasone	Panserin 401 2% FBS	Panserin 401 10 ng/ml EGF 1 ng/ml bFGF 1 ng/ml PDGF-BB 10 nM Dexamethasone

For adipogenic differentiation, hMSC were cultivated in DMEM containing 10% FCS, 0.5 µM dexamethasone, 0.5 µM indomethacin (Sigma, Steinheim, Germany), and 0.5 mM isobutyl-methyl-xanthine (Sigma). Medium was changed every 3 days for 3 weeks. Oil Red O staining (Sigma) was used to visualize lipid droplets formation in differentiated adipocytes. Osteogenic differentiation was induced by cultivation of hMSC in DMEM containing 10% FCS, 20 nM sodium β-glycerophosphate (Sigma), 1 nM dexamethasone, and 50 µg/ml 1-ascorbic acid 2-phosphate (Sigma). Medium was changed every 3 days for 3 weeks. Osteogenic differentiation was visualized by Alizarin-Red-S (Sigma) staining to demonstrate matrix mineralization associated with osteoblast differentiation.

5.3.2 Proliferation and cytotoxicity

Cell proliferation and cytotoxicity were measured using the CellTiter-Blue Cell Viability Assay and CytoTox-ONE Homogeneous Membrane Integrity Assay (Promega, Madison, USA) according to the manufacturer's protocol twice a week for three weeks without passaging cells. For cytotoxicity measurement, 100 µl of the supernatant were transferred into a black 96-well plate, and incubated with 100 µl CytoTox-ONE for 10 min at 37°C. To measure proliferation, CellTiter-Blue was diluted 1:5 in medium and 1 ml added to each well for 1h at 37°C and 5% CO_2. Subsequently, 200 µl of the supernatant were transferred into a black 96-well plate. For both assays fluorescence intensity was measured using the fluorometer FLUOstar OPTIMA (BMG Labtech, Jena, Germany) with an excitation at 560 nm and emission at 590 nm. After washing with PBS, 1 ml fresh medium was added to the cells and incubated until the following measurement.

5.3.3 Statistical analysis

All data are presented as the mean value ± SEM. Statistical differences were determined by one-way ANOVA followed by Bonferroni post hoc testing. A p value of less than 0.05 was considered to be significant. All the statistical analyses and the evaluation of data were performed using GraphPad Prism version 4.03 (GraphPad Software, San Diego, USA).

5.4 Results

Although the present investigation was unable to demonstrate the usefulness of Panserin 401 as a serum-free medium for the expansion of hMSC, its combination with 2% FBS and growth factors was found to be promote excellent hMSC proliferation. Cultivation of hMSC in non-supplemented DMEM resulted in the progressive detachment of the cells such that by 4 days *in vitro* (DIV), no substrate-bound cells could be detected (Figure 5.1A). The lack of cell binding to the substrate meant that cell death could not be measured in these samples (Figure 5.1B). Although hMSC grown in Panserin 401 were able to maintain adherence to the tissue culture plastic, minimal proliferation was observed up to day 4, and cell numbers actually decreased thereafter, eventually reaching a steady-state at a lower cell number (Figure 5.1A). The level of cell death under these conditions remained low throughout the whole duration of the experiment (Figure 5.1B). Cell detachment, as demonstrated in DMEM-only medium, may have been due to the lack of binding proteins (e.g. fibronectin) normally found in serum. Interestingly, serum-free Panserin 401 was capable of supporting the maintained attachment of relatively small numbers of cells, although the accompanying data sheet confirmed the absence of any cell adhesive ECM proteins. However, it was clear that Panserin 401 alone was not suitable for promoting the rapid proliferation of hMSC. The successful expansion of hMSC with Panserin 401 required the additional use of low amounts

of FBS (i.e. 2%) as well as growth factor supplements. The growth factors employed were PDGF, FGF2, EGF and the glucocorticoid dexamethasone, all of which have been shown to be potent mitogens for MSC (143-145).

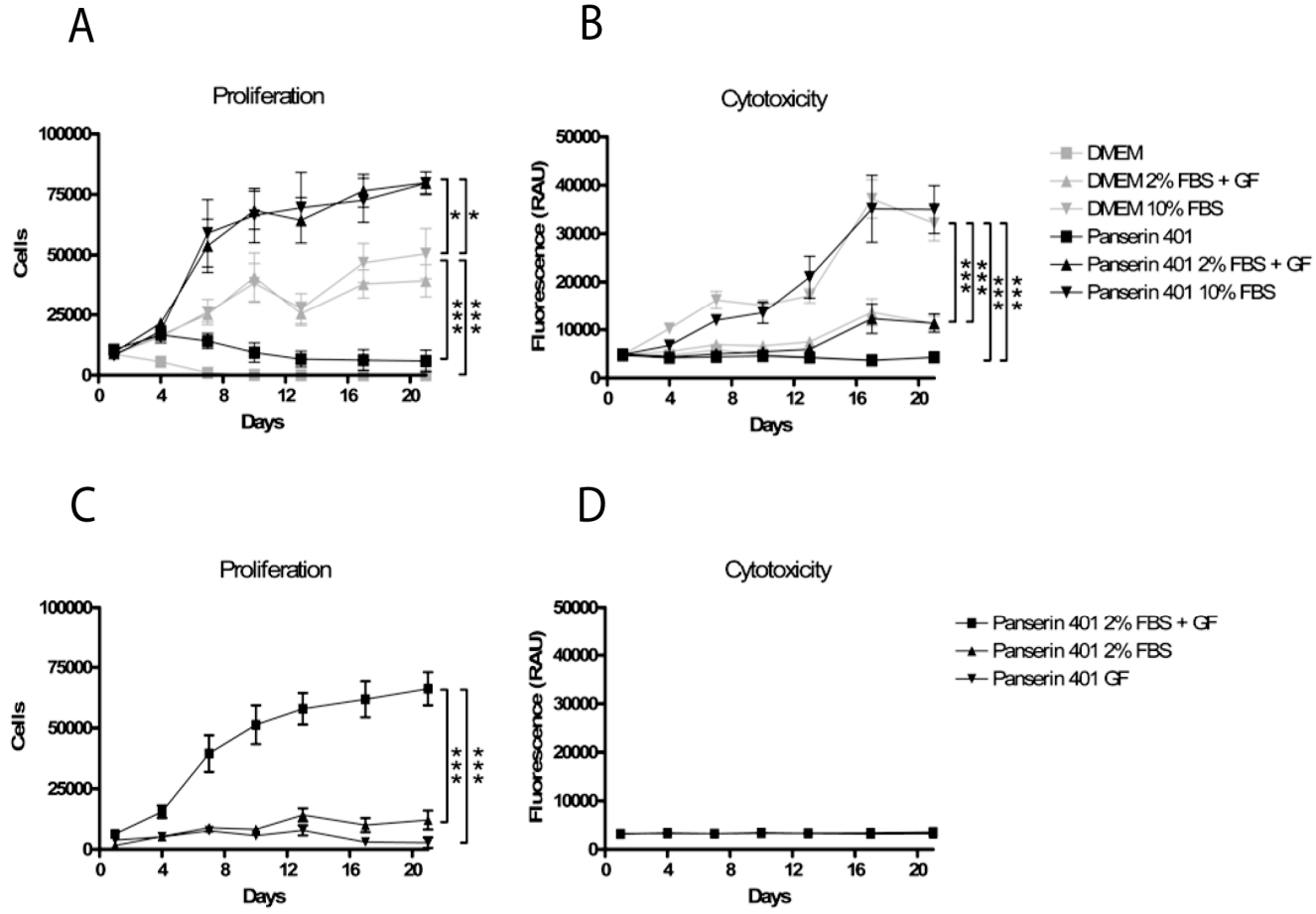

Figure 5.1: Human MSC demonstrate high proliferative capacity in Panserin 401 supplemented with 2% FBS and growth factors. Proliferation (A) and cytotoxicity (B) of four different donors were monitored over a total culture time of three weeks in DMEM, Panserin 401, DMEM supplemented with 2% FBS and growth factors (GF), Panserin 401 supplemented with 2% FBS and growth factors, DMEM with 10% FBS or Panserin 401 with 10% FBS. Furthermore, the role of the individual supplements on hMSC proliferation (C) and cytotoxicity (D) were monitored using Panserin 401 supplemented with 2% FBS-only or with GF-only. Data are expressed as mean value ± SEM and compared with the standard medium DMEM with 10% FBS. * $p<0.05$; *** $p<0.001$.

DMEM supplemented with 2% FBS and growth factors promoted a moderate increase in hMSC proliferation up to 10 DIV (reaching approximately 50 thousand cells per well), similar to that supported by DMEM/10% FBS (Figure 5.1A). Thereafter, cell numbers remained fairly constant in both media. Since elevated levels of cell death were detected between 13-21 DIV in DMEM/10% FBS, the relative stability of cell numbers at these times must have been due to the balance between cell death and cell proliferation. Similarly, a balance between relatively limited cell death and cell proliferation must have been established by hMSC in DMEM/2% FBS+GF between 13-21 DIV. In contrast, hMSC grown in Panserin

401/2% FBS+GF demonstrated the greater enhancement of cell proliferation that was evident by 7 DIV, a rate that could only be matched by incubation of cells in Panserin 401/10% FBS (Figure 5.1A). This rapid cell proliferation resulted in confluency (approximately 80 thousand cells per well) by 7 DIV with the densely packed hMSC appearing as swirls of similarly aligned, elongated cells and processes. Such densely packed swirls of confluent cells have been reported by others (28, 29). The Panserin 401/2% FBS+GF medium promoted only a minor increase of cell death that could be observed between 13-17 DIV.

To elucidate which media supplement was essential for promoting hMSC proliferation, cell growth was monitored using Panserin 401 supplemented solely with 2% FBS (Panserin 401/2% FBS) or solely with growth factors (Panserin 401/GF). HMSC cultivated in Panserin 401 with only one supplement demonstrated no cell growth, both supplements (i.e. 2% FBS and GF) were required for the optimal proliferation (Figure 5.1C). Interestingly, seeded cells adhered well to the tissue culture plastic and revealed no cytotoxicity (Figure 5.1D).

Isolation of hMSC from cancellous bone using the conventional medium DMEM/10% FBS revealed high numbers of adherent cells by one week after isolation (Figure 5.2A). However, isolation with Panserin 401/2% FBS+GF demonstrated even greater numbers of adherent cells by one week (e.g. Figure 5.2B). Low numbers of cells were isolated in Panserin 401 supplemented with 2% FBS-only (Figure 5.2C), whereas no attached cells were observed using Panserin 401 with growth factors (Figure 5.2D).

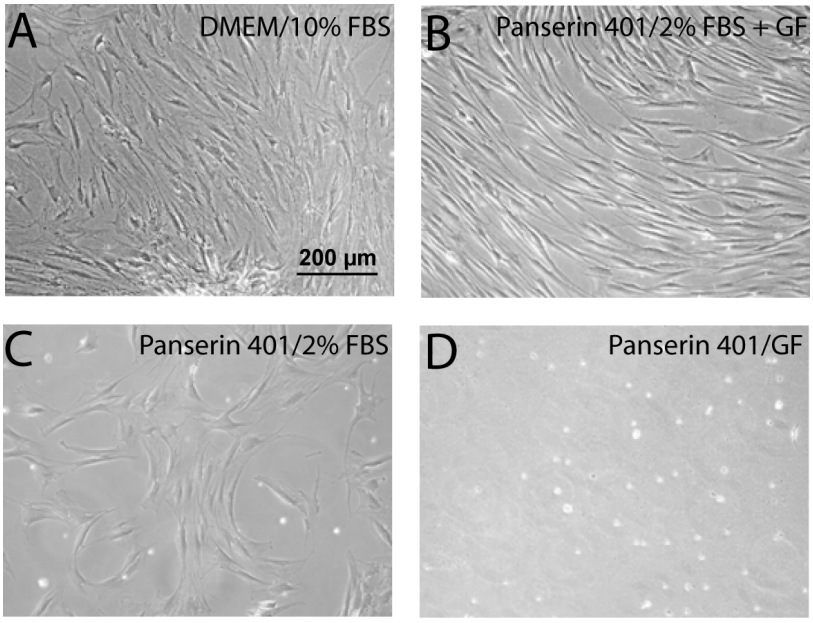

Figure 5.2: HMSC isolation applying different media. HMSC could be isolated from cancellous bone using DMEM/10% FBS (A), Panserin 401/2% FBS+GF (B), Panserin 401/2% FBS (C), but not using Panserin 401/GF (D) (1 week after isolation).

Those cells that were isolated directly with Panserin 401/2% FBS+GF could be efficiently expanded over a number of passages with no detrimental effects on multipotency as demonstrated by differentiation into adipocytes (Figure 5.3A) and osteocytes (Figure 5.3B).

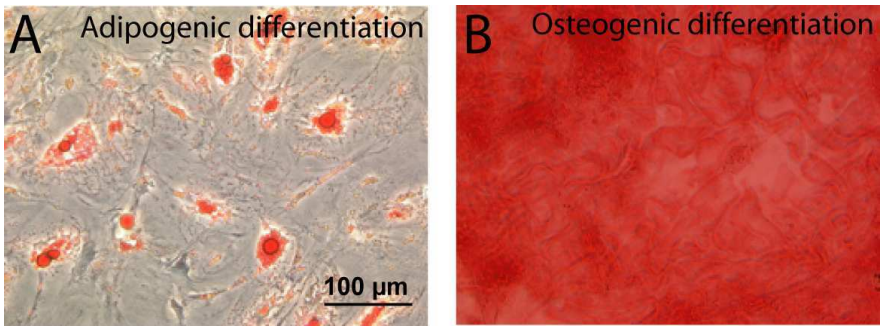

Figure 5.3: HMSC isolated and expanded in Panserin 401/2% FBS+GF maintain multipotent capacity. (A) Adipogenic differentiation resulted in the formation of lipid vacuoles which were stained with Oil Red O whereas (B) osteogenic differentiation resulted in immense mineral deposition demonstrated by Alician Red staining.

5.5 Discussion

Comparing all data generated using the different media, it could be demonstrated that the medium providing optimal cell proliferation with only moderate cell death was Panserin 401 supplemented with 2% FBS and growth factors. The employment of Panserin 401 medium for the expansion of hMSC enables the use of lower concentrations of animal serum, but this may still present a risk for infection or the development of host immune responses.

In an earlier attempt to develop serum-free culture conditions for hMSC, the group of Meuleman and colleagues described the use of UltraCulture medium supplemented with serum substitute “UltrosaG” (146). Although this medium and supplement induced a greater rate of cell expansion than that supported by α-MEM/15% FBS and maintained multipotency, it was later discovered that UltrosaG contained low amounts of animal serum (139). The present data support the notion that supplementation of serum-free media with low amounts of FBS and growth factors is capable of promoting excellent hMSC proliferation.

The present failure to demonstrate serum-free proliferation of hMSC suggests that alternative serum-free approaches using supplementation with bFGF, human albumin, hydrocortisone, selenite, insulin, transferrin and ethanolamine (141), should be considered for clinical expansion. However, although the above serum-free medium reported by Liu and colleagues promoted cell proliferation, it was unable to support the initial isolation of hMSC by adhesion (12). This suggests that undefined serum components were necessary for

colony formation. In a different approach, media supplemented with human platelet lysates (140, 141) proved to be excellent for hMSC isolation and cell proliferation. The aforementioned method still remains the most promising and safe method for large scale hMSC isolation and expansion without changing cell phenotype or loss of differentiation potential.

5.6 Conclusion

In summary, the present study demonstrated that Panserin 401, a medium specifically developed for serum-free cell cultivation, could not (acting alone) support hMSC expansion. However, supplementing Panserin 401 with 2% FBS and growth factors (PDGF, FGF2, EGF and dexamethasone) supported excellent isolation, proliferation and maintenance of multipotent differentiation capacity.

6. Growth factor and cytokine expression of human mesenchymal stromal cells is not altered in an *in vitro* model of tissue damage

6.1 Abstract

The beneficial effect of hMSC transplantation in a variety of cell-based intervention strategies is widely believed to be due to paracrine mechanisms. Here, the modification of hMSC cytokine and growth factor expression patterns have been studied following exposure to lipopolysaccharide (LPS) or to tissue homogenates (representing tissue debris) from normal and pathological tissues.

Human bone marrow-derived MSC were stimulated with LPS or exposed to homogenate from normal or pathological rat spinal cord or heart. The expression profiles of a number of cytokines and growth factors were investigated using quantitative RT-PCR with human specific primers. The effects of tissue homogenates on hMSC proliferation and migratory behaviour were also investigated.

Stimulation of hMSC with LPS resulted in an up-regulation of IL-1β, IL-6 and IL-8. However, the pattern of up-regulation varied between donor samples. Furthermore, LPS treatment resulted in a donor-dependent alteration of growth factor expression. Induction of a shift in expression pattern was not observed following exposure to homogenates from either normal or pathological tissues. Tissue homogenates did, however, stimulate cell proliferation but not migration.

HMSC expression pattern is apparently stable, even when cells are confronted by debris from different tissue types. However, treatment of hMSC with LPS is able to change the expression of cytokines and growth factors in a donor-dependent manner which may enhance their potential use in regenerative medicine.

6.2 Introduction

Cell-based intervention strategies using hMSC are of great interest to basic scientists and clinicians. Assessment of the beneficial effects after transplantation of autologous or allogenic MSC has been performed in a variety of clinical trials including spinal cord injury (61, 62), acute myocardial infarction (134), multiple sclerosis (135), graft-versus-host disease (136, 137), and osteogenesis imperfecta (138).

In the case of transplanting MSC into spinal cord lesions, motor and sensory improvement in rodent models (49, 53, 57) as well as in phase I clinical trials (62, 123) have been reported.

Migration of transplanted cells to the site of injury was associated with a significant reduction of secondary tissue degeneration (57). Injection of MSC directly into the infarcted heart has also been reported to improve the left ventricular function in rats (147, 148), dogs (149), and pigs (150, 151). Even the first clinical trial in diseased heart demonstrated an significant improvement in global and regional left ventricular function after an intra-coronary infusion of MSC (134).

The mechanism(s) responsible for such beneficial effects remain unclear. Four possible explanations have been proposed: (I) transplanted MSC differentiate into cells of the injured tissue (i.e. neurons and astrocytes in CNS, and cardiomyocytes in heart tissue) (37, 72, 79, 80, 125, 152, 153); (II) grafted cells fuse with cells of tissue origin (19, 20, 154); (III) MSC modulate the recipients' immune system (135, 155, 156); and (IV) donor cells release growth factors/cytokines which promote cell survival and proliferation of stem/progenitor cells residing in the damaged tissue as supporting the survival and regeneration of differentiated cells (127-129, 131, 157). The hypothesis that MSC differentiate into either neurons/astrocytes or cardiomyocytes has aroused great interest but such suggestions must be balanced by the observation that such transdifferentiation appears to be a rare event (124, 149). It would also seem that cell fusion is a similarly rare event (19, 154). Since it was shown that these two possible mechanisms occur at only very low frequency, it is unlikely that they make a major contribution to functional improvement. Therefore, the secretion of growth factors/cytokines by MSC is widely believed to promote the beneficial effects.

MSC are capable of expressing and releasing a variety of growth factors including VEGF, BDNF, NGF, bFGF and HGF (54). Neurotrophins such as BDNF and NGF increase the survival of injured CNS tissue *in vitro* and *in vivo* (158, 159). Similarly, a recent study has demonstrated cardioprotection by human MSC-derived conditioned medium in a porcine model myocardial infarction (160).

The expression of different toll-like receptors (TLRs) on hMSC has also been demonstrated (161). These receptors are normally found on immune cells and are activated by molecular components found on microbes. However, endogenous non-pathogenic molecules (e.g. extracellular matrix, heat shock proteins or proteolytic cleavage products) have been demonstrated to activate TLR2 and TLR4 (162-165). The release of molecules and debris into the extracellular space is greatly increased in pathological tissues and might thus, be expected to trigger a shift in the pattern of hMSC growth factor or cytokine expression. The present investigation was undertaken to assess the hypothesis that such changes in growth factor/cytokine expression might be altered in response to exposure to debris in a tissue-specific manner.

6.3 Material and methods

6.3.1 Cell culture

Cancellous bone fragments were obtained during operation procedures from fully anonymous patients (with informed consent according to local ethical board approval of the University Hospital, Aachen) and selected by their plastic adherence as demonstrated previously (see chapter 5.3.1) (166). Briefly, bone fragments were washed with Panserin 401 media (Pan Biotech GmbH, Aidenbach, Germany) and the collected media was centrifuged with 500 g for 5 min. The cell pellet was resuspended in 10 ml fresh Panserin 401 media supplemented with 2% fetal bovine serum (FBS) (Biowest, Nuaille, France) and growth factors (10 ng/ml epidermal growth factor (EGF), 1 ng/ml basic fibroblast growth factor (bFGF), 1 ng/ml platelet-derived growth factor BB (PDGF-BB) and 10 nM Dexamathasone (all Cell Concepts, Umkirch, Germany), transferred to a T75 flask (Greiner Bio-One, Frickenhausen, Germany) and maintained in a humidified cell culture incubator at 37°C and 5% CO_2. Non-adherent cells were removed by media exchange after one week. Medium exchange was performed every 3-4 days. When the cells reached nearly confluence, the cells were detached with trypsin/EDTA (PAA Laboratories GmbH, Pasching, Austria) and re-seeded with a density of 4000 cells/cm^2. For the following experiments cells in passage 5 were used.

Multipotent differentiation capacity and surface marker profile of the isolated hMSC were analyzed according to the guidelines set by the *Mesenchymal and Tissue Stem Cell Committee of the International Society for Cellular Therapy* (34) as demonstrated previously (see chapter 5.3.2) (142, 166).

6.3.2 TLR stimulation

TLR stimulation was performed by exposure of hMSC to 10 ng/ml lipopolysaccharide (LPS; Sigma, Steinheim, Germany) in normal culture medium for 4 hours (161).

6.3.3 Immunocytochemistry

Fluorescence immunocytochemistry was performed on hMSC seeded in 12-well plates at a density of 4000 cells/cm^2. After removal of the media and washing in PBS, cells were fixed with 4% paraformaldehyde in PBS for 30 min. Afterwards, the samples were washed three times with PBS and non-specific binding sites blocked by a 1 hour incubation in PBS containing 3% normal goat serum (Sigma), 1% bovine serum albumin (BSA, fraction 5, Serva, Heidelberg, Germany) and 1% Triton X-100 (Sigma). The primary antibody, anti-TLR4 (1:100, monoclonal, ab30667, Abcam, Cambridge, USA) was diluted in PBS containing 1% BSA and incubated at room temperature overnight. The secondary antibody goat-anti-mouse Alexa 594 (1:500, Invitrogen) was also diluted in PBS containing 1% BSA and incubated for 2.5 hours at

room temperature. Finally, nuclei were stained with diamidinophenylindole (DAPI, 1:1000, Roche), cover-slipped with Fluoroprep (bioMerieux, Marcy l'Etoile, France) and observed using a Leica DM RX microscope (Leica, Wetzlar, Germany) with 20x objective. Omission of primary antibodies served as negative control and resulted in no detectable staining.

6.3.4 Surgical procedure and tissue extraction

All surgical procedures were performed with female Lewis rats (body weight approximately 250 g) according to the guidelines of the regional ethical committee for North Rhine-Westfalia (AZ 50.203.2-Ac 23, 11/06 and 59.203.2-K 47, 43/03). Animals were housed under a 12:12 h dark light regime and allowed free access to water and standard laboratory chow.

Spinal cord injury: Animals (n = 3) were anesthetized by inhalation of a mixture of isoflurane and air (induction: 4% isoflurane, maintenance: 1.8% isofluorane). The dorso-lateral surfaces of the spinal cord were exposed by laminectomy at level Th13 and a lateral funiculotomy of the left side of the cord was performed. Haemostasis was established and the muscle and skin closed in layers.

Myocardial infarction: Induction of myocardial infarction was performed as described previously (167-169). Animals (n = 3) were anesthetized with an intraperitoneal injection of ketamine (50 mg/kg) and xylazine (10 mg/kg), intubated, and ventilated with room air. The chest was opened through the fourth intercostal space to expose the basal region of the heart. The left coronary artery was occluded by taking a stitch through the myocardium with a C-1 taper needle, attached to 5-0 polypropylene suture, from the atrioventricular groove to the region of the pulmonary cone to encircle the artery and then tying a double knot in the suture.

Harvesting of lesioned tissues: At 7 days post injury, animals were given terminal anaesthesia, the lesioned spinal cord or heart tissues were excised, frozen in liquid nitrogen and stored at -80°C. For homogenization, 1 ml of Panserin 401 was added and tissue was homogenized in a Retsch MM300 Shaker (Retsch GmbH, Haan, Germany) three times for 2 min at 25 Hz. In an attempt to standardise the content of the different samples, the amount of protein per sample was measured using a BCA protein assay kit (Pierce, Rockford, USA) following the manufacturers instructions. The homogenates were stored at –80°C prior to use. Homogenates from three individual animals were mixed such that each culture was treated in a similar manner. For *in vitro* experiments of the effect of the homogenates on hMSC expression patterns, a final homogenate-derived protein concentration of 0.1 mg/ml in normal culture medium was used.

6.3.5 Proliferation assay

Human MSC were plated in 12-well plates at a density of 4000 cells/cm^2 in either control medium or medium supplemented with 0.1 mg/ml tissue extract. After 1 and 4 days in culture, cell proliferation was measured using CellTiter-Blue (Promega, Madison, USA) according to the manufacturer's protocol.

6.3.6 Cell migration assay

For analysis of migration, a scratch assay was performed. A scratch with a 1 ml pipette tip was made through the diameter of confluent hMSC cultures in 12-well plates. To remove any non-adherent cells, the cultures were washed twice with 0.1 M phosphate buffered saline (PBS) and photographed (0 h) using an inverse phase contrast light microscope (DM IL Invers, Leica, Wetzlar, Germany) and Diskus software (Diskus, Königswinter, Germany). Afterwards, 1 ml of normal culture media (control), 100 ng/ml SDF1α (as positive control; Peprotech, Hamburg, Germany) (170), or homogenate was added to the cells and incubated at 37°C and 5% CO_2. After cultivation for 16 h and 24 h, samples were again photographed. For evaluation, the pixels of cell-free area were measured using ImageJ software (http://rsbweb.nih.gov/ij/). The area from 0 h was set as 100%.

6.3.7 RNA isolation and gene expression analysis

RNA was isolated using the RNeasy Micro Kit (Qiagen, Hilden, Germany) according to the manufacturer's protocol. The RNA concentration of each sample was measured using a Nanodrop photometer (Nanodrop Technologies, Montchanin, USA). Reverse transcription was performed using the Taqman RT Kit (Applied Biosystems, Carlsbad, USA).

Real-time PCR was carried out with an ABI Prism 7700 Sequence Detector using Taqman Universal PCR Master Mix (no UNG, Applied Biosystems) with the following pre-designed human-specific primer/probe sets (TaqMan® Gene Expression Assays, inventoried, Applied Biosystems): BDNF (Hs00380947), bFGF (Hs00266645_m1), EGF (Hs00153181M1), GAPDH (Hs99999905_m1), HGF (Hs00300159_m1), interleukin (IL) 1β (Hs00174097_m1), IL-6 (Hs00174131_m1), IL-8 (Hs00174103), NGF (Hs00171458_m1), neurotrophin (NT) 3 (Hs00267375_s1), NT4 (Hs01921834_s1), stromal-derived factor 1α (SDF1α) (Hs00171022_m1) and VEGFα (Hs00904634_m1). For each amplification, the template was equivalent to 10 ng of total RNA. Measurements were performed in duplicate; a no-template blank served as negative control. All assays were performed using the manufacturer recommended universal cycling parameters (40 cycles of 94ºC for 20 s and 62ºC for 1 min). Amplification curves and gene expression were normalized to the house-keeping gene glyceraldehyde-3-phosphate dehydrogenase (GAPDH). Gene expression was calculated using the ddCT method.

6.3.8 Statistical analysis

Data are shown as average ± SD. Multiple group comparison was performed by one-way analysis of variance (ANOVA) followed by the Tukey *post-hoc* test (Prism4, GraphPad Software, Inc., San Diego, USA). Values of $p<0.05$ were considered as statistically significant.

6.4 Results

6.4.1 Characterization of hMSC

Characterization of isolated hMSC was performed according to the *Mesenchymal and Tissue Stem Cell Committee of the International Society of Cellular Therapy* (34). As demonstrated previously in chapter 5, hMSC expressed CD73, CD90 and CD105, but were negative for CD11b, CD19, CD34, CD45 and HLA-DR. Multipotency was confirmed by differentiation into adipocytes, osteocytes and chondrocytes.

Since the potential beneficial effects of hMSC transplantation (either spinal cord injury or the infracted heart) is thought to be due to the release of growth factors and cytokines, the basal expression of these factors by all three donors was investigated using quantitative RT-PCR (Figure 6.1). Donor heterogeneity could be observed in the basal expression of BDNF, HGF, NGF, SDF1α, IL-1β and IL-6, whereas the expression of bFGF, EGF, NT3, NT4, VEGFα and IL-8 was quite homogeneous.

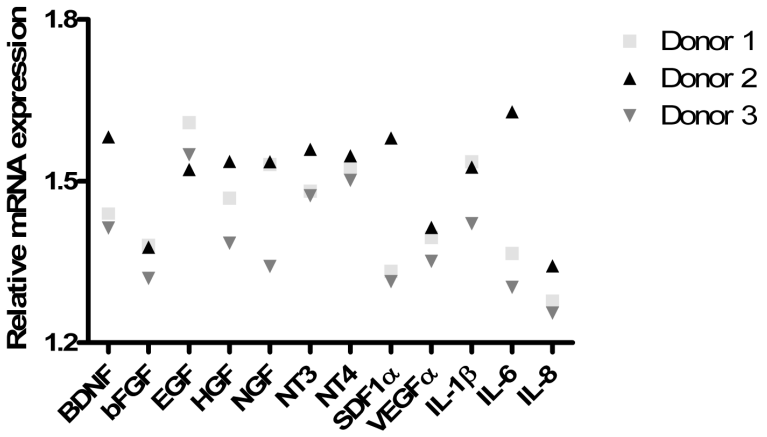

Figure 6.1: Basal expression of growth factors and cytokines is donor dependent. Quantitative RT-PCR was performed on three independent hMSC samples. Donor dependent-heterogeneity was detected in the basal expression of BDNF, HGF, NGF, SDF1α, IL-1β and IL-6, whereas the expression of bFGF, EGF, NT3, NT4, VEGFα and IL-8 appeared to be similar between donor samples.

6.4.2 LPS treatment of hMSC leads to an altered expression of cytokines and growth factors

TLR4 expression by hMSC was confirmed by immunofluorescence (Figure 6.2A). Stimulation of TLR4 by exposure to LPS resulted in the up-regulation of cytokines IL-1β (133.74 ± 155.30-fold) , IL-6 (24.11 ± 32.63-fold) and IL-8 (94.38 ± 60.21-fold) by hMSC obtained from three donors (Figure 6.2B) (161). However, the pattern of increased expression demonstrated apparent donor-dependent variability. Furthermore, LPS treatment revealed an altered growth factor expression as demonstrated by quantitative RT-PCR (Figure 6.2C). A down-regulation by cells from all three donors could be detected for the growth factors BDNF (0.09 ± 0.05-fold), EGF (0.04 ± 0.02-fold), NT3 (0.07 ± 0.02-fold), NT4 (0.07 ± 0.02-fold) and VEGFα (0.26 ± 0.26-fold), whereas an up-regulation could be detected for bFGF (10.69 ± 16.05-fold). Interestingly, LPS stimulation resulted in an up-regulation in HGF (5.02 ± 7.49), NGF (3.26 ± 2.41-fold) and SDF1α (9.93 ± 12.06-fold) expression by two of the investigated donors, whereas down-regulation of these factors could be observed for the third donor.

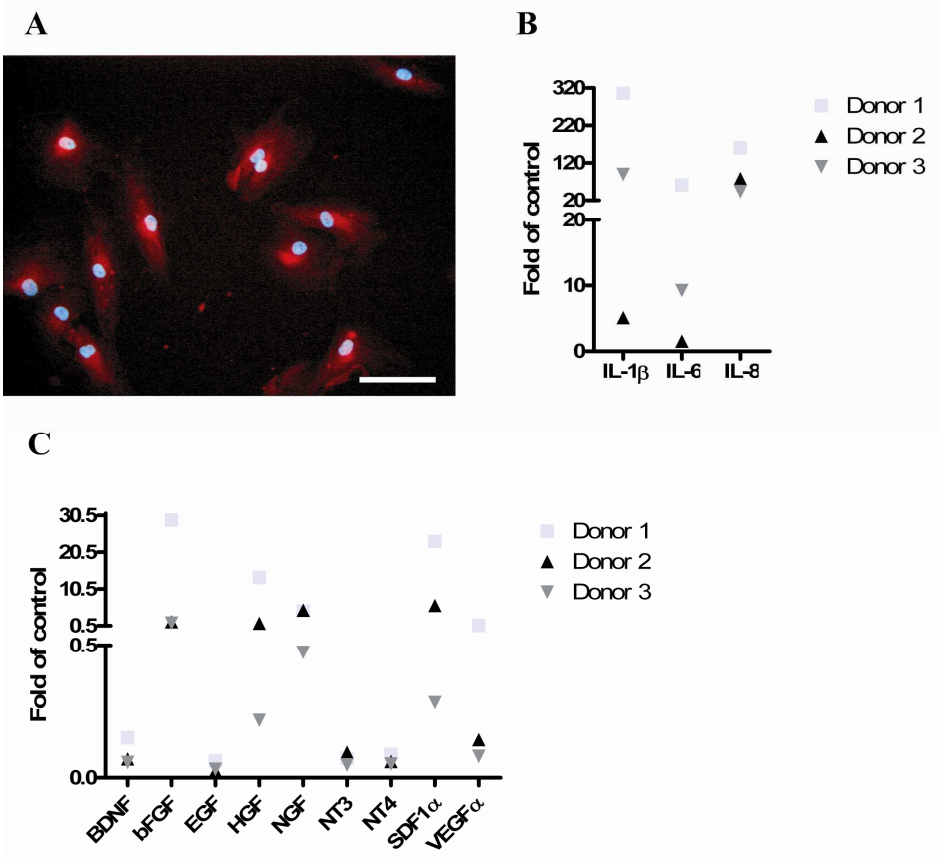

Figure 6.2: LPS treatment of hMSC leads to an altered cytokine and growth factor expression. TLR4 expression by hMSC was demonstrated by immunofluorescence (scale bar 100 µm) (A). Quantitative RT-PCR revealed an enhanced expression of the cytokines IL-1β, IL-6 and IL-8 after LPS stimulation compared to control cultures (B). Altered growth factor expression after LPS treatment was demonstrated by quantitative RT-PCR. BDNF, EGF, NT3, NT4 and VEGFα were down-regulated, whereas bFGF, HGF, NGF and SDF1α were up-regulated (C).

6.4.3 hMSC exposure to tissue homogenates does not alter cytokine or growth factor expression patterns

To investigate if a shift in cytokine and growth factors expression patterns could also be induced by exposure to endogenous molecules liberated within debris, tissue homogenate from either normal or pathological rat spinal cord or heart was supplemented to the hMSC cultures. Quantitative RT-PCR using human-specific primers revealed no induction of the cytokine expression of IL-1β, IL-6 or IL-8, in contrast that the pattern of expression induced by exposure to LPS (Figure 6.3).

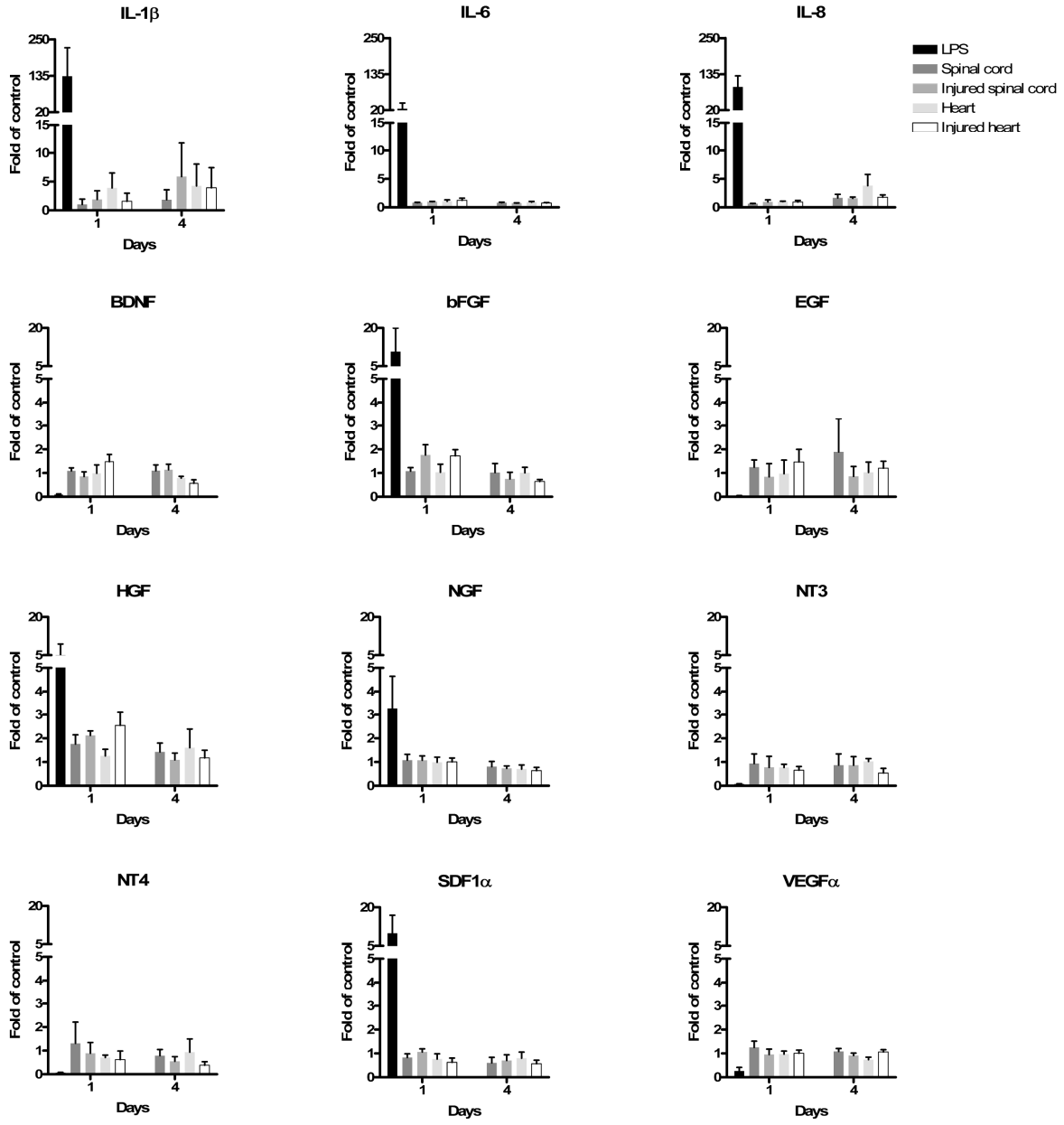

Figure 6.3: Co-cultivation with tissue homogenate from normal or pathological tissue does not affect cytokine and growth factor expression. In contrary to LPS treated cultures, no induction in cytokine expression could be detected after treatment with tissue homogenate from either normal or pathological tissue. Furthermore, no altered growth factor expression was observed after co-cultivation. (n=3; *p<0.05).

Furthermore, the induction or reducing of the growth factor expression could not be detected after exposure to tissue homogenate from either normal or lesioned samples.

6.4.4 Stimulation with tissue homogenate triggers hMSC proliferation but not migration

To investigate whether the supplementation of tissue homogenate from either normal or pathological tissue has an effect on hMSC cultures, proliferative and migratory activity was investigated. As early as 1 day after exposure to tissue homogenate, an increase in cell numbers could be detected compared to control cultures (Figure 6.4A). After 4 days of exposure, the cell numbers of treated cultures were significantly increased. The effect of tissue homogenate on the migratory capacity was examined by scratch assays and revealed no effect on migratory behavior (Figure 6.4B). The migration of hMSC showed a trend for enhancement in response to SDF1α but this effect did not reach the level of statistical significance when compared to the control cells.

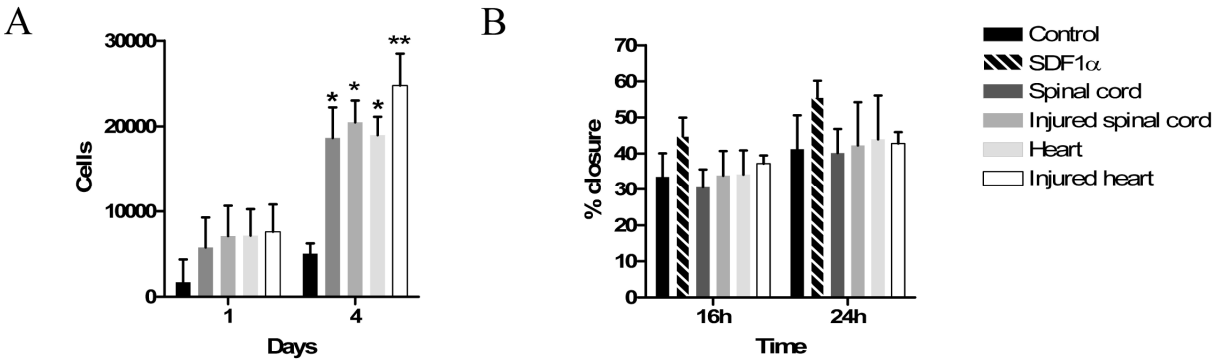

Figure 6.4: Stimulation of hMSC with tissue homogenate induces proliferation but not migration. Induced cultures demonstrated significantly enhanced proliferation after 4 days of treatment (A). No effect after 16h or 24h of stimulation could be observed in migratory activity as shown by scratch assays (B). (n=3; *p<0.05; **p<0.01).

6.5 Discussion

The present *in vitro* study was undertaken in an attempt to evaluate the possible mechanism(s) of action by which implanted hMSC exert the beneficial effects that have been reported in models of tissue pathology as well as in clinical trials. We tested the hypotheses that exposure of hMSC to homogenates (intended to represent tissue debris) from various tissues would cause a shift in cytokine and growth factor expression patterns, and that the expected shifts would be dependent on the type of tissue used to generate the homogenate. Although a shift of cytokine and growth factor expression could be clearly demonstrated after

exposure to LPS, no significant shift of expression patterns could be observed after exposure of cells to tissue homogenate (from any investigated source).

The basal expression of the investigated molecules was donor dependent, supporting other reports (127, 161). Activation of TLR4 by LPS treatment led to an increase in the expression of the cytokines IL-1β, IL-6 and IL-8, by all donor samples, confirming the results of others (161). However, the present study demonstrated variability of the intensity of cytokine expression by the three different donors. An LPS-mediated shift of expression of growth factors bFGF, HGF and VEGFα has been previously reported (171, 172). However, these studies reported an increase in the expression of the above growth factors by all donors. The present investigation confirms the increased expression of bFGF (detected in all three donors), however, decreased VEGFα expression was demonstrated by all hMSC samples. Furthermore, LPS treatment in the current investigation led to an increase of HGF expression by two donors, whereas reduced expression was observed in the third donor sample. Such an apparent variability of donor cell responses to a single stimulus is a novel observation, as is the LPS-induced alterations of BDNF, EGF, NGF, NT3, NT4 and SDF1α expression.

As mentioned above, the only growth factor that was up-regulated by all three donors after LPS treatment was bFGF. It has been reported that bFGF is involved in tissue remodelling and regeneration, has neurotrophic activity and seems to be a survival factor that blocks the apoptosis of neural cells (reviewed in (173)). Furthermore, bFGF is involved in cardiac protection (174) and initiates neovascularisation (neo-angiogenesis) in hypoxic or ischemic tissues (175).

Interestingly, differences regarding the response to LPS stimulation could be observed for the growth factors HGF, NGF and SDF1α. The expression of these factors was increased in two donor samples, but was decreased in the third sample. HGF facilitates the growth, motility, and morphogenesis of various types of cells, i.e. vascular endothelial cells (176), neural cells (177, 178), hepatocytes (179) or hematopoietic cells (180). Moreover, HGF promotes repair, protection, and functional improvement of injured spinal cord (177) or heart (181). NGF is involved in the survival of CNS (reviewed in (182)) as well as cardiac tissue (183, 184) *in vitro* and *in vivo*. SDF1α acts as a potent cell attractant for lymphocytes (185) and has been reported to promote the survival of cardiomyocytes after myocardial infarction (186). Moreover, application of SDF1α leads to an outgrowth of postnatal dorsal root ganglions on inhibitory central myelin (187). Although it is well known, that the basal expression of different factors is donor dependent, an altered reaction to the same stimulus has not previously been reported. These observations confirm and extend the information regarding the apparent heterogeneity between MSC samples obtained from different donors (127, 142). Such

heterogeneity may have considerable consequences for the ability of certain populations of donor cells to deliver the anticipated beneficial effects.

LPS treatment further led to a down-regulation of the growth factors BDNF, EGF, NT-3, NT-4, and VEGFα. BDNF facilitates almost all aspects of nervous system development and regeneration such as neuronal proliferation, neuronal migration, axon pathfinding, dendritic growth, and neuronal survival (188-190). Furthermore, BDNF is involved in vascularisation of the developing heart as well as promotes blood flow recovery and capillary density after cardiac injury (191, 192). EGF is involved in cell proliferation, differentiation, motility and blood vessel recruitment (reviewed in (193)). NT3 and NT4 belong to the family of neurotrophins which promote the survival and differentiation of existing and developing neurons (194). Application of NT3 after spinal cord injury supported re-growth of axons across the dorsal root entry zone and established functional connections with cells of the dorsal horn (195). NT3 has further been reported to be involved in the development of the heart (196) as well as impairs resting heart rates (197). VEGFα is involved in angiogenesis, functions as a chemoattractant for macrophages (198) and attenuates left ventricle fibrosis and cardiac dysfunction in ischemic heart (199) presumably by activating resting cardiac stem cells (200). Moreover, VEGFα has been reported to promote neural repair by gliogenesis, angiogenesis, and tissue sparing after contusion of rat the spinal cord (201, 202). Recently, Yao and colleagues (203) described, for the first time, the application of LPS-stimulated MSC in a disease model. Transplantation of LPS-stimulated MSC into the infarcted rat myocardium ameliorated cardiac function and reduced fibrosis to a more significant extent than non-treated MSC. Furthermore, such pre-conditioned MSC demonstrated greater engraftment and ensuing vascularisation. Since an increase of VEGF expression by LPS-stimulated MSC could be detected, the group assumed VEGF to be the factor responsible for the improvement. However, the current results indicate that LPS changes the expression of a number of factors, some of these changes being in a donor-dependent manner.

Despite the apparent sensitivity (and variability) of donor hMSC responses to exposure to LPS, there were, surprisingly, no detectable changes in either cytokine or growth factor expression following exposure to tissue homogenate from either normal or pathological tissues. It could be argued that the choice of the concentration and storage of homogenate that was added to the culture medium (i.e. 0.1 mg/ml) was insufficient to be able to provoke a physiological response, but the observation of enhanced proliferation in all donor samples would argue against this possibility. Since the local ethics committee policy dictated that the age of donors as well as the anatomical origin of bone fragments used for hMSC isolation be kept fully anonymous, it cannot be excluded that the observed variability of expression patterns may have been due to differences in donor age or sample site. Furthermore,

although the novel (Panserin-based) medium with supplements was used to induce a more robust proliferation of donor hMSC, it cannot be excluded that that this choice of medium may have altered the sensitivity of the samples to the tissue homogenates as well as their ability to demonstrate changes of growth factor and cytokine expression (166).

The composition of the Panserin-based medium used for hMSC isolation and expansion might also have influenced the results obtained from the migration assay. No differences in the migratory capacity of tissue homogenate stimulated cells could be observed when compared to the non-stimulated control cells. Indeed, the inclusion of a positive control for hMSC migration, SDF1α, induced a trend for increased migration when compared with the unstimulated control cells, but this did not reach statistical significance. Since the culture medium used was supplemented with bFGF, EGF, and PDGF-BB, all of which are known to enhance hMSC migration (204, 205), the further addition of SDF1α might have had little effect on an already stimulated population of cells.

The present observations are in contrast to those of Chen and colleagues who reported an increase in growth factor (BDNF, NGF, VEGF and HGF) production of hMSC that had been exposed to conditioned medium derived from traumatic brain injury tissues (54). Although Chen and colleagues used ELISA for the demonstration of elevated levels of growth factors, there was no data presented about possible changes in the proliferation of the hMSC. Since the present study demonstrated homogenate-induced stimulation of cell proliferation, it is feasible that the increased levels of growth factors reported by Chen and colleagues may have been due to conditioned medium effects on cell numbers. Another possible reason for the apparent differences of hMSC to molecules/debris released by damaged brain and spinal cord may be related to the fact that these different regions of CNS undergo different responses to particular insults. For example, the exposure of brain and spinal cord to particular pro-inflammatory cytokines (e.g. recombinant TNFα or IL-1β) resulted in strikingly different tissue responses: blood brain barrier breakdown being more prominent in spinal cord than in brain tissue (206, 207).

6.6 Conclusion

These observations lead to the conclusion, that the pattern of cytokine and growth factor expression by hMSC is not altered when exposed to debris or molecules from normal or pathological spinal cord or heart tissue. The improvement in the regeneration of spinal cord injuries or myocardial infarctions after hMSC transplantation seems to be due to the donor-dependent cytokine and growth factor expression pattern which, according to the present data, would not change when the cells encounter such tissues. However, pre-stimulation of cells with LPS results in a shifted pattern of cytokine and growth factor which may enhance

their potential use in regenerative medicine. Nonetheless, care must be exercised in the choice of candidate donor cells for pre-stimulation because considerable donor variability appears to remain a confounding issue.

7. Mesenchymal stromal cells immobilized in an oriented 3D scaffold transiently accelerate functional recovery after acute spinal cord injury

7.1 Abstract

HMSC have important features that make them of high interest in the repair of the injured spinal cord: (1) hMSC express and release a variety of growth factors important for supporting axonal outgrowth, (2) the morphology of the hMSC extracellular matrix they produce is capable of influencing the direction of axonal outgrowth. In an attempt to combine both important features, hMSC were seeded into 3D, type-I collagen scaffolds (that were engineered to present a highly oriented porous microstructure) and implanted into acute lateral resection injuries of the rat thoracic spinal cord to investigate aspects of graft-host integration and tissue repair. For this purpose, green fluorescent protein (GFP)-transduced hMSC were seeded onto the collagen scaffolds, and human fibroblast (hFbl)-seeded scaffolds and empty scaffolds served as controls. Motor and sensory function were investigated weekly for up to 8 weeks. Immunohistochemistry was then performed to evaluate axonal regeneration as well the astrocytic and inflammatory responses.

Already 1 week after implantation, animals which received hMSC-seeded scaffolds demonstrated better functional improvement than the control animals, which was even significant after four weeks. This difference, however, was no longer significant at 8 weeks. Although only small numbers of hMSC could be identified within the scaffold at 8 weeks, transplantation of hMSC-seeded scaffolds had resulted in the regeneration of increased numbers of axons into the implant as well as decreased astroglial and inflammatory responses. The hMSC detected at 8 weeks were found to be chondroitin sulphate proteoglycan (CSPG)-positive and were located in a scaffold that contained elevated levels of CSPG. The combination of an oriented type-I collagen scaffold and hMSC thus resulted in the transient acceleration of functional recovery in the present model of acute spinal cord injury. This effect might be associated with their expression of CSPGs as well as the reported growth factor and cytokine release.

7.2 Introduction

Several different cell types are currently under investigation as therapeutic cell-based intervention strategies for spinal cord injury (SCI). Such cell types include Schwann cells (44, 208), olfactory ensheathing cells (45), neural stem/progenitor cells from embryonic (46), foetal (47) or adult sources (209). Other encouraging cell-types include the MSC which can be

readily isolated from tissues such as bone marrow, expanded *in vitro* (28) and reintroduced into the patient as an autograft (62, 123).

Transplantation of MSC in spinal cord lesions has been reported to result in motor and sensory improvements in rodent models of injury (49, 53, 57) as well as in phase I clinical trials (62, 123). Migration of transplanted cells to the site of injury was associated with a significant reduction of secondary tissue degeneration (57). Furthermore, donor MSC were observed to form longitudinally orientated guidance structures which supported axonal growth *in vitro* (210) as well as *in vivo* (49). The beneficial effects of MSC engraftment in SCI are likely to be due to the release of growth factors/cytokines which may promote cell survival and proliferation of host stem/progenitor cells residing in or near the damaged tissue, as well as supporting the survival and axonal regeneration of differentiated neurons (127, 129, 210, 211). Human MSC express a variety of cytokines such as IL-1β, IL-6 and IL-8 as well as growth factors including several neurotrophic factors such as BDNF, NGF, NT-3 and NT-4 (210, 211). Apart from the release of growth factors, the orientation of hMSC (and their extracellular matrix) is essential for the control of the direction of axon regeneration (210). It would be therapeutically advantageous to be able to control the orientation of donor hMSC and their ECM in relatively large lesions. Therefore, in the present thesis, hMSC were seeded into type-I collagen scaffolds that presented an oriented microstructure (212) and were implanted into an rat model of acute spinal cord injury to investigate issues of graft-host integration the regeneration of damaged axons.

7.3 Materials and methods

7.3.1 Cell culture

HMSC: The GFP-expressing hMSC were provided by Drs Seguera and Mallet (University of Paris, France) as part of the EU funded collaboration on stem-cell based intervention strategies for SCI (acronym: RESCUE). HMSC were cultivated in Panserin 401 medium supplemented with 2% fetal bovine serum (FBS) (Biowest, Nuaille, France) and growth factors (10 ng/ml epidermal growth factor (EGF), 1 ng/ml basic fibroblast growth factor (bFGF), 1 ng/ml platelet-derived growth factor BB (PDGF-BB) and 10 nM Dexamathasone (all Cell Concepts, Umkirch, Germany)), transferred to a T75 flask (Greiner Bio-One, Frickenhausen, Germany) and maintained in a humidified cell culture incubator at 37°C and 5% CO_2 (166)

Adipogenic- and osteogenic differentiation capacity of the GFP-transduced hMSC were determined as described earlier in chapter 5.3.1 (142, 166).

HFbl: A human foreskin fibroblast cell line (SM3) was used as a control cell-type. The cells were generated and provided by Drs. Devos and Klein (University of Montpellier, France)

following informed patient consent and approval of the local ethics committee. The cells were provided by colleagues as part of the EU-funded collaboration on stem-cell based intervention strategies for SCI (acronym: RESCUE). Fibroblasts were cultured on normal tissue culture plastic in DMEM/F12 (Lonza) containing 10% FBS and penicillin/streptomycin (PAA Laboratories GmbH).

7.3.2 Scaffold seeding

Three-dimensional scaffolds were provided by a local bioenterprise (Matricel GmbH, Herzogenrath, Germany) and cut into cylinders (2 mm diameter x 3 mm length) using sterile biospy punches (Kai Industries, Japan). Seeding was performed using a cell suspension with either 10^4 cells/µl (hMSC) or $2x10^4$ cells/µl (hFbl). These different seeding densities were chosen due to size differences of both cell types. Furthermore, higher cell numbers of hMSC block the pores of the scaffold, leading to unequal distribution of the cells. For seeding, dry scaffold cylinders were dropped into the cell suspension and transferred into 12-well plates. To allow cell attachment, seeded scaffolds were incubated at 37°C for 3 h with a drop of media next to the scaffold to prevent dehydration. Afterwards cell-specific media were added.

Some of the hMSC-seeded scaffolds were further processed for cell proliferation and distribution data after 1, 7 and 14 days *in vitro.* After fixation in 4% PFA, samples were embedded in a 5% gelatine (Merck, Darmstadt, Germany), 5% (w/v) sucrose (Merck) solution in 0.1M PBS and kept in a humidified chamber at 45°C overnight. Gelatine was allowed to polymerize the next day, at 4°C, for half an hour and was then frozen at -80°C in isopentane. 20 µm thick longitudinal sections were cut using a cryostat and either processed for immunocytochemistry or proliferation analysis. Proliferation was evaluated by counting DAPI-stained nuclei from 15 non-overlapping, randomly chosen, microscopic fields (100x magnification) from three scaffolds per time point.

7.3.3 Behavioural analysis

Female adult Lewis rats (Charles River, Sulzfeld, Germany) were maintained in accordance with the guidelines of the German animal protection statute and experimental protocols were approved by the regional ethical committee for North Rhine-Westphalia (AZ 50.203.2-Ac 23, 11/06). A total of 29 female Lewis rats (Charles River, Sulzfeld, Germany) with a body weight of approximately 200 g were used. The animals were housed under temperature controlled conditions at 21 ± 1 °C, with a normal 12:12 h light/dark cycle. The animals were kept on a food-restriction protocol throughout the pre-operative training period and post-surgery. This food-restriction protocol involved a 12 g diet per day (which allowed the adult rats to maintain a stable body weight) with free access to water. The assessment of animal weight and behavioural analysis after surgery was performed on a weekly basis for up to 8 weeks.

7.3.3.1 CatWalk Gait Analysis

Animals were trained daily on the CatWalk (Noldus Information Technology, Wageningen, The Netherlands) for 2-3 weeks prior to surgery. The use of the CatWalk for computer-assisted gait analysis and the required training protocol have already been described elsewhere (213-215). Briefly, the CatWalk system consists of a glass runway (109 x 15 x 0.6 cm), located in a darkened room, which contains light from a white fluorescent tube. Internal reflection causes the light to be restricted to the glass surface plate under normal circumstances. Only at those points where an animal's paw touches the surface of plate does light exit from glass floor. The scattered light demonstrates the contact area of the paw and is detected by a video camera (Sony 3CCD Color Video Camera; DXC-990/990P) positioned underneath the walk-way. The signal is digitized (50 half-frames/s) by an S-RGB frame grabber (Matrix Vision GmbH, Oppenheimer, Germany) and the acquired data compressed and stored for eventual analysis using the CatWalk software program (Hamers et al., 2001). Thus, a wide range of gait parameters can be measured from each run that a rat makes across the glass runway. The dietary food restriction of 12 g per day was used to motivate the animals, since each run was rewarded by access to a small number of foot pellets (Noyes Precision pellets PJPPP-0045; Sandown Chemical Ltd., Hempaton, UK) which were placed at the end of the runway. The training period ended after all animals were able to make at least three consecutive runs without interruptions. Importantly, the crossing time was controlled by only recording runs that required a duration of between 1 - 2 s. For correct locomotor analysis, the following walkway crossing criteria were used: (1) the rat needed to cross the walkway, without any interruption or problem, and (2) a minimum of three correct crossings per animal were required (but 8 were recorded). For correct evaluation of the gait analysis, the three runs with crossing times closest to 1.4 seconds were chosen. In the present study, all individual crossings were analyzed for the duration of walkway crossing, the regularity index, base of support (hind-limbs), intensity of paw placement, paw print area, paw max area, stance duration, swing duration, stride length and duty cycle (hind-limbs).

7.3.3.2 Grid-walk

The grid-walk provides a quantitative assessment of the animal's ability to precisely control hind-paw placing while traversing a wire mesh walkway. The walkway consisted of wire mesh with regularly spaced diagonal bars (distance between bars is 3 cm). For correct analysis, the following criteria concerning grid-walk crossing were used: (1) the rat needed to cross the walkway, without any interruption or problem, and (2) a minimum of four correct crossings per animal were required. All runs were recorded using a video camera (Sony) to ensure correct analysis. Stepping errors consisting of misplacement of the hind-paw (such that it falls through the grid meshwork) were counted and the mean error rate from all four runs was calculated.

7.3.3.3 Von Frey sensory analysis

Animals were placed in a plastic cage with a metal mesh floor, allowing them to move freely. They were acclimatised to this environment for approximately 10 min prior to testing, to allow for behavioural accommodation. A series of ten von Frey-type filaments with different stiffness (0.4, 0.6, 1, 1.4, 2, 4, 6, 10, 15, and 26 g; Stoelting, Wood Dale, USA) was employed to determine the 50% threshold for paw withdrawal to light mechanical stimulation, using a previously described “up-and-down paradigm” (216). Von Frey filaments were applied to the mid-plantar surface of each paw through the mesh floor. Probing was only performed when all paws of the animal were in contact with the floor. Each probe was applied to the foot until it just bent, and was kept in this position for 6–8 s. Interval between consecutive filaments was at least 5 s. The 50% paw withdrawal threshold was determined by initiation with the 2 g filament. In the absence of a paw withdrawal response, the next strongest stimulus in the filament series was presented. Once a paw withdrawal was observed, the next weakest stimulus in the filament series was chosen. After the first paw withdrawal, 5 further stimuli were presented until the series ended.

Values obtained from animals one day prior to surgery were used for the demonstration of normal, baseline behaviour.

7.3.4 Surgical procedure

The day before surgery, animals were started on an immune suppression strategy to prevent rejection of donor human cells. For this purpose animals received 10 mg/kg cyclosporine (Novartis AG, Basel, Switzerland) and 4 mg/ml azathioprine sodium (GlaxoSmithKline, London, UK) intraperiteonal (i.p.).

Under isoflurane inhalation anaesthesia, the back of the animal was shaved and the skin sterilized with 70% alcohol prior to incision along the midline, exposing the back musculature. Using blunt dissection, the superficial and deep muscle layers were cleared and retracted to expose the dorsal surface of the T9-T12 vertebrae. Fine bone rongeurs were used to perform a laminectomy of the T10-T11 vertebra, exposing the dorsal surface of the spinal cord. The dura was cut and reflected, after which a 2 mm long lateral funiculotomy was performed, followed by haemostasis using Spongostan. Subsequently, either a non-seeded scaffold, or a hFbl- or hMSC-seeded scaffold was implanted into the resection injury. 10/0 sutures were then used to secure the dural flap over the scaffold, thus helping to stabilize its position. The muscle layers were then closed using resorbable 6/0 suture. The skin was closed using 4/0 sutures. After surgery, animals received immunosupression (i.p. 10 mg/kg cyclosporine, 4 mg/kg azathioprine sodium and 2 mg/ml methylprednisolone (Sanofi-Aventis, Bridgewater, USA) according to the method of Pedersen and colleagues (217). Rats were also given 10 ml

of saline and antibiotics (0.01% baytril, Bayer, Leverkusen, Germany) subcutaneously, and were allowed to recover. The following day, the vast majority of the animals moved freely in their cage, and fed/drank without any indication of pain or discomfort. In those few cases of bladder dysfunction, which usually lasted for not more than 7 days, the bladders were manually voided on a daily basis. Immunosupression was performed until the end of the experiment using 10 mg/kg cyclosporine, 2 mg/kg azathioprine sodium and decreasing concentrations of methylprednisolone (1-7 days 2 mg/kg; 8-14 days 1 mg/kg; 15-end 0.5 mg/kg) as recommended by Pedersen and colleagues (217).

7.3.5 Tissue preparation

Under terminal isoflurane inhalation anaesthesia, animals were perfused transcardially with 50 ml PBS followed by approximately 300 ml of cooled 4% paraformaldehyde (PFA) in PBS. After perfusion, the spinal cord was carefully removed, post-fixed in 4% PFA for 24h and stored in 20% sucrose for three days at 4°C. For histological processing, spinal cord segments including the lesion area were frozen in isopropanol (-80°C) and stored until required at –80°C.

7.3.6 Immunohistochemistry

Adjacent serial longitudinal spinal cord sections (20 µm thick) were cut on a cryostat and collected onto adjacent SuperFrost Plus Gold glass slides (Menzel-Glaeser, Braunschweig, Germany), dried at 37°C for 4 h and stored at -80°C. For immunohistochemistry, the samples were washed three times with PBS and non-specific binding sites were blocked by a 1 h incubation in PBS containing 3% normal goat serum (Sigma), 1% bovine serum albumin (BSA; fraction 5, Serva, Heidelberg, Germany) and 1% Triton X-100 (Sigma). The primary antibodies were diluted in PBS with 1% BSA and 3% normal goat serum and incubated at room temperature overnight. The following monoclonal primary antibodies were used: anti-chondroitin sulfate proteoglycans (CSPG, 1/200, Sigma), anti-GFP (1/200, Chemicon, Temecula, USA), anti-neurofilament 200 kDa (NF200, 1/2000, Sigma), and anti-human nuclei (hNuclei, 1/200, Millipore, Billerica, USA) as well as the following polyclonal antibodies: anti-glial fibrilary acidic protein (GFAP, 1/2000, DAKO, Hamburg, Germany), anti-GFP (1/500, Chemicon), and anti-ionized calcium binding adaptor molecule 1 (Iba1, 1/1000, Wako, Neuss, Germany). Primary antibodies were detected by incubation of the appropriate combination of fluorochrome-conjugated secondary antibodies, i.e. either Alexa-Fluor 488 or 594 goat anti-mouse IgG and Alexa-Fluor 488 or 594 goat anti-rabbit (1/500, Invitrogen, Carlsbad, USA) diluted in PBS with 1% BSA and 4,6-diamidino-2-phenylindole dihydrochlorid (DAPI, 1/1000, Invitrogen) for 2.5 h at room temperature. Coverslips were then mounted onto the samples using Fluoroprep (BioMerieux, Nürtingen, Germany). Sections were visualized using an

inverted Zeiss Axioplan fluorescence microscope coupled to an on-line digital camera (Axiovision software).

7.3.7 Evaluation of immunohistochemistry

For quantification of the staining intensity, 8 sections (with an inter-section distance of 140 µm) were analyzed per animal and marker.

NF200: The whole transplantation area was photographed by employing the automatic image acquisition and mosaic reconstruction feature of the Zeiss AxioVision software using a 40x objective. The number of axons which crossed lines drawn across the images of the scaffold, 100 µm from the rostral and caudal graft-host interfaces, as well as through the mid-portion of the scaffold, was counted (e.g. see Figure 7.1A). Any spinal nerve roots within the field were excluded from the quantification.

GFAP: To assess the astrocytic response at the implant-host interface, 3 pictures of the implantation site rostral, caudal and medial were taken using a 40x objective (Figure 7.1B). For quantification, images were all captured using the same exposure time and the mean grey value of each picture was evaluated using ImageJ software (http://rsbweb.nih.gov/ij/). The mean grey values of completely white and completely black images were used to set maximal and minimal values at 100% and 0%.

Iba1: For the evaluation of the inflammatory response, 4 pictures of each section including the rostral, caudal, medial graft-host interfaces as well as from the central position within the scaffold were taken using a 40x objective (Figure 7.1C). Quantification was performed following same protocol as described for the GFAP staining (above).

CSPG: To evaluate the level of extracellular matrix-related protein CSPG, within the scaffold, 3 pictures of the implantation site including the rostral-, caudal- and medial graft-host interfaces were taken using a 40x objective (Figure 7.1D). Quantification was performed following same protocol as described for the GFAP staining (above).

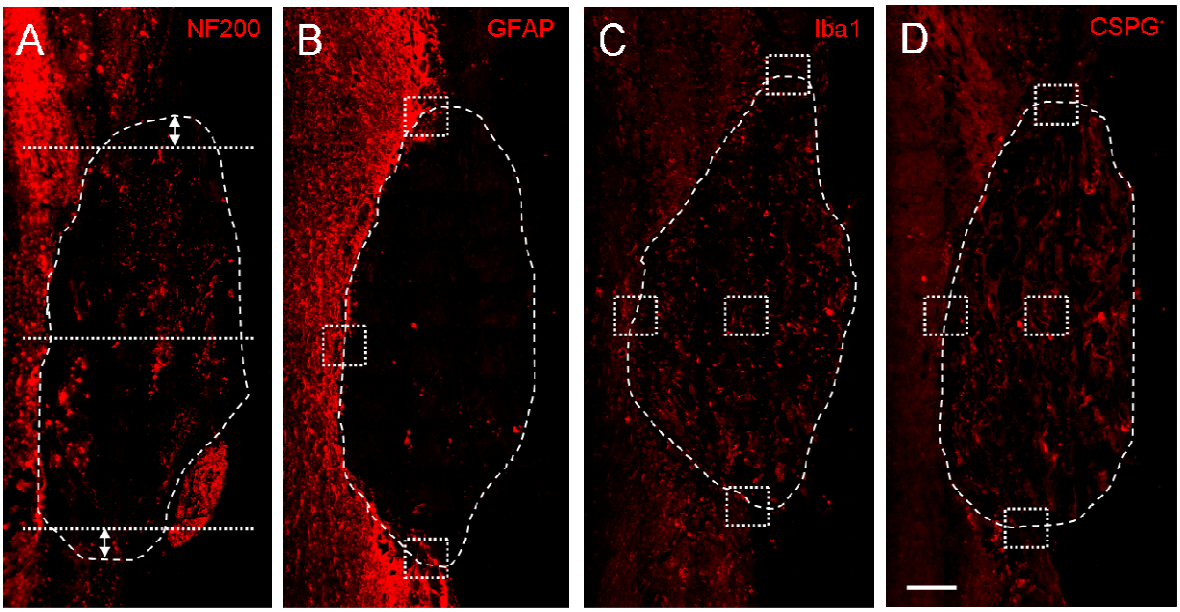

Figure 7.1: Examples of the acquistion protocols for the quantification of immunohistochemical stainings. Regenerating axons (A) were stained for NF200 and all axons crossing the rostral and caudal lines within the scaffolds (arrows) as well as the middle line (dotted lines) were counted. For quantification of the astrocytic response (B), 3 pictures (squares) of the graft-host interface at rostral-, caudal- and medial positions of GFAP stained samples were taken and evaluated. The inflammatory response (C) was evaluated in Iba1-stained sections by taking 4 pictures including the graft-host interface at rostral-, caudal- and medial positions as well as the central position (squares). Extracellular matrix deposition (D) was evaluated in CSPG-stainined sections from 3 pictures of the graft-host interface at the rostral-, caudal- and medial positions (squares). Addiontally, the CSPG staining of the scaffold center was evaluated. Scale bar: 200 µm.

7.3.8 Statistical analysis

Data are shown as average values ± SEM. Multiple group comparisons were performed by one-way analysis of variance (ANOVA) followed by the Bonferroni *post-hoc* test (Prism4, GraphPad Software, Inc., San Diego, USA). Values of $p<0.05$ were considered as statistically significant.

7.4 Results

7.4.1 Characterization of hMSC

After transduction of hMSC, all cells constitutively expressed GFP (Figure 7.2A). This had no apparent effect on hMSC multipotent characteristics as demonstrated by the differentiation into osteocytes (Figure 7.2B) and adipocytes (Figure 7.2C).

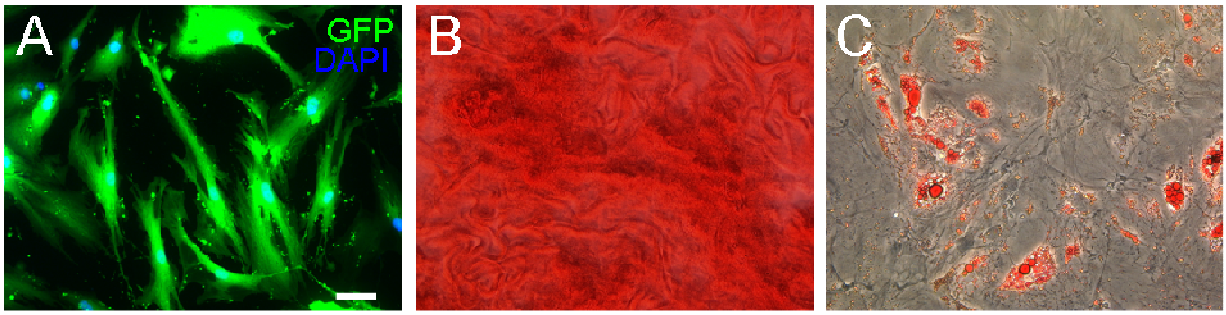

Figure 7.2: Transduced hMSC remain their differentiation capacity. Transduced hMSC expressed constitutively GFP in culture (A) and remained their differentiation capacity into osteocytes (B) and adipocytes (C). Scale bar: 20 µm.

7.4.2 *In vitro* cytocompatibility of the scaffold

The 3D collagen scaffold used in this study presented continuous, longitudinally oriented guidance channels with numerous interconnected pores, as demonstrated by scanning electron microscopy (Figure 7.3A and B). Such oriented microstructure was intended to support the longitudinal orientation of the seeded cells as well the ensuing host axon regeneration. One day after seeding hMSC onto the biomaterial, the cells adhered and demonstrated an even distribution throughout the scaffold (Figure 7.3C-E). Interestingly, some of the hMSC expressed low levels of GFP, but these could still be clearly identified by anti-GFP immunofluorescence (Figure 7.3F). Seeded scaffolds cultivated for up two 2 weeks *in vitro* revealed hMSC proliferation (Figure 7.3G), demonstrating the biocompatibility of the scaffold.

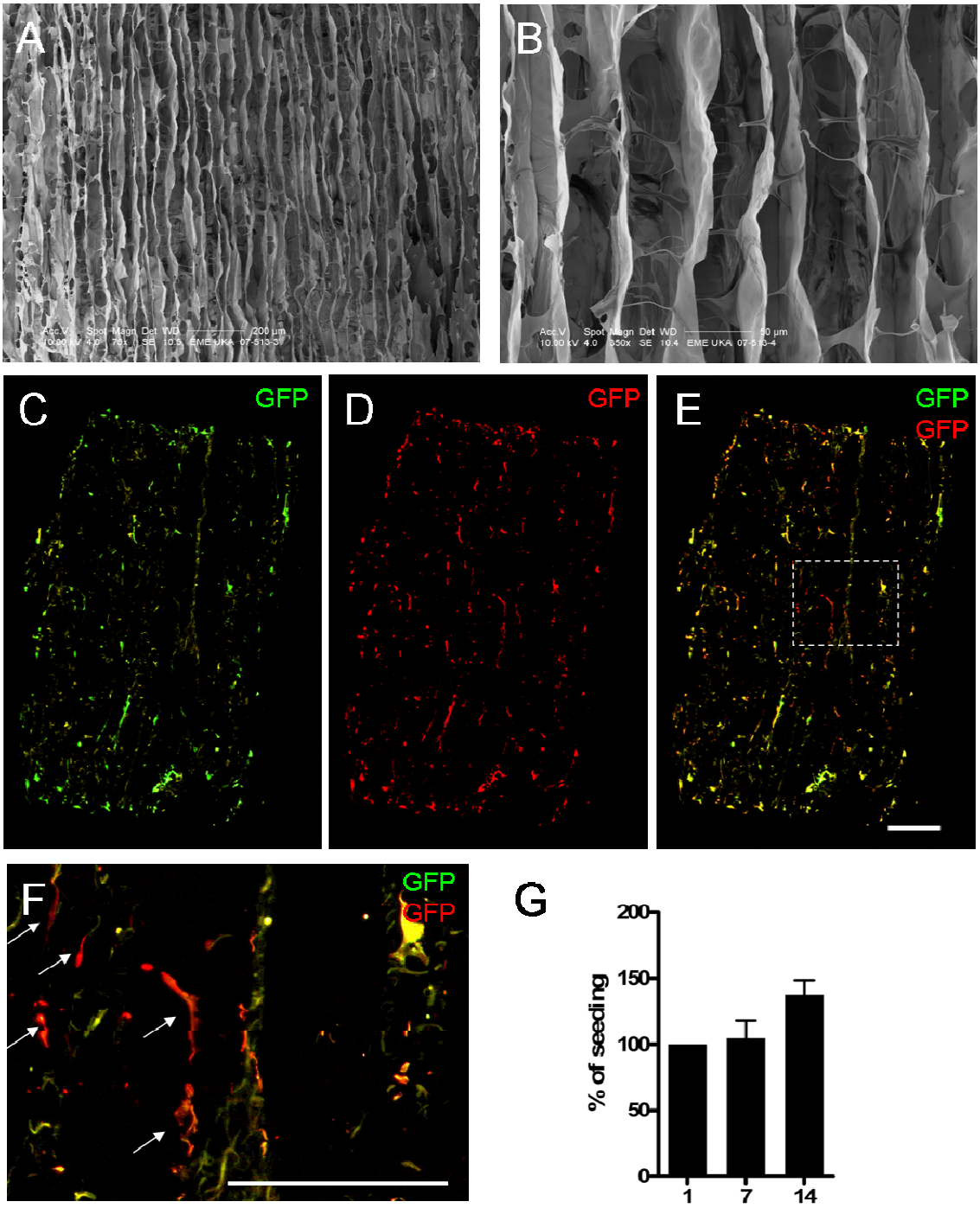

Figure 7.3: HMSC grow on oriented porous collagen scaffold. The scaffold consisted of oriented interconnected pores as demonstrated by electron microscopy (A+B). Seeded hMSC were evenly distributed throughout the scaffold (C-E) and could be stained for GFP (D). Interestingly, some cells expressed low visual levels of GFP, but could be identified by GFP staining (E+F). HMSC proliferated onto the collagen scaffold, demonstrating the biocompatibility of the material (G). Scale bar: 500 µm.

7.4.3 Behavioural analysis after scaffold implantation

All animals received a right-sided Th10-11 lateral funiculotomy and the lesion gap was directly replaced by either non-seeded (control) scaffolds (n=9) or hMSC-seeded scaffolds (n=10). Furthermore, hFbl-seeded scaffolds (n=10) were implanted as cellular controls. The

behavioural analysis was performed weekly after the surgery; however, to provide a better overview of the behavioural trends, data from 1, 4 and 8 weeks post surgery have been presented.

7.4.3.1 Body weight

Although all 29 animals showed a drop in body weight in the first week postoperatively, they all gained body weight in the weeks thereafter (Figure 7.4A). One week after surgery, significant ($p<0.01$) loss of weight compared to baseline level (BL: 201.6±1.25 g; indicated by dotted line) could be observed in animals receiving scaffold only (control: 185.3±2.82 g; hFbl: 192.1±2.60 g; hMSC: 191.9±2.49). After 4 weeks, all animals recovered to BL level (control: 197.6±2.19 g; hFbl: 206.0±2.69 g; hMSC: 206.5±2.29 g). At 8 weeks postoperatively, animals which received hMSC-seeded scaffold demonstrated significant ($p<0.01$) weight gain compared to BL values (control: 205.5±3.97 g; hFbl: 211.5±3.36 g; hMSC: 216.2±4.21 g). However, all three groups of animals did not display a significant difference in body weight at any time point in the study.

7.4.3.2 Grid-walk

In pre-operative BL measurements, all animals showed a mean stepping error rate of 0.55±0.08 per run (as indicated by the dotted line) (Figure 7.4B). Evaluation of miss-steps 1 week postoperatively could not be performed since the animals started to drag the hindlimbs after the first miss-step. Four weeks after surgery, all three groups demonstrated significantly ($p<0.001$) higher numbers of foot-falls compared to BL (control: 6.80±0.84; hFbl: 4.75±0.53; hMSC: 4.45±0.44). Furthermore, animals which received cell-loaded scaffolds presented significant ($p<0.001$) lower miss-steps than control animals. Eight weeks after surgery, the number of foot-falls by all three groups had decreased (control: 5.00±0.78; hFbl: 4.18±0.38; hMSC: 3.03±0.45), however these values were still significantly (control/hFbl: $p<0.001$; hMSC: $p<0.05$) higher than the baseline. The animals receiving hMSC-seeded scaffolds demonstrated still significant ($p<0.001$) lower error rates compared to animals of control and hFbl group.

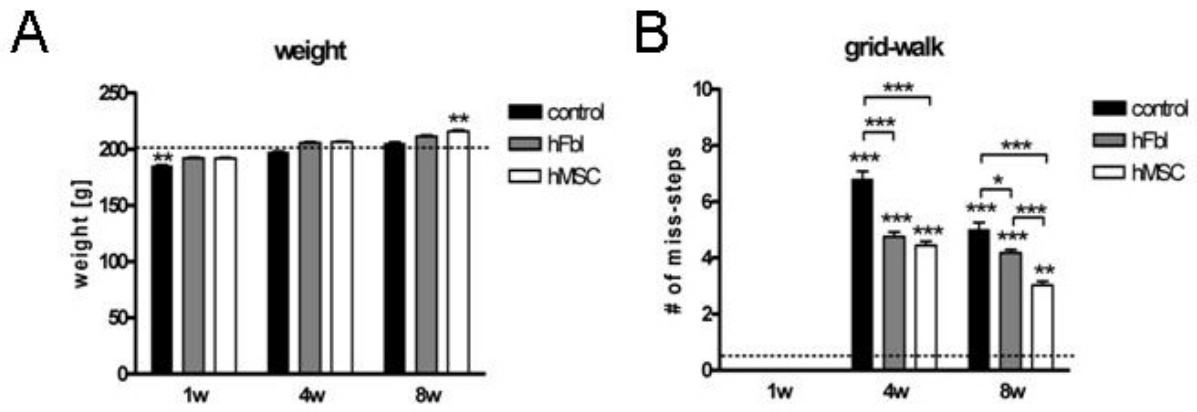

Figure 7.4: Animals transplanted with hMSC show best weight recovery and significant increased coordination. Animals of all three groups demonstrated loss of weight 1 week after surgery (A). Control animals significantly lost weight compared to BL level (dotted line). Eight weeks after implantation, animals of the hMSC group significantly gained weight compared to BL. However, no significant weight differences could be observed between all three groups. Coordination was assessed by the number of miss-steps on a grid-walk (B). Four and 8 weeks postoperatively, all groups presented significant higher numbers in miss-steps as compared to BL level (dotted line). Animals which received hMSC demonstrated significantly enhanced coordinative abilities at four and eight weeks after injury compared to control and hFbl groups. *p<0.05; **p<0.01; ***p<0.001.

7.4.3.3 Von Frey filaments

Using von Frey filaments enables the detection of sensory responses to a certain stimulus. Furthermore, detection of a sensory over-reaction, so-called allodynia, is possible. The pre-operative 50% paw withdrawal threshold of the (ipsilateral) right hind-limb (RHL) was 5.03±0.83 g (baseline and variation are indicated by dotted lines) (Figure 7.5A). The BL did not differ significantly from the thresholds after 1 week (control: 8.12±2.54 g; hFbl: 4.42±0.90 g; hMSC: 7.437±1.54 g), 4 weeks (control: 6.36±2.07 g; hFbl: 4.75±1.45 g; hMSC: 6.32±2.77 g) or 8 weeks (control: 5.33±1.95 g; hFbl: 7.02±1.54 g; hMSC: 4.14±0.91 g) of all three transplantation groups. The BL of the (contralateral) left hind-limb (LHL) was 4.88±1.06 g. No significant differences could be observed after 1 week (control: 3.82±0.94 g; hFbl: 4.21±1.11 g; hMSC: 4.86±1.73 g), 4 weeks (control: 4.33±1.35 g; hFbl: 1.84±0.24 g; hMSC: 2.82±0.66 g) or 8 weeks (control: 2.71±0.44 g; hFbl: 3.47±0.91 g; hMSC: 4.19±1.32 g) after implantation of the (seeded) scaffolds (Figure 7.5B).

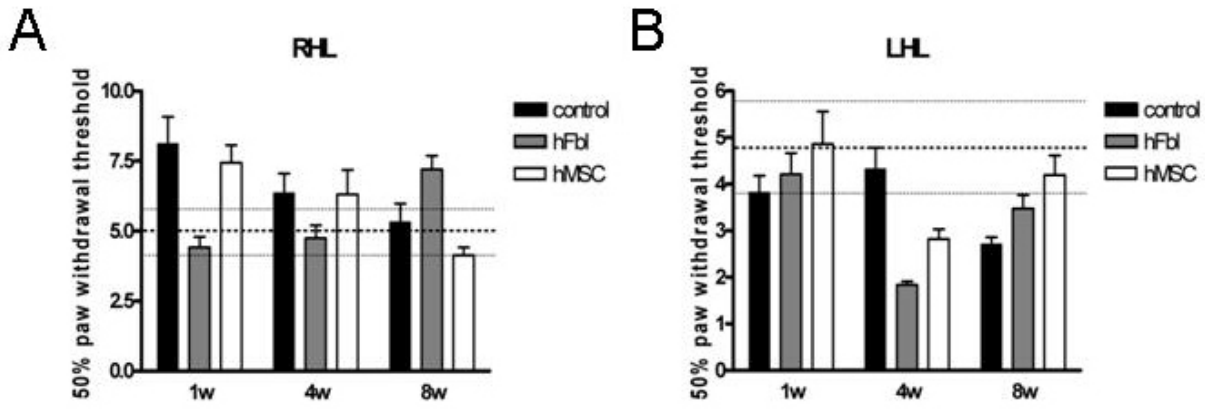

Figure 7.5: Sensory function is not impaired after scaffold implantation. Sensory function of both hind-paws was assessed with von Frey filaments. The dashed lines indicate the BL ± variation before injury. No significant differences could be observed between the groups or to BL levels.

Although the BL of all limbs was around 5 g, the high standard error in BL experiments as well as after surgery impeded conclusive evidence of enhanced/decreased paw sensitivity.

7.4.3.4 CatWalk gait analysis

For correct data analysis of the different gait parameters between all three groups, the *crossing time* is of great importance. Significant differences in the crossing time between the investigated groups could lead to false conclusions. Therefore, only 3 runs out of 8 recodings that were nearest to 1.4 s were used for evaluation. Pre-operative training on the CatWalk resulted in rapid runway crossings of 1.38±0.01 s (dotted line; Figure 7.6A). By 1 week after surgery, animals of all three groups were slower than in BL measurements (control: 1.48±0.03 s; hFbl: 1.48±0.02 s; hMSC: 1.44±0.02 s). Furthermore, animals of the control group needed significantly ($p<0.05$) longer for each run compared to BL values. Four and 8 weeks postoperatively, the crossing time remained at BL levels (4 weeks: control: 1.38±0.02 s; hFbl: 1.36±0.02 s; hMSC: 1.34±0.02 s; 8 weeks: control: 1.32±0.02 s; hFbl: 1.33±0.01 s; hMSC: 1.35±0.02 s). Since there were no differences between the three groups, a legitimate comparison of data between all three groups can be made at all three time points.

Regularity index. The regularity index defines coordination as the exclusive use of normal step sequence pattern during uninterrupted locomotion. Healthy animals have a regularity index of 100% (dotted line; Figure 7.6B). One week after scaffold implantation, the regularity index of all three groups decreased significantly (control/hMSC: $p<0.001$; hFbl: $p<0.01$) compared to BL values (control: 91.54±2.47%; hFbl: 95.53±1.42%; 92.51±1.75%). Four weeks after surgery, the regularity index of all three groups nearly reached again 100% (control:

98.24±1.13%; hFbl: 99.80±0.20%; hMSC: 99.13±0.54%). Eight weeks after surgery, animals which received empty or hFbl-seeded scaffolds demonstrated a regularity index of 100%, whereas animals of the hMSC group had a lower regularity index of 97.93±0.78%.

Stride length. The stride length gives the distance between the print of one hind-paw in one step cycle to the print of the same paw in the next step cycle. In uninjured animals the BL ratio of the ipsilateral to the contralateral side was 100% (dotted line; Figure 7.6C). The week after implantation of the scaffolds, the stride length was increased in all three groups (control: 113.00±5.96%; hFbl: 103.90±4.81%; hMSC: 106.00±3.35%). The increase in stride length of the control animals was significant ($p<0.001$) compared to BL. Animals of all three groups presented almost normal stride length at 4 weeks (control: 103.90±3.84%; hFbl: 97.84±1.47%; hMSC: 96.92±3.46) and 8 weeks after surgery (control: 101.50±0.93%; hFbl: 97.43±1.31%; hMSC: 99.14±1.46%).

Stance duration. The stance duration gives the time period in which one hind-paw is in contact with the CatWalk. In uninjured animals the ratio of the ipsilateral to the contralateral side was 102±2.12% (dotted lines; Figure 7.6D). One week after surgery, the stance duration decreased in all three groups compared to BL (control: 64.56±6.10%; hFbl: 83.75±2.94%; hMSC: 92.05±3.38%). This decrease was significant ($p<0.001$) in animals of the control group. At 4 weeks after injury, the stance phase was still decreased (control: 65.72±5.27%; hFbl: 80.93±4.35%; hMSC: 88.24±4.67%) whereas this decrease was significant to BL levels in animals receiving empty ($p<0.001$) or hFbl-seeded ($p<0.01$) scaffolds. Furthermore, the animals of the hMSC group demonstrated significantly ($p<0.05$) better recovery in stance duration compared to the control group. Eight weeks after injury all three groups presented recovery (but still lower than BL) in stance duration with no statistical differences (control: 86.30±5.20%; hFbl: 87.98±2.96%; hMSC: 92.77±4.01%).

Swing duration. The swing duration gives the time period in which one hind-paw has no contact to the CatWalk and therefore behaves complimentarily to the stance phase. The BL ratio of the ipsilateral to the contralateral side of all animals was 99.83±1.20% before surgery (dotted line; Figure 7.6E). Accordingly, the swing duration was increased 1 week after surgery compared to BL (control: 206.90±23.15%; hFbl: 159.70±21.69%; hMSC: 137.70±10.49%), whereas this increase was significant in animals receiving empty ($p<0.001$) or hFbl-seeded ($p<0.001$) scaffolds. Furthermore, animals of the hMSC group presented significantly ($p<0.001$) better recovery in swing duration compared to control animals. After 4 weeks, the swing duration of all three groups was still increased (control: 165.00±13.77%; hFbl: 131.00±6.75%; hMSC: 112.40±5.76%). The difference of control animals to BL values as well as to animals of the hMSC group was still significant ($p<0.001$). Eight weeks after surgery, the swing duration of all three groups decreased towards BL levels (control: 134.50±7.19%; hFbl:

115.40±4.51%; hMSC: 110.70±4.52%). However, the swing duration of control animals was still significantly ($p<0.05$) higher compared to BL.

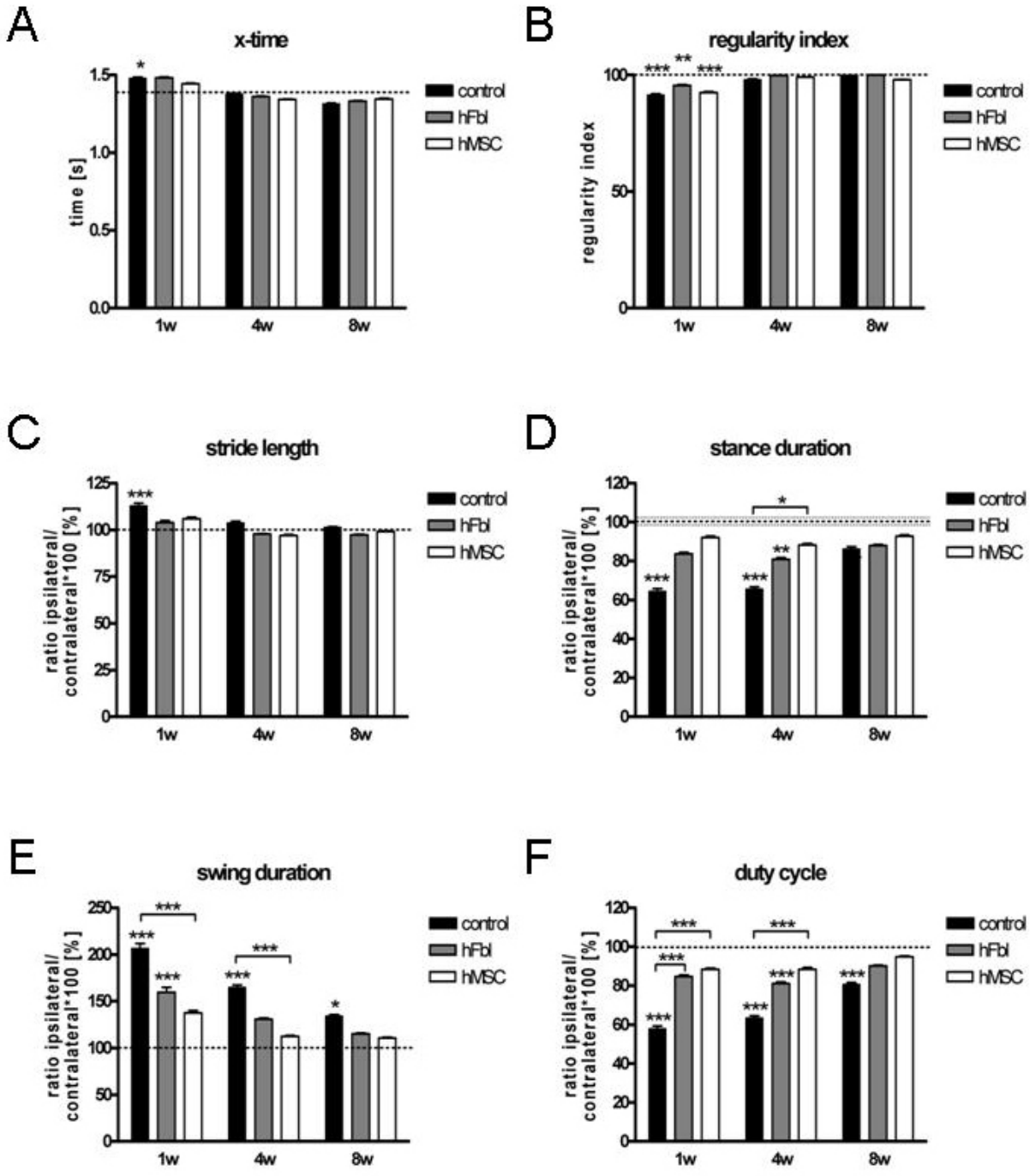

Figure 7.6: Animals of the hMSC group showed a transient improvement in the recovery of gait parameters as assessed by CatWalk. No differences between all three groups could be observed in crossing-time (x-time) (A), regularity index (B) and stride length (C). However, significantly improved function in stance duration (D), swing duration (E) and duty cycle (F) was observed in hMSC-transplanted animals at 1 and 4 weeks with almost normal levels achieved by 8 weeks after injury. The dotted line indicates the values before injury. *p<0.05; **p<0.01; ***p<0.001.

Duty cycle. The duty cycle is a parameter that gives the stance duration as a percentage of the step cycle. Before injury the ratio of the ipsilateral to the contralateral side of the duty cycle was 100.10±0.84% (dotted line; Figure 7.6F). One week postoperatively, the duty cycle of all three groups decreased (control: 58.07±5.58%; hFbl: 84.72±3.10%; hMSC: 88.49±2.54%), however, this decrease was significant ($p<0.001$) only for the control group to BL values. Furthermore, the performance of control animals was significantly ($p<0.001$) lower than of animals which received hFbl- or hMSC-seeded scaffolds. At 4 weeks, the duty cycle of animals of the control and hFbl group was significantly ($p<0.001$) lower than the BL (control: 63.58±4.92%; hFbl: 81.19±4.04%; hMSC: 88.45±4.68%). Animals of the hMSC group presented the same performance as after 1 week, but this was still significantly ($p<0.001$) better than of the control group. Eight weeks after injury, the duty cycle of all three groups maintained below BL (control: 80.89±3.95%; hFbl: 90.12±2.40%; hMSC: 94.83±2.08%). However, the control group was still significantly ($p<0.001$) lower than the BL. No statistical difference between all three groups could be identified.

Base of support. The base of support (BOS) gives the average width between the hind-paws. Before injury the BOS of the hind-paws was 15.91±0.28 mm (dotted lines; Figure 7.7A). One week postoperatively, the BOS of the control and hFbl group was lower, the BOS of the hMSC group higher than BL (control: 14.90±1.47 mm; hFbl: 15.04±0.91 mm; hMSC 17.84±0.85 mm). At 4 weeks after injury, the BOS of animals which received hFbl-seeded scaffolds was at BL level, whereas the BOS of control animals and animals which received hMSC was increased (control: 18.54±0.89 mm; hFbl: 16.30±0.99 mm; hMSC: 18.99±1.04 mm). After 8 weeks, the BOS of all three groups was higher than BL values (control: 18.04±0.87 mm; hFbl: 18.02±0.92 mm; hMSC: 18.67±0.83 mm). However, no statistically differences between all three groups or to BL values could be detected for any time point.

Print area. The print area gives the average area of the footprint during contact to the CatWalk. The ratio of the print area of the ipsilateral to the contralateral side was 104.10±2.97% in uninjured animals (dotted lines; Figure 7.7B). One week postoperatively, animals of all three groups presented a significant ($p<0.001$) decrease in print area compared to BL values (control: 34.31±5.85%; hFbl: 49.38±2.33%; 67.06±4.32%). Although there was no statistical difference detectable between all three groups, animals with cell-seeded scaffolds performed better than animals of the control group. Furthermore, better performance was presented by animals which received hMSC than those with hFbl. After 4 weeks, the print area of all three groups increased, but was still significantly (control/hFbl: $p<0.001$; hMSC: $p<0.01$) lower than the BL (control: 42.54±5.59%; hFbl: 64.61±5.82%; hMSC: 77.40±5.28%). However, the print area of the hMSC group was significantly ($p<0.05$) higher than that of the control group. At 8 weeks, the print area maintained below BL values (control: 70.72±6.66%;

hFbl: 77.47±6.66%; hMSC 82.87±4.87%) and was even significantly lower than BL in animals of the control ($p<0.001$) and hFbl ($p<0.01$) group. Although animals that received hMSC-seeded scaffolds still presented the best recovery in print area at eight weeks, the improvement was no longer significant.

Maximum area. The maximum area (max area) indicates the size of the footprint at the maximum contact to the CatWalk. The max area is given as the ratio of the ipsilateral to the contrlateral hind-paw. Before surgery, the BL of the max area was 105.50±3.42% (dotted lines; Figure 7.7C). The data for the max area was very similar to that already described for the print area. The week after surgery, the max area decreased significantly (control/hFbl: $p<0.001$; hMSC: $p<0.05$) in all three groups (control: 36.11±5.78%; hFbl: 56.24±2.67%; hMSC: 74.27±5.05%). After 4 weeks, the max area of all three groups was slightly increased, but still significantly ($p<0.001$) below BL in animals of the control and hFbl group (control: 43.96±5.63%; hFbl: 71.20±6.59%; hMSC: 83.32±5.84%). The improvement in max area was, however, significantly ($p<0.01$) increased in animals which received hMSC-seeded scaffolds compared to control animals. Eight weeks after implantation, the max area of all three groups maintained below BL values (control: 73.19±6.30%; hFbl: 83.83±6.98%; hMSC: 89.63±4.89%) and for animals of the control group, this difference was still significant ($p<0.01$). Although animals which received hMSC-seeded scaffolds still presented the best recovery in max area after 8 weeks, the improvement was no longer significant.

Intensity. The intensity is defined as the average intensity of max area. The more pressure the animals paw exerts, the larger is the total area of skin-floor contact and the brighter the pixel. The BL ratio of the ipsilateral to contralateral side of the intensity was 104.20±2.30% (dotted lines; Figure 7.7D). One week after implantation, the intensity of all three groups was below BL level (control: 60.11±7.10%; hFbl: 82.44±4.63%; hMSC: 91.20±4.36%), whereas the intensity of the control animals was significantly ($p<0.001$) decreased. This gait parameter demonstrated the most striking effect of implanting hMSC-seeded scaffolds with almost BL values already after one week. At 4 weeks, the intensity of animals of the control and hFbl group was significantly ($p<0.001$) lower than BL values, whereas animals of the hMSC group remained at BL level (control: 56.55±4.29%; hFbl: 74.46±5.14%; 98.13±5.96%). Additonally, the intensity of animals receiving the hMSC was significantly ($p<0.001$) improved compared to control animals. By 8 weeks, however, this difference decreased, but was still detectable. Furthermore, animals of the control and hFbl group presented some recovery in intensity, whereas the control group remained significantly below BL values (control: 77.52±5.35%; hFbl: 82.79±4.66%; hMSC: 94.92±5.17%).

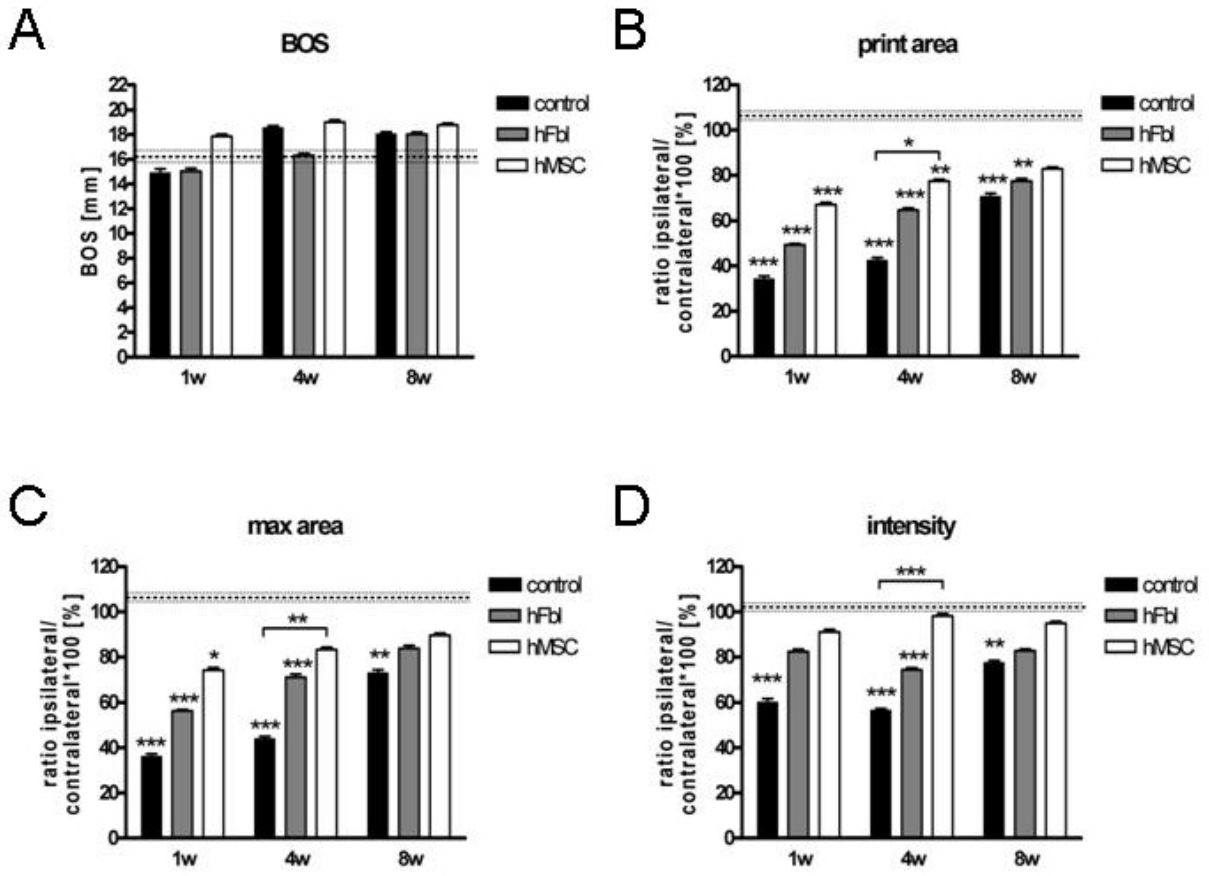

Figure 7.7: HMSC-transplanted animals showed a transient improvement in the recovery of gait parameters as assessed by the CatWalk. No significant differences between all three groups could be observed in base of support (BOS) of the hind-paws (A). However, improved function in print area (B), max area (C) and intensity (D) was recorded in hMSC-transplanted animals as early as 1 week after injury. Furthermore, animals of the hMSC group presented significant recovery in these gait parametes compared to control animals at 4 weeks after injury. This difference, however, was reduced at 8 weeks. *p<0.05; **p<0.01; ***p<0.001.

7.4.4 Histological analysis of transplant-host interactions

7.4.4.1 Survival of transplanted cells

Transplanted cells within the scaffolds were identified by immunohistochemical staining of hMSC with anti-GFP antibody (Arrows; Figure 7.8A-D) and of hFbl with anti-human nuclei antibody (Figure 7.8E+F). Staining for GFP was essential due to low levels of GFP expression determined in the *in vitro* experiments, prior to implantation. Interestingly, hMSC demonstrated a substantially better survival than hFbl. In particular, hMSC could be identified in 60% (6 out of 10) whereas hFbl could be detected in only 10% (1 out of 10) of the animals in each group (Figure 7.8G). Furthermore, transplanted hMSC could only be identified near the center of the scaffold (Figure 7.8A+B) with no evidence of migrated cells into the host tissue. However, some autofluorescence could be detected within the host's tissue in some cases (asterisk;

Figure 7.8A). In the one case where hFbl could be identified at eight weeks after implantation, these cells were also found within the scaffold with no sign of migration into the host's tissue (Figure 7.8E+F). However, due to the staining of the human nuclei, only a high magnification image can be presented. Interestingly, although only few transplanted cells could be identified, the transplanted scaffolds were heavily infiltrated with cells (Figure 7.8C-F).

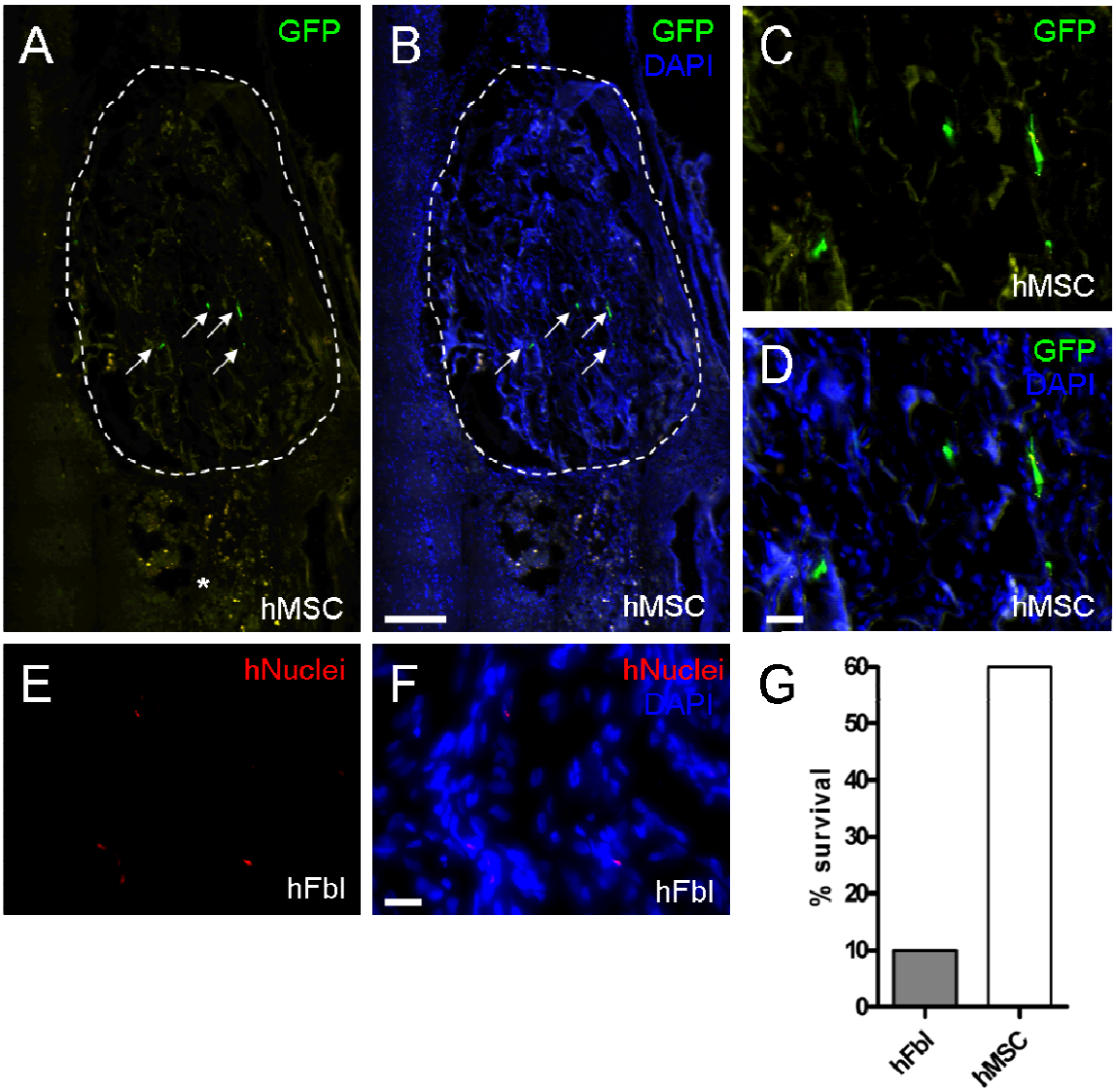

Figure 7.8: Transplanted hMSC can be identified eight weeks after implantation. Immunofluorescence stainings of longitudinal spinal cord sections were prepared to identify transplanted cells. Only a few donor hMSC (arrows) could be identified within the collagen scaffold (dotted line) and there was no migration into surrounding host tissue (A+B). However, some autofluorescence within the host tissue could be identified in some cases (asterisk in A). Higher magnification of identified hMSC revealed high infiltration of host's cells into the scaffold (C+D). Few transplanted hFbl could only be identified in one animal at eight weeks after implantation (E+F). Quantification revealed better survival of hMSC than hFbl up to 8 weeks after surgery (G). Scale bar: 200 µm (A+B); 50 µm (C+D); 20 µm (E+F).

7.4.4.2 Host axonal regeneration

The re-growth of axons into the site of the injury is an important parameter to evaluate axonal regeneration. Regenerating axons were visualized using NF200 staining and could be identified in all three animal groups (Figure 7.9A-C). However, quantification revealed significantly higher numbers of regenerating neurons in hMSC-seeded scaffolds compared to non-seeded controls (control: 9.77±1.07; hMSC: 15.43±0.92; $p<0.01$). Numbers of axons within the hFbl group were 11.31±1.08 compared to 9.77±1.07 in the control group (not significant; figure 7.9G). For the quantification process only axons within the scaffold were counted and any present spinal nerve roots were excluded (asterisk; Figure 7.9C+D). Interestingly, the regenerating axons formed bundles and grew along the pores of the scaffold which was fully covered by infiltrated cells (Figure 7.9D-F).

7.4.4.3 Host astrocytic response

The astrocytic response after injury to the spinal cord leads to the formation of a glial scar which separates the damaged tissues from the intact tissue. The glial scar is characterized by elevated GFAP expression and could be detected at the host-scaffold interface in all three transplantation groups (Figure 7.10A-C). Furthermore, occassional GFAP-positive astrocytes were found to have migrated up to 200 µm along the pores of cell-seeded scaffolds (Figure 7.10B-F). Quantification of the astrocytic response revealed a significantly ($p<0.001$) lower expression of GFAP in animals which received cell-seeded transplants compared to the control, non-seeded group (control: 1.11±0.03%; hFbl: 0.88±0.02%; hMSC 0.85±0.02%) (Figure 7.10G).

7.4.4.4 Inflammatory response

To evaluate the inflammatory response provoked by the transplantation of the cell-seeded and non-seeded scaffolds, staining of Iba1, a marker for microglia and macrophages was performed. The expression of Iba1 could be identified in all three groups around the lesion as well as throughout the scaffold (Figure 7.11A-C). Although many macrophages/microglia infiltrated the scaffold, DAPI counterstaining indicated that there were still numerous cells of unknown phenotype that had infiltrated into the scaffolds in high numbers (Figure 7.11D-F). Quantification of the inflammatory response revealed a significant ($p<0.001$) decrease of Iba1 expression in animals that received the cell-seeded implants compared to control, non-seeded implants (control: 1.34±0.01%; hFbl: 1.21±0.01%; hMSC: 0.87±0.00%). Furthermore, hMSC-seeded implants provoked a significantly lower inflammatory response than was induced by hFbl-seeded scaffolds ($p<0.001$; Figure 7.11G).

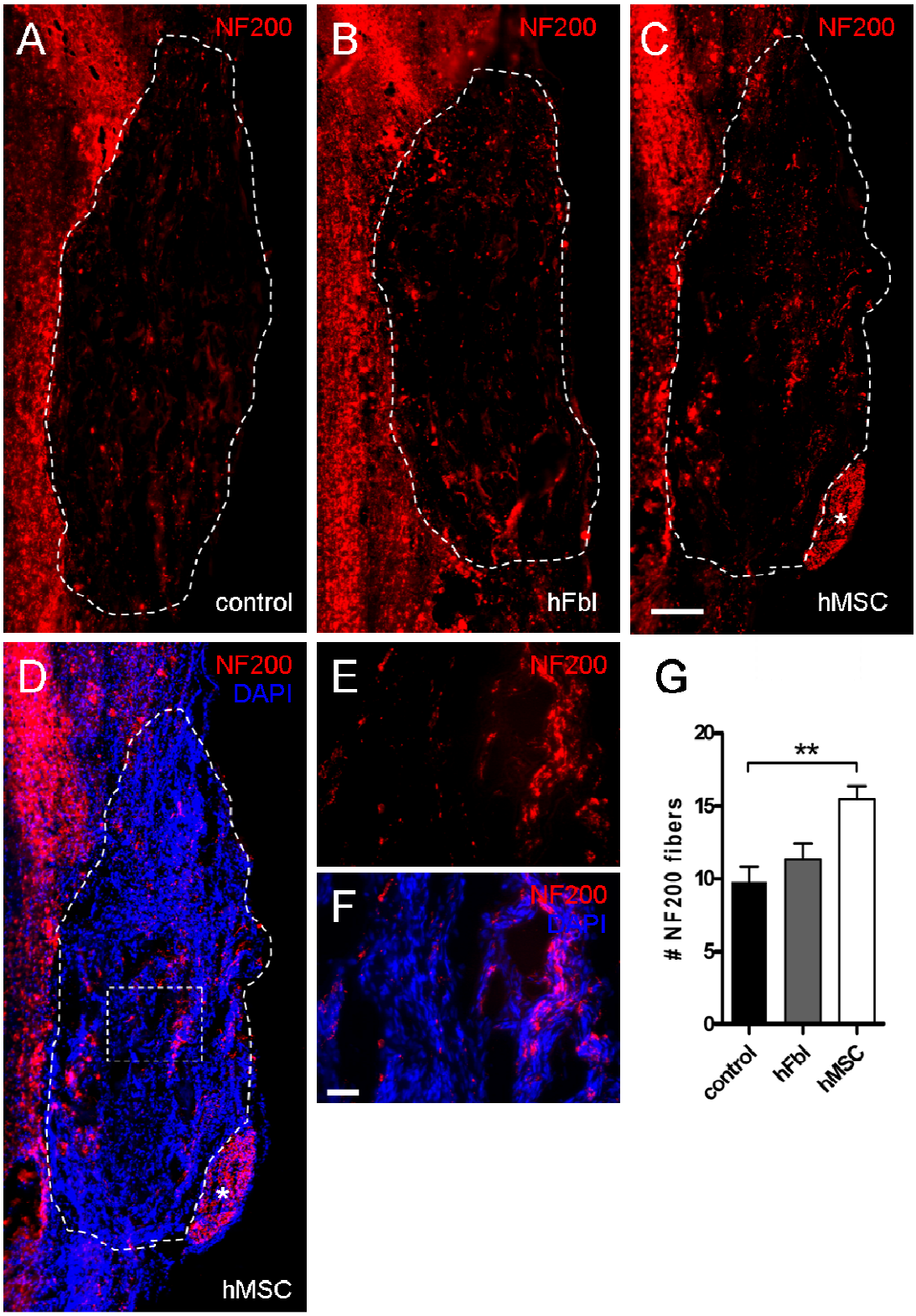

Figure 7.9: Immunohistochemitstry of longitudinal sections of the implants for NF200 to demonstrate that axonal regeneration is greater in animals which received hMSC-seeded scaffolds. Axonal outgrowth into the scaffold (highlighted by dotted line) could be detected by NF200 staining in all three groups at 8 weeks after implantation (A-C). DAPI staining revealed that regenerating axons grew along the pores of the scaffold which had been infiltrated with cells of unknown phenotype as seen by the overview picture (D) and in higher magnification from D (E-F). Quantification of the axonal ingrowth (without any spinal nerve roots marked by an asterisk in C) revealed significant higher numbers of regenerating neurons in hMSC-transplanted animals compared to non-seeded controls, with intermediate values being observed in hFbl-seeded scaffolds (G). Scale bar: 200 µm (A-D); 50 µm (E+F). **p<0.01.

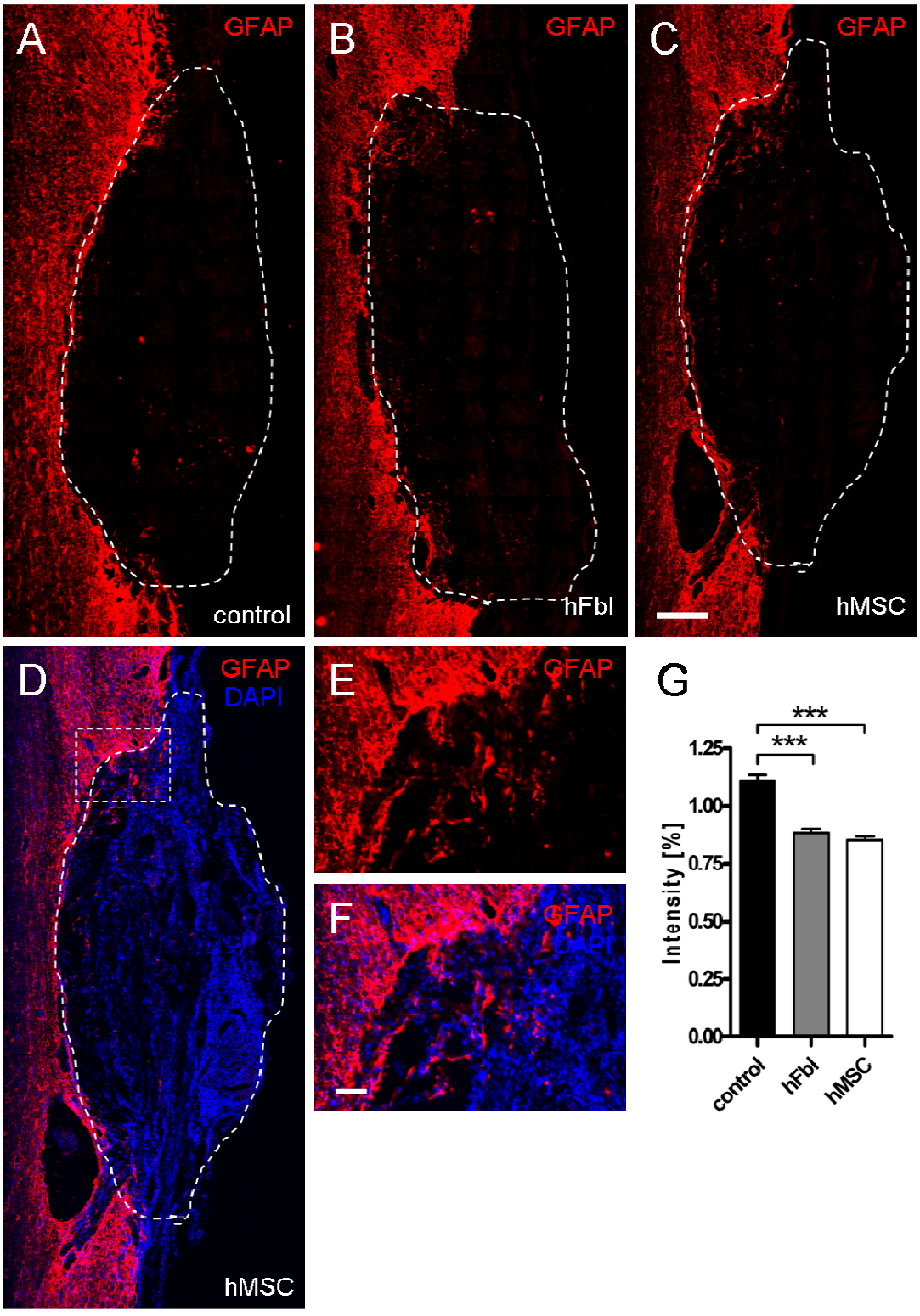

Figure 7.10: Immunohistochemistry for GFAP demonstrates that cell-seeded implants induce a reduced host astrocytic response after implantation. Astrocytic response to the scaffold (dotted line) could be detected with GFAP staining in all three groups (A-C). Occassional astrocytic profiles were found to migrate up to 200 µm into cell-seeded scaffolds (B-D). High magnification image of the host-scaffold interface from D (square) demonstrates the alignment of ingrowing astrocytes (E+F). Quantification of the astrocytic response revealed that both groups which received cell-seeded scaffolds (i.e. hFbl or hMSC) demonstrated significant lower GFAP staining at the graft-host interface than was seen in the group receiving the non-seeded scaffold. Scale bar: 200 µm (A-D); 50 µm (E, E'). ***p<0.001.

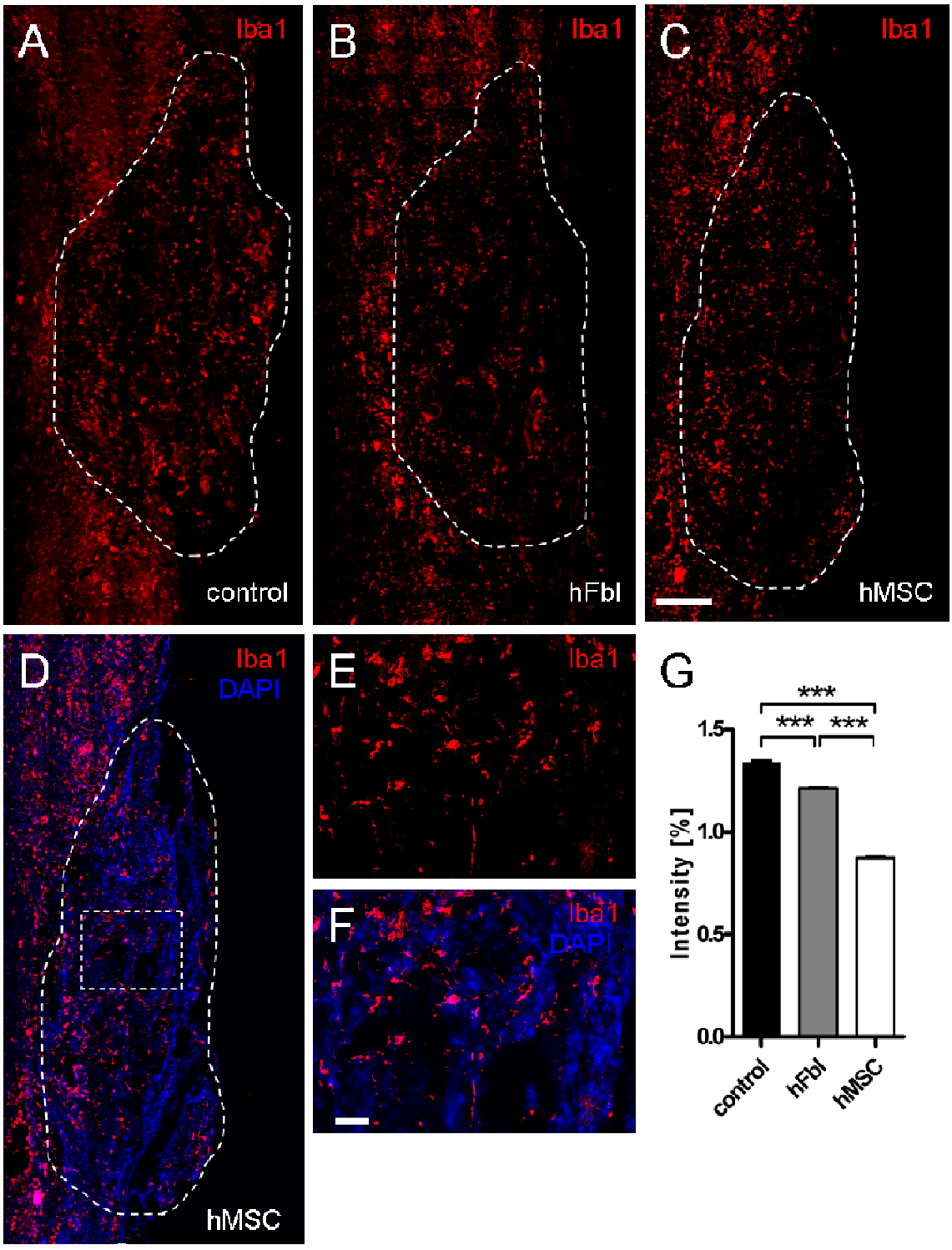

Figure 7.11: Immunohistochemistry for Iba1 demonstrated that hMSC-seeded scaffolds induce the lowest extent of host inflammation. Macrophages and microglia could be identified by Iba1 staining throughout the scaffold and the surrounding host tissue in all three groups (A-C). Although macrophages and microglia could be detected within the scaffold, the majority of cells within the scaffold's pores remained unidentified (D; high er magnification: E+F). Quantification the inflammatory response revealed significantly decreased staining in cell-seeded implants (i.e. hFbl and hMSC) compared to empty scaffolds. Furthermore, hMSC-seeded scaffolds demonstrated significantly lower inflammatory responses than were seen in response to the hFbl-seeded scaffolds. Scale bar: 200 µm (A-D); 50 µm (E+F). ***p<0.001.

7.4.4.5 Extracellular matrix production

The highly sulphated extracellular matrix-related protein, CSPG, is a major constituent of the glial scar and its expression is markedly elevated following tissue injury (218, 219). CSPG expression could be detected around the lesion in all three implantation groups (Figure 7.12A-C). However, a markedly intense CSPG staining could be identified in the center of hMSC-seeded implants (Figure 7.12C). Although only few donor hMSC survived until the end of the experiment, the remaining, viable cells were found to be responsible for the intense CSPG expression (Figure 7.12D-F). Moreover, the expression and secretion of CSPG by hMSC was further confirmed subsequent in *in vitro* investigations (Figure 7.12G-I). Quantification of the CSPG staining demonstrated a significantly ($p<0.05$) lower expression around hFbl-seeded scaffolds compared to control- and hMSC-seeded scaffold implants (control: 0.65±0.01%; hFbl: 0.59±0.01%; hMSC: 0.66±0.02%) (Figure 7.12J). However, quantification of the CSPG staining within the center of hMSC-seeded implants was significantly ($p<0.001$) higher than in non- and hFbl-seeded implants (control: 0.38±0.01%; hFbl: 0.41±0.01%; hMSC: 1.53±0.06%) (Figure 7.12K).

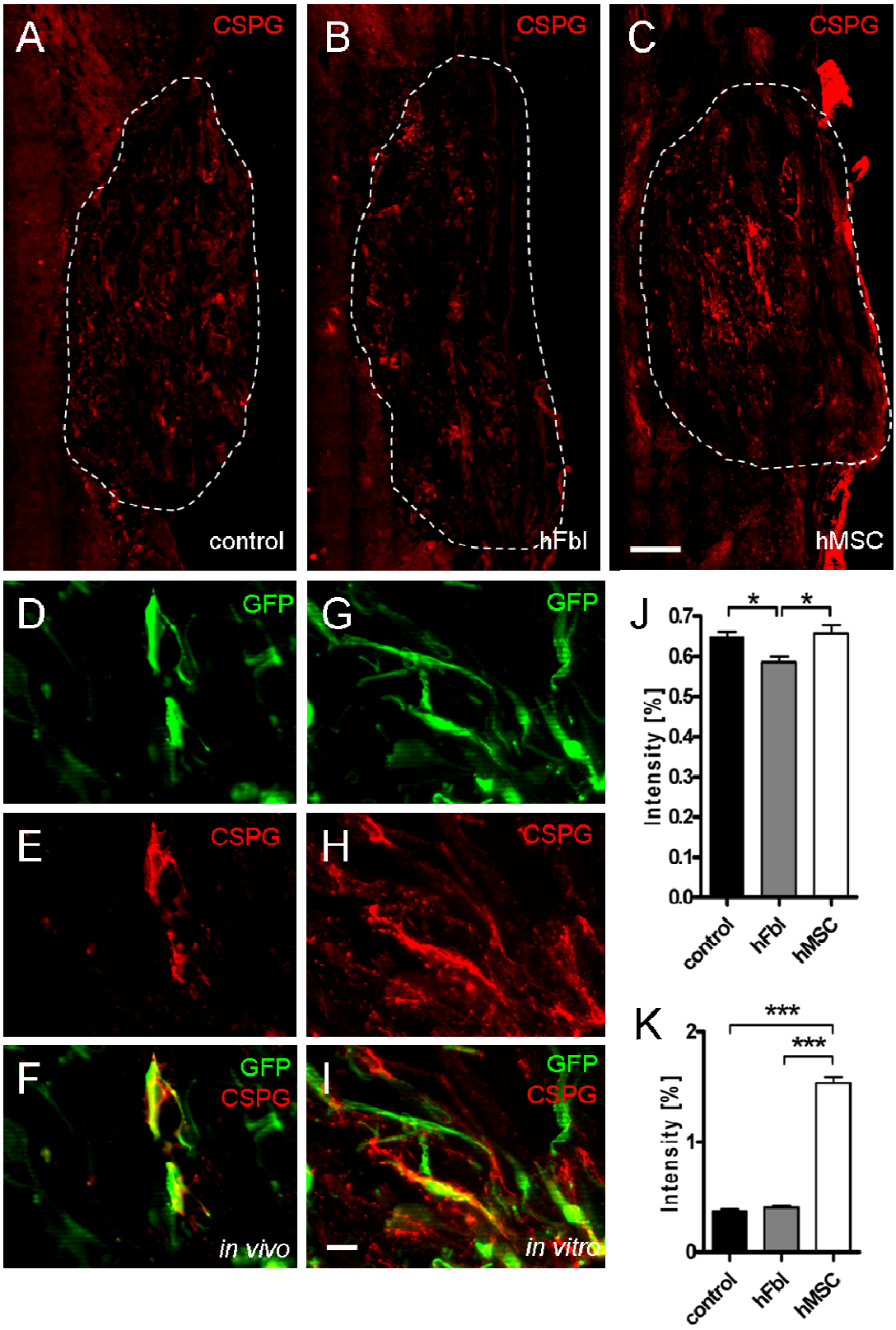

Figure 7.12: CSPG immunoghistochemistry demonstrates the expression of this important ECM-related molecule by hMSC *in vivo* and *in vitro*. The extracellular matrix protein CSPG was expressed around the implant in all three groups (A-C). Interestingly, CSPG could additionally be identified within the scaffold of hMSC-seeded implants (C). Double immunofluorescence demonstrated that hMSC expressed CSPG in vivo (D-F) and in vitro (G-I). Quantification revealed significantly decreased CSPG staining only around hFbl-seeded implants (J). However, quantification of the CSPG staining revealed significantly increased expression in the center of hMSC-seeded scaffolds compared to non- and hFbl-seeded scaffolds (K). Scale bar: 200 µm (A-C); 20 µm (D-I). *p<0.05; ***p<0.001.

7.4.4.6 Correlation of behavioural performance and axonal regeneration

To evaluate if the number of NF200-positive axons detected by immunohistochemistry may have an impact on the behavioural performance in grid-walk experiments at 8 weeks after surgery, these parameters from each individual animal were correlated.

As observed in the behavioural analysis, animals of the hMSC group presented a significantly lower numbers of foot-falls in grid-walk experiments compared to animals of the control and hFbl groups (see figure 7.4B). Furthermore, immunohistochemistry revealed higher numbers of axons in the hMSC-seeded scaffolds (see figure 7.9G). However, no significant correleation could be observed between these two paramaters (R^2=0.03; Figure 7.13).

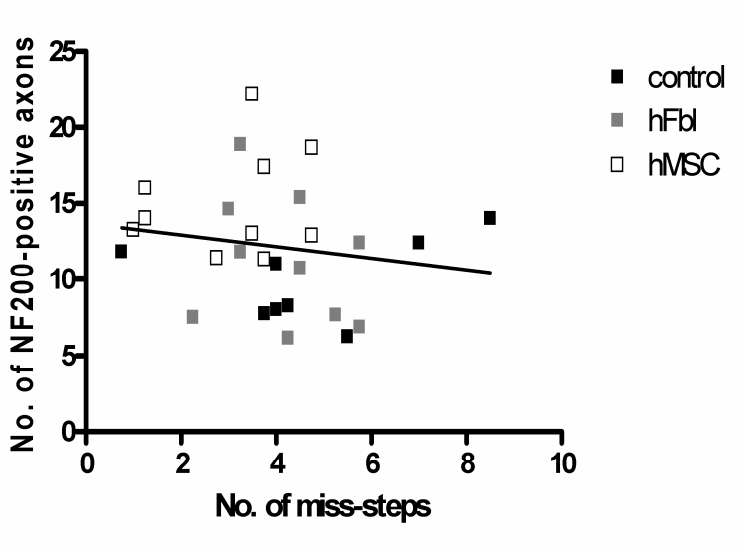

Figure 7.13: Correlation of behavioural analysis with axonal regeneration into the scaffolds. For correlation analysis, the following parameters were evaluated for each animal at 8 weeks after scaffold implantation: number of miss-steps in grid-walk experiments and the number of NF200-positive axons found in the scaffolds. Although animals with higher numbers of NF200-positive axons had fewer miss-steps, the correlation between these 2 parameters was weak.

7.5 Discussion

Implantation of immobilized MSC has the great advantage that the cells should stay at the area of interest rather than migrating to other areas. A number of different biomaterials have been investigated for the delivery of MSC into spinal cord lesions, such as hydrogels (220) or denuded human amniotic membrane (221). However, these biomaterials have no intrinsic guiding or orientational structures that could enable a directed axonal regeneration through the lesion site.

After implantation of the oriented biomaterial, animals of all three groups presented a minor weight loss at 1 week. This expected surgery-induced weight loss was compensated at 4 weeks and further increased at 8 weeks.

The present use of an oriented biomaterial for such a strategy (i.e. a collagen scaffold seeded with hMSC) has demonstrated a transient acceleration of functional recovery in an acute model of spinal cord injury. Furthermore, the porous microstructure of the scaffold persisted in all three groups during the whole experimental procedure and could, in theory, facilitate further axonal regeneration beyond 8 weeks. Implantation of hMSC, however, demonstrated to have an early effect directly after surgery, suggesting that hMSC influence the host tissue by tissue sparing. Due to the high heterogeneity between different hMSC samples (211), this effect might be donor-dependent. Since only cells of one donor were used in this study, further investigations need to correlate the ECM, growth factor and cytokine composition of different donor samples with the behavioural results to identify hMSC with the highest improving properties.

The use of the CatWalk gait analysis system enabled an objective and reliable method of evaluating locomotor parameters after lateral funiculotomy and the direct implantation of oriented scaffolds. Although all animals were trained to run continuously onto the CatWalk and only 3 runs out of 8 were evaluated that were nearest to 1.4 s, animals of all three groups presented longer runtimes 1 week postoperatively. Four and 8 weeks after surgery, the crossing time of all animals decreased and was even a little bit lower than before surgery. Since there were no significant differences in body weight and crossing time between all three groups, the results of the CatWalk gait analysis system can be objectively valuated. The regularity index, a measure for the exclusive use of normal step sequence pattern, was significantly reduced at 1 week compared to BL values, but was almost normalized in all three groups after 4 and 8 weeks. At 8 weeks, however, one animal of the hMSC group still presented some irregularities.

As early as 1 week after implantation, functional parameters like stance and swing duration, duty cycle, print and max area, as well as intensity of paw placement all showed a significant but transient increase in the rate of improvement (at 4 weeks post implantation) in animals which received hMSC-seeded scaffold compared to control animals. However, 8 weeks after implantation, the statistical significance of this effect was no longer detectable, but the positive trend was nonetheless clear. Furthermore, front-limb/hind-limb coordination was additionally significantly improved after 4 and 8 weeks in the hMSC-seeded scaffold group compared to control animals, as demonstrated by grid-walk experiments. Interestingly, this functional improvement was detectable in all animals despite the fact that only low numbers of donor cells could be detected within the scaffold in 60% of the animals. Although, the number of detectable donor cells was low, there was no evidence of cell migration into the host tissue. This suggests that there was a relatively poor survival rate of donor cells which may have been caused by the immediate transplantation of cells and scaffold into the lesion site. It has already been demonstrated in a contusion injury model that rat MSC show a significantly better survival rate when transplanted 1 week after injury, when compared with cells that were implanted directly after injury (49). Interestingly, the survival of hFbl, which served as a cellular control, was even lower: only 10% of the animals revealed viable donor hFbl. The better survival of hMSC might be due to their reported immunosuppressive properties (222-225). Others have suggested that these immunosuppressive properties might also be responsible for the reduced astrocyte and macrophage/microglia reactivity (226).

The sensory function of both hind-paws was not consistently changed during the whole experimental procedure as demonstrated by von Frey filaments. This is likely due to the fact that the ascending sensory fibers located in the dorsal funiculus, were not affected by the lateral funiculotomy.

Significantly higher numbers of NF200-positive axons could be identified in animals which received hMSC-seeded scaffolds compared to control animals, even though only few donor hMSC could be detected within the scaffolds at 8 weeks after transplantation. The regenerating axons formed bundles in a direction that followed the pores of the scaffold. Interestingly, these pores were filled by host cells of unknown phenotype. These cells, presumably Schwann cells or fibroblasts, must have invaded the scaffold after implantation. Schwann cells could be easily be identified by staining for the low affinity nerve growth factor receptor p75. Identification of fibroblasts is, however, more complicated due to the lack of cell-specific markers. One possibility to identify fibroblasts would be the staining for fibronectin (227). Unfortunately, hMSC and other cell types express fibronectin as well (228) and double-immunofluorescence staining might not satisfactorily clarify the phenotype of these cells. Due to the limited amount of spinal cord sections and the difficulties to perform double-

immunofluorescence staining, these investigations could not be performed in this study, but should be included in further investigations.

Elevated GFAP staining surrounding the implant could be identified in all three groups. However, implantation of either hMSC- or hFb-seeded scaffolds resulted in a significantly decreased astrocytic response. The decreased astrogliosis in animals which received cell-seeded implant might have contributed to the increased ingrowth of regenerating axons.

CSPG, a major component of the glial scar, is widely believed to limit axonal growth after spinal cord injury (218, 219). Staining of CSPG could be identified around the implanted scaffold in all three groups. Decreased CSPG expression surrounding the implant could only be detected in animals which received hFbl-seeded implants. Interestingly, animals receiving hMSC-seeded scaffolds demonstrated significantly higher CSPG expression within the scaffold compared to non- and hFbl-seeded scaffolds. Double-immunofluorescence demonstrated that hMSC express CSPG *in vitro* and *in vivo*. Therefore, it is likely that the strong CSPG expression found within the scaffold of hMSC-seeded implants was a residue of early proteoglycan expression from donor hMSC, which were subsequently lost. Although CSPG expression in spinal cord lesions is regarded to have a negative impact on regenerative capacity (229-231), a recent report by Rolls et al. suggests that beneficial effects of CSPGs on axonal regeneration are also possible (232). This beneficial effect of CSPG has been reported to be due to the modulation of macrophage and microglia behaviour, therefore affecting the overall repair process. Furthermore, regulation of other aspects of macrophage/microglia phenotype by CSPGs, i.e. phagocytosis or neurotrophic factor secretion has also been suggested. Expression of CSPG directly after injury promotes spinal cord repair and decreases tissue loss at the injury site. These observations lead to the conclusion that the acute implantation of highly CSPG-expressing hMSC into the lesion site may have promoted some degree of spinal cord repair. This might further explain the prominent behavioural effects observed 1 week after the implantation of hMSC-seeded scaffolds. In the present investigation no double-immunofluorescence staining of CSPG and NF200 could be performed due to the GFP expression by transplanted hMSC and the limited amount of sections. Further investigations should include such double-staining to correlate the regrowing axons with the CSPG expression within the scaffold.

Since CSPG expression is thought to modulate macrophage and microglia function, the distribution and intensity of Iba1 staining in the present investigation is of particular interest. Iba1 expression was present in all three implantation groups and could be found in the host tissue as well as in the scaffold. However, decreased levels of Iba1 staining were detected in the hMSC group, suggesting lower macrophages/microglia infiltration than in the control- and hFbl groups. This observation tends to support the observations of Roll et al. (18) and might

contribute to an understanding of the apparent (but transient) beneficial effects brought about by hMSC-seeded scaffold implantation.

Macrophages and microglia induce a reactive process of secondary tissue degeneration and cell death in the area surrounding the original injury by their expression and release of metalloproteinases, proteolytic- and oxidative enzymes (233, 234). The extent of such secondary tissue degeneration around the implant has been investigated with NeuN staining, as demonstrated recently by Davies et al. (235). It would be interesting to know if implantation of hMSC- seeded scaffolds would be able to preserve more neurons around the lesion than control scaffolds. The observed behavioural improvement already 1 week after injury suggests that the beneficial effect by hMSC-seeded implants is the result of spared tissue rather than regrowing axons. Therefore, future investigations should include NeuN-staining of these implants already after 1 week after injury.

However, macrophages have also been reported to promote beneficial effects after spinal cord injury through the phagocytosis of myelin debris, which is known to inhibit axonal regeneration (236, 237). However, the inflammatory response in the spinal cord proceeds at a slower rate than in other tissues, leading to only a slow removal of tissue and myelin debris (238). The influence of the inflammatory response after spinal cord injury is clearly a complex and somewhat controversially discussed area of research, however a consequence of inflammation would be to induce the production of neurotrophic factors like NGF, FGF, and GDNF (239, 240).

7.6 Conclusion

It is clear that the regeneration process of the injured spinal cord is a very complex issue in which numerous factors play crucial roles, including ECM-, growth factor- and cytokine release by resident and implanted cells. Their impact on tissue sparing, axon regeneration and myelination are issues that can profoundly affect functional outcome after injury and implantation. The present study has demonstrated some interesting but transient beneficial effects of acutely transplanted hMSC-seeded scaffolds into experimental spinal cord lesions. However, there are clearly many more questions that need to be answered before any firm conclusion can be drawn about the potential usefulness of such an intervention strategy in promoting tissue repair or axon regeneration after spinal cord injury.

8. General discussion

The aim of this thesis was to broaden the knowledge about the fate and function of MSC in their use in transplantation strategies for spinal cord injury. Four different explanations for their beneficial effects in SCI had already been suggested:

(1) MSC transdifferentiate into cells of the neural lineage and replace lost cells (72-80)

(2) Grafted MSC fuse with cells of the host's nervous system to impart their beneficial effects (19)

(3) Grafted MSC modulate the host's immune system (156)

(4) Grafted MSC produce a number of different growth factors that promote neuronal survival and axonal growth (54, 127, 129, 131).

In vitro transdifferentiation using chemical agents or growth factors has aroused great scepticism since this effect occurred within a time scale of minutes to hours after induction, a speed that was not comparable with the pace of the normal developmental process (114). The neuronal-like morphological changes induced by such stimulation were interpreted as being due to environmental stress, leading to physical contraction of the cells without an increased expression of neuronal markers (241). To further support this notion, several other stressors, such as detergents, chloride and extreme pH were also found to induce similar morphological changes. Time-lapse video-microscopy revealed that cellular shrinkage was responsible for the appearance of the neurite-like processes (241). This mechanism was further determined to be due to the breakdown of the actin cytoskeleton (115).

The fusion of MSC with cells of host's nervous system and the subsequent apparent adoption phenotype of the recipient cells was suggested to improve functional recovery after SCI. However, the frequency of spontaneous fusion is very low and therefore can not explain spinal cord regeneration (19).

Modulation of the host's immune system by transplanted MSC certainly could explain the functional recovery after SCI. Indeed, MSC have the capacity to inhibit the cell division of immune-competent cells, resulting in a lower inflammatory response (242).

The last issue of the expression of growth factors could also contribute to tissue sparing and axon regeneration. Several growth factors are reported to be expressed by MSC, i.e. BDNF, bFGF, NGF and VEGF (54, 131). However, this growth factor expression exhibits donor variability which influences the extend of neuritic outgrowth (127).

In the following section, the main results in this thesis will be summarized and discussed. Furthermore, the implications of the present results for future research will be considered.

8.1 HMSC express neural-related markers

In the last ten years, several *in vitro* and *in vivo* investigations have been performed which claimed to demonstrate the ability of MSC to differentiate into cells of the neural lineage (49, 65, 72-80). These studies aroused great interest since such a capacity would open extensive possibilities for autologous therapeutic treatments in a variety of neurological disorders. However, many of these studies suffered from the methodological weakness of evaluating expression patterns for neural-related markers only after induction or implantation (37, 72, 113).

In this thesis, the expression of several neural-related markers could be demonstrated in undifferentiated hMSC by PCR and immunocytochemistry. The hMSC expressed neural-related markers such as nestin, Enolase2, Nurr1 and MAP1b. More interestingly, however, was the identification of the immense donor-dependent heterogeneity between the samples. For example, DRD2, NFL, MBP and STX1A could only be identified in some of the donor samples, although all cells had been isolated from the patient bone marrow and expanded using the same culture medium and protocol. This inter-donor variability in neural-related marker expression is of immense importance when attempting to understand the apparent controversy regarding the ability of such cells to transdifferentiate.

This on-going discussion has been stimulated by recent reports of hMSC transdifferentiation. It has been claimed that hMSC isolated from placenta (243) or umbilical cord (244) are capable of such transdifferentiation. Macias and colleagues described an elevated expression of β-III tubulin and NF200 after induction of placenta-derived hMSC using a differentiation medium containing dimethylsulfoxide (DMSO) (243). Although all 3 donor hMSC samples demonstrated a dramatic change in cell morphology and marker expression, it is most likely that the DMSO-containing induction protocol resulted in cellular shrinkage and breakdown of the actin cytoskeleton, as demonstrated previously with bone marrow-derived hMSC (115, 241). Furthermore, the data of the present thesis has demonstrated that there are immense differences in marker gene expression between donors. Therefore, the evaluation of only two markers without corresponding functional investigations is insufficient to support claims of efficient transdifferentiation. The report by Zhang and colleagues has suggested transdifferentiation of hMSC derived from umbilical cord to a neural stem cell phenotype after cultivation in serum-free medium supplemented with bFGF, EGF and B27 (244). Formation of spheres and expression of nestin was regarded as functional conversion to neural stem cells. However, nestin expression prior to transdifferentiation had not been evaluated. As clearly

demonstrated in the present thesis, nestin expression may be detected in 100% of the bone marrow-derived hMSC and, thus, cannot be regarded as incontrovertible evidence of transdifferentiation.

Although there is a substantial number of publications claiming to present protocols capable of supporting transdifferentiation (e.g. application of chemical compounds (37, 68-71), growth factors (72-75) or neurosphere-like cultivation (76-81)), by hMSC derived from different sources, the heterogeneity between different donor hMSC samples suggests that true transdifferentiation of hMSC is an unlikely event, or at best, still remains to be clearly defined.

8.2 Serum-reduced expansion of hMSC

For the translation of MSC-based transplantation strategies from the laboratory bench to the clinic, the use of a standardized serum-free medium is essential. The conventional medium used for laboratory expansion of MSC contains 10% serum. Such animal- or donor-derived sera might transfer infectious agents or lead to an elevated immune response (139). Therefore, it was deemed timely to assess the potential of the newly developed and commercially available serum-free medium, Panserin 401, on the isolation and expansion of hMSC.

Isolation and proliferation of hMSC were investigated in Panserin 401 media without serum, supplemented with 10% FBS or with 2% FBS and growth factors, and compared with the conventional medium of DMEM with 10% FBS. Although Panserin 401 was designed for serum-free expansion of a number of different cell types, hMSC could not be isolated and expanded without serum. However, the combination of Panserin with reduced serum (2% FBS) and growth factors was able to support significantly greater hMSC proliferation than was seen with conventional medium. Furthermore, Panserin 401 supplemented with 2% FBS and growth factors did not change hMSC multipotency as demonstrated by adipogenic and osteogenic differentiation. Thus, the identification of a serum-free cultivation protocol for the clinical application of hMSC was not achieved in this thesis. However, a substantial reduction of serum levels was accomplished which, furthermore, presented improved cell proliferation. Due to this lower serum concentration, the possibility of using the patients own serum for hMSC isolation and expansion could be considered.

However, the development of functional serum-free culture conditions for the expansion of bone marrow-derived hMSC has recently been reported by two individual groups (245, 246). Mimura and colleagues applied a medium that was initially developed for embryonic stem cell cultivation (247), which was further supplemented with bFGF, heparin, and TGF-β1. The cultivated hMSC cell line (UE7T-13) maintained the expression of CD73, CD90 and CD105,

as well as adipogenic and osteogenic differentiation capacity. Since these results were obtained with a single hMSC cell line, the capacity of efficient isolation and expansion of hMSC by this serum-free medium needs to be further investigated. Chase and colleagues employed a commercially available medium (StemPro MSC SFM by Invitrogen) supplemented with PDGF-BB, bFGF and TGF-β1 (246). This serum-free medium revealed the same proliferation rate and differentiation capacity as with the conventional medium (DMEM supplemented with 10% FBS). However, even though these initial experiments were performed using a pool of four different donors, it cannot be excluded that the cells from the individual donors grew with different proliferation rates. Clearer data would have been generated if the investigators had decided to analyze the responses of the individual donors separately. The comparison of isolation efficiency and the generation of sufficient cell numbers between the serum-free and conventional medium was, however, not presented.

Although a growth factor composition, including bFGF and PDGF-BB, was applied in the present thesis, serum-free cultivation of hMSC could not be achieved. The novel and promising results presented by the Mimura and Chase research groups suggest that further investigations into serum-free cultivation using Panserin 401 should also include the supplementation of TGF-β1.

8.3 Growth factor and cytokine expression by hMSC

Increasing evidence has indicated that the beneficial effects of donor MSC in tissue defects might be due to the expression of growth factors and cytokines (248). Although the expression of some of these molecules has already been presented (54, 127, 131), the question as to whether the expression of molecules might be differentially regulated by the local environments of specific damaged host tissues had not been addressed.

In this thesis, it could be demonstrated that the basal expression of the investigated growth factors and cytokines was donor-dependent. Interestingly, the regulation of growth factor and cytokine expression by LPS was additionally found to be donor-dependent. Since it was of interest to determine whether hMSC change their growth factor and cytokine expression patterns when implanted into lesioned spinal cord, an *in vitro* assay with tissue extract from normal and injured rat spinal cord was performed. To further evaluate the tissue-specificity of the expression pattern change, the effects of tissue extracts from normal and injured rat heart were also investigated. Although the growth factor and cytokine expression pattern could be altered by LPS stimulation, cultivation with tissue extract did not influence this pattern. However, it could be demonstrated that tissue extract enhanced hMSC proliferation but had no effect on cell migration.

These results indicate that hMSC maintain their expression patterns when implanted into spinal cord lesions. In contrast to the observations of this thesis, a recent report by Nicaise et al. describes the existence of growth factor expression changes of rat MSC after incubation with brain or spinal cord extract from amyotophic lateral sclerosis affected rats (249). The stimulation with the extracts resulted in a significant increase in NGF, BDNF and VEGF expression, whereas bFGF, IGF1, GDNF and HGF remained unaffected. A change in the growth factor expression of rat MSC upon stimulation with rat tissue extract is possible, but if these results can be transferred to human MSC remains unknown.

By further investigating the effect of heart tissue, it could be similarly demonstrated that there was no tissue-specificity in the growth factor and cytokine expression pattern. Therefore, the immense differences in basal expression patterns between different donors could influence the anticipated beneficial effect after hMSC transplantation in spinal cord lesions. It has to be suggested that some donor cells may not improve functional recovery after SCI due to their inappropriate expression pattern. However, LPS-treatment was demonstrated to alter the growth factor and cytokine expression which may, in theory, enhance the beneficial properties of hMSC when used in regenerative medicine.

In the report of Neuhuber and colleagues, it could be demonstrated that the variability in growth factor and cytokine expression by different hMSC samples had an immense impact on the functional and histological outcome after implantation into rat spinal cord lesions (127). To further support their results, dorsal root ganglia were incubated with conditioned media from different donors. Interestingly, although all conditioned media supported axonal outgrowth compared to normal culture medium, no correlation between the *in vitro* and *in vivo* results could be observed (127).

These results suggest that such *in vitro* data may not be representative of the underlying mechanism of functional improvement that have been observed *in vivo*.

8.4 Accelerated but transient spinal cord recovery induced by implantation of a microstructured 3D scaffold seeded with hMSC

The regenerative properties of MSC in spinal cord injury have mainly been investigated using compression models of SCI followed by the injection of MSC directly into the lesion site (49, 50, 56) or the surrounding tissue (57, 250). However, sufficient bridging of the lesion may require the immobilization of MSC within a biomaterial. Therefore, the goal of this thesis was to investigate the potential beneficial effects of combining hMSC and a microstructured 3D scaffold for experimental spinal cord repair. The oriented pores of the microstructured scaffold were intended to guide regrowing axons through the lesion site.

Earlier investigations of spinal cord regeneration by MSC have used the BBB score (251) to rate the functional outcome (49, 50, 53, 56, 127, 221). This score, however, was developed for contusion injuries of the spinal cord and the (subjective) correct rating is impeded by fast moving animals. In this thesis, the gait analysis was performed using the CatWalk gait analysis sytem which enables reliable objective quantitative data on numerous gait parameters after different spinal cord injury models (213, 214). Furthermore, this was the first application of the CatWalk gait analysis system to investigate the effect of MSC transplantation in acute spinal cord lesions.

The implanted hMSC-seeded scaffolds demonstrated an early increase in recovery of motor function by 1 week after implantation, which was statistically significant by 4 weeks. However, little further improvement could be detected by the end of the experiment. It therefore has to be concluded that hMSC have an important function in the early recovery after SCI. On the other hand, Hofstetter and colleagues compared direct and delayed (7 days post injury) transplantation of rat MSC into a T9 contusion injury and reported functional improvement only after delayed application (49). However, others have reported that delayed (9 days) transplantation of rat MSC in a T9 clip compression model resulted in no functional improvement (56). Therefore, it might be possible that the application of MSC preparations from different species in a number of spinal cord injury models may have led to the apparent variability in their effects on functional outcome.

Immunohistochemistry revealed that, by 8 weeks post implantation, only small numbers of hMSC could be identified in 60% of the animals. However, significantly more regenerating axons could be detected in animals which had received hMSC-seeded scaffolds. Furthermore, the glial and inflammatory responses were reduced in the scaffold+hMSC group. HMSC-seeded scaffolds were found to be filled with CSPG and double immunofluorescence revealed that remaining hMSC were CSPG-positive. Since *in vitro* investigations have revealed that the extracellular matrix of hMSC is capable of directing (to some extent) the axonal outgrowth from dissociated adult rat dorsal root ganglia (252), it may be concluded that CSPG, shown in the present thesis to be expressed by these cells, may have contributed to this effect.

The reduction in the astrocytic and inflammatory responses might be related to the immuno-modulatory properties of hMSC (226). CSPG expression has widely been regarded to impair axon regeneration in the lesioned spinal cord. However, a beneficial effect of elevated CSPG expression has also been reported (232). This effect is considered to be due to the modulation of macrophage/microglia function and an early increase of expression has been reported to promote spinal cord repair. By implanting CSPG-expressing hMSC directly into the lesion, such modulation might have taken place, resulting in the early effect observed by the behavioural analysis. However, since the present investigation only included

immunohistochemical analyses at the later, 8 week, survival time, such a suggestion must remain pure speculation. Nonetheless, the early (though transient) improvement of function suggests that the likely mechanism of action of donor hMSC is by modulation of the local environment (e.g. tissue sparing) within the injured spinal cord by the release of growth factors, cytokines and ECM molecules. Such tissue sparing has been previously reported following the implantatiojn of MSC from a range of different species into a number of different spinal cord injury lesion models (53, 56, 57, 127).

8.5 Future perspectives

In this thesis it became evident that each donor hMSC preparation had its own individual growth factor and cytokine expression pattern and that not all samples are likely to be suitable for cell implantation strategies for spinal cord repair. Therefore, it is of great importance to determine which expression pattern for these molecules is most likely to promote spinal cord repair. Such information will be crucial for the transfer of such a therapeutic approach to a clinical application.

The combination of hMSC and an oriented 3D scaffold was also demonstrated to have important properties in the transient acceleration of spinal cord repair following acute lesions. The present thesis suggests that such improved function is likely to be due to the production of growth factors, cytokines and ECM which modulate the environment rather than transdifferentiating into cells of the neural lineage.

The transfer to clinical application of an autologous combinatory intervention strategy is, so far, limited. If it is known which donor hMSC have the best regenerative properties, an autologous approach may still be impracticable, since isolation and characterization of the cells is too time-consuming to provide the early effects of hMSC transplantation. However, the use of well characterized allogenic hMSC for transplantation might be practicable. Since hMSC have hypoimmunogenic properties (253), transplantation can also be performed with mismatched individuals. Furthermore, transplanted hMSC do not replace cells of the destroyed tissue but modulate the initially injured microenvironment. Long survival of the transplanted hMSC in the spinal cord seems to be not essential.

9. References

1. Potten CS, Loeffler M. Stem cells: attributes, cycles, spirals, pitfalls and uncertainties. Lessons for and from the crypt. Development 1990;110(4):1001-20.

2. Spangrude GJ, Heimfeld S, Weissman IL. Purification and characterization of mouse hematopoietic stem cells. Science 1988;241(4861):58-62.

3. Prockop DJ. Marrow stromal cells as stem cells for nonhematopoietic tissues. Science 1997;276(5309):71-4.

4. Alison M, Sarraf C. Hepatic stem cells. J Hepatol 1998;29(4):676-82.

5. Watt FM. Epidermal stem cells: markers, patterning and the control of stem cell fate. Philos Trans R Soc Lond B Biol Sci 1998;353(1370):831-7.

6. Gage FH. Mammalian neural stem cells. Science 2000;287(5457):1433-8.

7. Potten CS. Stem cells in gastrointestinal epithelium: numbers, characteristics and death. Philos Trans R Soc Lond B Biol Sci 1998;353(1370):821-30.

8. Adams GB, Scadden DT. The hematopoietic stem cell in its place. Nat Immunol 2006;7(4):333-7.

9. de Rooij DG, Grootegoed JA. Spermatogonial stem cells. Curr Opin Cell Biol 1998;10(6):694-701.

10. Weissman IL. Stem cells: units of development, units of regeneration, and units in evolution. Cell 2000;100(1):157-68.

11. Vats A, Tolley NS, Polak JM, Buttery LD. Stem cells: sources and applications. Clin Otolaryngol Allied Sci 2002;27(4):227-32.

12. Spalding KL, Bhardwaj RD, Buchholz BA, Druid H, Frisen J. Retrospective birth dating of cells in humans. Cell 2005;122(1):133-43.

13. Spradling A, Drummond-Barbosa D, Kai T. Stem cells find their niche. Nature 2001;414(6859):98-104.

14. Lin H. The stem-cell niche theory: lessons from flies. Nat Rev Genet 2002;3(12):931-40.

15. Schofield R. The relationship between the spleen colony-forming cell and the haemopoietic stem cell. Blood Cells 1978;4(1-2):7-25.

16. Moore KA, Lemischka IR. Stem cells and their niches. Science 2006;311(5769):1880-5.

17. Slack JM, Tosh D. Transdifferentiation and metaplasia--switching cell types. Curr Opin Genet Dev 2001;11(5):581-6.

18. Westmacott A, Burke ZD, Oliver G, Slack JM, Tosh D. C/EBPalpha and C/EBPbeta are markers of early liver development. Int J Dev Biol 2006;50(7):653-7.

19. Terada N, Hamazaki T, Oka M, Hoki M, Mastalerz DM, Nakano Y, et al. Bone marrow cells adopt the phenotype of other cells by spontaneous cell fusion. Nature 2002;416(6880):542-5.

20. Ying QL, Nichols J, Evans EP, Smith AG. Changing potency by spontaneous fusion. Nature 2002;416(6880):545-8.

21. Verfaillie CM, Pera MF, Lansdorp PM. Stem cells: hype and reality. Hematology Am Soc Hematol Educ Program 2002:369-91.

22. Morrison SJ, Kimble J. Asymmetric and symmetric stem-cell divisions in development and cancer. Nature 2006;441(7097):1068-74.

23. Marshman E, Booth C, Potten CS. The intestinal epithelial stem cell. Bioessays 2002;24(1):91-8.

24. Brawley C, Matunis E. Regeneration of male germline stem cells by spermatogonial dedifferentiation in vivo. Science 2004;304(5675):1331-4.

25. Tang DG, Tokumoto YM, Apperly JA, Lloyd AC, Raff MC. Lack of replicative senescence in cultured rat oligodendrocyte precursor cells. Science 2001;291(5505):868-71.

26. Shen CN, Slack JM, Tosh D. Molecular basis of transdifferentiation of pancreas to liver. Nat Cell Biol 2000;2(12):879-87.

27. Friedenstein AJ, Chailakhyan RK, Latsinik NV, Panasyuk AF, Keiliss-Borok IV. Stromal cells responsible for transferring the microenvironment of the hemopoietic tissues. Cloning in vitro and retransplantation in vivo. Transplantation 1974;17(4):331-40.

28. Pittenger MF, Mackay AM, Beck SC, Jaiswal RK, Douglas R, Mosca JD, et al. Multilineage potential of adult human mesenchymal stem cells. Science 1999;284(5411):143-7.

29. Gronthos S, Franklin DM, Leddy HA, Robey PG, Storms RW, Gimble JM. Surface protein characterization of human adipose tissue-derived stromal cells. J Cell Physiol 2001;189(1):54-63.

30. Jankowski RJ, Deasy BM, Huard J. Muscle-derived stem cells. Gene Ther 2002;9(10):642-7.

31. Kuznetsov SA, Mankani MH, Gronthos S, Satomura K, Bianco P, Robey PG. Circulating skeletal stem cells. J Cell Biol 2001;153(5):1133-40.

32. Rosada C, Justesen J, Melsvik D, Ebbesen P, Kassem M. The human umbilical cord blood: a potential source for osteoblast progenitor cells. Calcif Tissue Int 2003;72(2):135-42.

33. Tsai MS, Lee JL, Chang YJ, Hwang SM. Isolation of human multipotent mesenchymal stem cells from second-trimester amniotic fluid using a novel two-stage culture protocol. Hum Reprod 2004;19(6):1450-6.

34. Dominici M, Le Blanc K, Mueller I, Slaper-Cortenbach I, Marini F, Krause D, et al. Minimal criteria for defining multipotent mesenchymal stromal cells. The International Society for Cellular Therapy position statement. Cytotherapy 2006;8(4):315-7.

35. Kim S, Honmou O, Kato K, Nonaka T, Houkin K, Hamada H, et al. Neural differentiation potential of peripheral blood- and bone-marrow-derived precursor cells. Brain Res 2006.

36. Krampera M, Marconi S, Pasini A, Galie M, Rigotti G, Mosna F, et al. Induction of neural-like differentiation in human mesenchymal stem cells derived from bone marrow, fat, spleen and thymus. Bone 2006.

37. Woodbury D, Schwarz EJ, Prockop DJ, Black IB. Adult rat and human bone marrow stromal cells differentiate into neurons. J Neurosci Res 2000;61(4):364-70.

38. Sato Y, Araki H, Kato J, Nakamura K, Kawano Y, Kobune M, et al. Human mesenchymal stem cells xenografted directly to rat liver are differentiated into human hepatocytes without fusion. Blood 2005;106(2):756-63.

39. Lange C, Bassler P, Lioznov MV, Bruns H, Kluth D, Zander AR, et al. Liver-specific gene expression in mesenchymal stem cells is induced by liver cells. World J Gastroenterol 2005;11(29):4497-504.

40. Friedenstein AJ, Chailakhjan RK, Lalykina KS. The development of fibroblast colonies in monolayer cultures of guinea-pig bone marrow and spleen cells. Cell Tissue Kinet 1970;3(4):393-403.

41. Horwitz EM, Le Blanc K, Dominici M, Mueller I, Slaper-Cortenbach I, Marini FC, et al. Clarification of the nomenclature for MSC: The International Society for Cellular Therapy position statement. Cytotherapy 2005;7(5):393-5.

42. Richardson PM, McGuinness UM, Aguayo AJ. Axons from CNS neurons regenerate into PNS grafts. Nature 1980;284(5753):264-5.

43. Asada Y, Kawaguchi S, Hayashi H, Nakamura T. Neural repair of the injured spinal cord by grafting: comparison between peripheral nerve segments and embryonic homologous structures as a conduit of CNS axons. Neurosci Res 1998;31(3):241-9.

44. Blakemore WF, Crang AJ. The use of cultured autologous Schwann cells to remyelinate areas of persistent demyelination in the central nervous system. J Neurol Sci 1985;70(2):207-23.

45. Ramon-Cueto A, Plant GW, Avila J, Bunge MB. Long-distance axonal regeneration in the transected adult rat spinal cord is promoted by olfactory ensheathing glia transplants. J Neurosci 1998;18(10):3803-15.

46. McDonald JW, Liu XZ, Qu Y, Liu S, Mickey SK, Turetsky D, et al. Transplanted embryonic stem cells survive, differentiate and promote recovery in injured rat spinal cord. Nat Med 1999;5(12):1410-2.

47. Han SS, Liu Y, Tyler-Polsz C, Rao MS, Fischer I. Transplantation of glial-restricted precursor cells into the adult spinal cord: survival, glial-specific differentiation, and preferential migration in white matter. Glia 2004;45(1):1-16.

48. Koda M, Okada S, Nakayama T, Koshizuka S, Kamada T, Nishio Y, et al. Hematopoietic stem cell and marrow stromal cell for spinal cord injury in mice. Neuroreport 2005;16(16):1763-7.

49. Hofstetter CP, Schwarz EJ, Hess D, Widenfalk J, El Manira A, Prockop DJ, et al. Marrow stromal cells form guiding strands in the injured spinal cord and promote recovery. Proc Natl Acad Sci U S A 2002;99(4):2199-204.

50. Chopp M, Zhang XH, Li Y, Wang L, Chen J, Lu D, et al. Spinal cord injury in rat: treatment with bone marrow stromal cell transplantation. Neuroreport 2000;11(13):3001-5.

51. Wehner T, Bontert M, Eyupoglu I, Prass K, Prinz M, Klett FF, et al. Bone marrow-derived cells expressing green fluorescent protein under the control of the glial fibrillary acidic protein promoter do not differentiate into astrocytes in vitro and in vivo. J Neurosci 2003;23(12):5004-11.

52. Hess DC, Hill WD, Martin-Studdard A, Carroll J, Brailer J, Carothers J. Bone marrow as a source of endothelial cells and NeuN-expressing cells After stroke. Stroke 2002;33(5):1362-8.

53. Ankeny DP, McTigue DM, Jakeman LB. Bone marrow transplants provide tissue protection and directional guidance for axons after contusive spinal cord injury in rats. Exp Neurol 2004;190(1):17-31.

54. Chen X, Katakowski M, Li Y, Lu D, Wang L, Zhang L, et al. Human bone marrow stromal cell cultures conditioned by traumatic brain tissue extracts: growth factor production. J Neurosci Res 2002;69(5):687-91.

55. Crigler L, Robey RC, Asawachaicharn A, Gaupp D, Phinney DG. Human mesenchymal stem cell subpopulations express a variety of neuro-regulatory molecules and promote neuronal cell survival and neuritogenesis. Exp Neurol 2006;198(1):54-64.

56. Parr AM, Kulbatski I, Wang XH, Keating A, Tator CH. Fate of transplanted adult neural stem/progenitor cells and bone marrow-derived mesenchymal stromal cells in the injured adult rat spinal cord and impact on functional recovery. Surg Neurol 2008;70(6):600-7; discussion 607.

57. Sykova E, Jendelova P. Magnetic resonance tracking of implanted adult and embryonic stem cells in injured brain and spinal cord. Ann N Y Acad Sci 2005;1049:146-60.

58. Himes BT, Neuhuber B, Coleman C, Kushner R, Swanger SA, Kopen GC, et al. Recovery of function following grafting of human bone marrow-derived stromal cells into the injured spinal cord. Neurorehabil Neural Repair 2006;20(2):278-96.

59. Deng YB, Liu XG, Liu ZG, Liu XL, Liu Y, Zhou GQ. Implantation of BM mesenchymal stem cells into injured spinal cord elicits de novo neurogenesis and functional recovery: evidence from a study in rhesus monkeys. Cytotherapy 2006;8(3):210-4.

60. Iwashita Y, Crang AJ, Blakemore WF. Redistribution of bisbenzimide Hoechst 33342 from transplanted cells to host cells. Neuroreport 2000;11(5):1013-6.

61. Moviglia GA, Fernandez Vina R, Brizuela JA, Saslavsky J, Vrsalovic F, Varela G, et al. Combined protocol of cell therapy for chronic spinal cord injury. Report on the electrical and functional recovery of two patients. Cytotherapy 2006;8(3):202-9.

62. Sykova E, Homola A, Mazanec R, Lachmann H, Konradova SL, Kobylka P, et al. Autologous bone marrow transplantation in patients with subacute and chronic spinal cord injury. Cell Transplant 2006;15(8-9):675-87.

63. Moviglia GA, Varela G, Gaeta CA, Brizuela JA, Bastos F, Saslavsky J. Autoreactive T cells induce in vitro BM mesenchymal stem cell transdifferentiation to neural stem cells. Cytotherapy 2006;8(3):196-201.

64. Azizi SA, Stokes D, Augelli BJ, DiGirolamo C, Prockop DJ. Engraftment and migration of human bone marrow stromal cells implanted in the brains of albino rats--similarities to astrocyte grafts. Proc Natl Acad Sci U S A 1998;95(7):3908-13.

65. Kopen GC, Prockop DJ, Phinney DG. Marrow stromal cells migrate throughout forebrain and cerebellum, and they differentiate into astrocytes after injection into neonatal mouse brains. Proc Natl Acad Sci U S A 1999;96(19):10711-6.

66. Brazelton TR, Rossi FM, Keshet GI, Blau HM. From marrow to brain: expression of neuronal phenotypes in adult mice. Science 2000;290(5497):1775-9.

67. Mezey E, Chandross KJ, Harta G, Maki RA, McKercher SR. Turning blood into brain: cells bearing neuronal antigens generated in vivo from bone marrow. Science 2000;290(5497):1779-82.

68. Deng W, Obrocka M, Fischer I, Prockop DJ. In vitro differentiation of human marrow stromal cells into early progenitors of neural cells by conditions that increase intracellular cyclic AMP. Biochem Biophys Res Commun 2001;282(1):148-52.

69. Munoz-Elias G, Woodbury D, Black IB. Marrow stromal cells, mitosis, and neuronal differentiation: stem cell and precursor functions. Stem Cells 2003;21(4):437-48.

70. Lee OK, Ko YC, Kuo TK, Chou SH, Li HJ, Chen WM, et al. Fluvastatin and lovastatin but not pravastatin induce neuroglial differentiation in human mesenchymal stem cells. J Cell Biochem 2004;93(5):917-28.

71. Jori FP, Napolitano MA, Melone MA, Cipollaro M, Cascino A, Altucci L, et al. Molecular pathways involved in neural in vitro differentiation of marrow stromal stem cells. J Cell Biochem 2005;94(4):645-55.

72. Sanchez-Ramos J, Song S, Cardozo-Pelaez F, Hazzi C, Stedeford T, Willing A, et al. Adult bone marrow stromal cells differentiate into neural cells in vitro. Exp Neurol 2000;164(2):247-56.

73. Jin K, Mao XO, Batteur S, Sun Y, Greenberg DA. Induction of neuronal markers in bone marrow cells: differential effects of growth factors and patterns of intracellular expression. Exp Neurol 2003;184(1):78-89.

74. Jiang Y, Henderson D, Blackstad M, Chen A, Miller RF, Verfaillie CM. Neuroectodermal differentiation from mouse multipotent adult progenitor cells. Proc Natl Acad Sci U S A 2003;100 Suppl 1:11854-60.

75. Tao H, Rao R, Ma DD. Cytokine-induced stable neuronal differentiation of human bone marrow mesenchymal stem cells in a serum/feeder cell-free condition. Dev Growth Differ 2005;47(6):423-33.

76. Wislet-Gendebien S, Leprince P, Moonen G, Rogister B. Regulation of neural markers nestin and GFAP expression by cultivated bone marrow stromal cells. J Cell Sci 2003;116(Pt 16):3295-302.

77. Croft AP, Przyborski SA. Generation of neuroprogenitor-like cells from adult mammalian bone marrow stromal cells in vitro. Stem Cells Dev 2004;13(4):409-20.

78. Suzuki H, Taguchi T, Tanaka H, Kataoka H, Li Z, Muramatsu K, et al. Neurospheres induced from bone marrow stromal cells are multipotent for differentiation into neuron, astrocyte, and oligodendrocyte phenotypes. Biochem Biophys Res Commun 2004;322(3):918-22.

79. Hermann A, Gastl R, Liebau S, Popa MO, Fiedler J, Boehm BO, et al. Efficient generation of neural stem cell-like cells from adult human bone marrow stromal cells. J Cell Sci 2004;117(Pt 19):4411-22.

80. Wislet-Gendebien S, Hans G, Leprince P, Rigo JM, Moonen G, Rogister B. Plasticity of cultured mesenchymal stem cells: switch from nestin-positive to excitable neuron-like phenotype. Stem Cells 2005;23(3):392-402.

81. Bunnell BA, Ylostalo J, Kang SK. Common transcriptional gene profile in neurospheres-derived from pATSCs, pBMSCs, and pNSCs. Biochem Biophys Res Commun 2006;343(3):762-71.

82. Scintu F, Reali C, Pillai R, Badiali M, Sanna MA, Argiolu F, et al. Differentiation of human bone marrow stem cells into cells with a neural phenotype: diverse effects of two specific treatments. BMC Neurosci 2006;7:14.

83. Hermann A, Liebau S, Gastl R, Fickert S, Habisch HJ, Fiedler J, et al. Comparative analysis of neuroectodermal differentiation capacity of human bone marrow stromal cells using various conversion protocols. J Neurosci Res 2006;83(8):1502-14.

84. Peister A, Mellad JA, Larson BL, Hall BM, Gibson LF, Prockop DJ. Adult stem cells from bone marrow (MSCs) isolated from different strains of inbred mice vary in surface epitopes, rates of proliferation, and differentiation potential. Blood 2004;103(5):1662-8.

85. Johnstone B, Hering TM, Caplan AI, Goldberg VM, Yoo JU. In vitro chondrogenesis of bone marrow-derived mesenchymal progenitor cells. Exp Cell Res 1998;238(1):265-72.

86. Grandy DK, Litt M, Allen L, Bunzow JR, Marchionni M, Makam H, et al. The human dopamine D2 receptor gene is located on chromosome 11 at q22-q23 and identifies a TaqI RFLP. Am J Hum Genet 1989;45(5):778-85.

87. Marangos PJ, Zis AP, Clark RL, Goodwin FK. Neuronal, non-neuronal and hybrid forms of enolase in brain: structural, immunological and functional comparisons. Brain Res 1978;150(1):117-33.

88. Sato-Yoshitake R, Shiomura Y, Miyasaka H, Hirokawa N. Microtubule-associated protein 1B: molecular structure, localization, and phosphorylation-dependent expression in developing neurons. Neuron 1989;3(2):229-38.

89. Zhang R, Maksymowych AB, Simpson LL. Cloning and sequence analysis of a cDNA encoding human syntaxin 1A, a polypeptide essential for exocytosis. Gene 1995;159(2):293-4.

90. Wiedenmann B, Franke WW. Identification and localization of synaptophysin, an integral membrane glycoprotein of Mr 38,000 characteristic of presynaptic vesicles. Cell 1985;41(3):1017-28.

91. Binder LI, Frankfurter A, Rebhun LI. The distribution of tau in the mammalian central nervous system. J Cell Biol 1985;101(4):1371-8.

92. Bignami A, Dahl D. Specificity of the glial fibrillary acidic protein for astroglia. J Histochem Cytochem 1977;25(6):466-9.

93. Popko B, Puckett C, Lai E, Shine HD, Readhead C, Takahashi N, et al. Myelin deficient mice: expression of myelin basic protein and generation of mice with varying levels of myelin. Cell 1987;48(4):713-21.

94. Deloulme JC, Assard N, Mbele GO, Mangin C, Kuwano R, Baudier J. S100A6 and S100A11 are specific targets of the calcium- and zinc-binding S100B protein in vivo. J Biol Chem 2000;275(45):35302-10.

95. Lo LC, Johnson JE, Wuenschell CW, Saito T, Anderson DJ. Mammalian achaete-scute homolog 1 is transiently expressed by spatially restricted subsets of early neuroepithelial and neural crest cells. Genes Dev 1991;5(9):1524-37.

96. Shimizu C, Akazawa C, Nakanishi S, Kageyama R. MATH-2, a mammalian helix-loop-helix factor structurally related to the product of Drosophila proneural gene atonal, is specifically expressed in the nervous system. Eur J Biochem 1995;229(1):239-48.

97. Pfaff SL, Mendelsohn M, Stewart CL, Edlund T, Jessell TM. Requirement for LIM homeobox gene Isl1 in motor neuron generation reveals a motor neuron-dependent step in interneuron differentiation. Cell 1996;84(2):309-20.

98. Simon HH, Saueressig H, Wurst W, Goulding MD, O'Leary DD. Fate of midbrain dopaminergic neurons controlled by the engrailed genes. J Neurosci 2001;21(9):3126-34.

99. Law SW, Conneely OM, DeMayo FJ, O'Malley BW. Identification of a new brain-specific transcription factor, NURR1. Mol Endocrinol 1992;6(12):2129-35.

100. Takayama S, Kochel K, Irie S, Inazawa J, Abe T, Sato T, et al. Cloning of cDNAs encoding the human BAG1 protein and localization of the human BAG1 gene to chromosome 9p12. Genomics 1996;35(3):494-8.

101. Lendahl U, Zimmerman LB, McKay RD. CNS stem cells express a new class of intermediate filament protein. Cell 1990;60(4):585-95.

102. Tsujimura T, Makiishi-Shimobayashi C, Lundkvist J, Lendahl U, Nakasho K, Sugihara A, et al. Expression of the intermediate filament nestin in gastrointestinal stromal tumors and interstitial cells of Cajal. Am J Pathol 2001;158(3):817-23.

103. Vanderwinden JM, Gillard K, De Laet MH, Messam CA, Schiffmann SN. Distribution of the intermediate filament nestin in the muscularis propria of the human gastrointestinal tract. Cell Tissue Res 2002;309(2):261-8.

104. Li L, Mignone J, Yang M, Matic M, Penman S, Enikolopov G, et al. Nestin expression in hair follicle sheath progenitor cells. Proc Natl Acad Sci U S A 2003;100(17):9958-61.

105. Bertelli E, Regoli M, Lucattelli M, Bastianini A, Fonzi L. Nestin expression in rat adrenal gland. Histochem Cell Biol 2002;117(4):371-7.

106. Kachinsky AM, Dominov JA, Miller JB. Intermediate filaments in cardiac myogenesis: nestin in the developing mouse heart. J Histochem Cytochem 1995;43(8):843-7.

107. Terling C, Rass A, Mitsiadis TA, Fried K, Lendahl U, Wroblewski J. Expression of the intermediate filament nestin during rodent tooth development. Int J Dev Biol 1995;39(6):947-56.

108. Akazawa C, Ishibashi M, Shimizu C, Nakanishi S, Kageyama R. A mammalian helix-loop-helix factor structurally related to the product of Drosophila proneural gene atonal is a positive transcriptional regulator expressed in the developing nervous system. J Biol Chem 1995;270(15):8730-8.

109. Johnson JE, Birren SJ, Anderson DJ. Two rat homologues of Drosophila achaete-scute specifically expressed in neuronal precursors. Nature 1990;346(6287):858-61.

110. Julien JP. Neurofilament functions in health and disease. Curr Opin Neurobiol 1999;9(5):554-60.

111. Raponi E, Agenes F, Delphin C, Assard N, Baudier J, Legraverend C, et al. S100B expression defines a state in which GFAP-expressing cells lose their neural stem cell potential and acquire a more mature developmental stage. Glia 2007;55(2):165-77.

112. Alberi L, Sgado P, Simon HH. Engrailed genes are cell-autonomously required to prevent apoptosis in mesencephalic dopaminergic neurons. Development 2004;131(13):3229-36.

113. Fu L, Zhu L, Huang Y, Lee TD, Forman SJ, Shih CC. Derivation of neural stem cells from mesenchymal stemcells: evidence for a bipotential stem cell population. Stem Cells Dev 2008;17(6):1109-21.

114. Liu Y, Rao MS. Transdifferentiation--fact or artifact. J Cell Biochem 2003;88(1):29-40.

115. Neuhuber B, Gallo G, Howard L, Kostura L, Mackay A, Fischer I. Reevaluation of in vitro differentiation protocols for bone marrow stromal cells: disruption of actin cytoskeleton induces rapid morphological changes and mimics neuronal phenotype. J Neurosci Res 2004;77(2):192-204.

116. Tremain N, Korkko J, Ibberson D, Kopen GC, DiGirolamo C, Phinney DG. MicroSAGE analysis of 2,353 expressed genes in a single cell-derived colony of undifferentiated human mesenchymal stem cells reveals mRNAs of multiple cell lineages. Stem Cells 2001;19(5):408-18.

117. Woodbury D, Reynolds K, Black IB. Adult bone marrow stromal stem cells express germline, ectodermal, endodermal, and mesodermal genes prior to neurogenesis. J Neurosci Res 2002;69(6):908-17.

118. Somoza R, Conget P, Rubio FJ. Neuropotency of human mesenchymal stem cell cultures: clonal studies reveal the contribution of cell plasticity and cell contamination. Biol Blood Marrow Transplant 2008;14(5):546-55.

119. Hockfield S, McKay RD. Identification of major cell classes in the developing mammalian nervous system. J Neurosci 1985;5(12):3310-28.

120. Pierret C, Spears K, Maruniak JA, Kirk MD. Neural crest as the source of adult stem cells. Stem Cells Dev 2006;15(2):286-91.

121. Colter DC, Sekiya I, Prockop DJ. Identification of a subpopulation of rapidly self-renewing and multipotential adult stem cells in colonies of human marrow stromal cells. Proc Natl Acad Sci U S A 2001;98(14):7841-5.

122. Nagoshi N, Shibata S, Kubota Y, Nakamura M, Nagai Y, Satoh E, et al. Ontogeny and multipotency of neural crest-derived stem cells in mouse bone marrow, dorsal root ganglia, and whisker pad. Cell Stem Cell 2008;2(4):392-403.

123. Park HC, Shim YS, Ha Y, Yoon SH, Park SR, Choi BH, et al. Treatment of complete spinal cord injury patients by autologous bone marrow cell transplantation and administration of granulocyte-macrophage colony stimulating factor. Tissue Eng 2005;11(5-6):913-22.

124. Li Y, Chen J, Chen XG, Wang L, Gautam SC, Xu YX, et al. Human marrow stromal cell therapy for stroke in rat: neurotrophins and functional recovery. Neurology 2002;59(4):514-23.

125. Deng J, Petersen BE, Steindler DA, Jorgensen ML, Laywell ED. Mesenchymal stem cells spontaneously express neural proteins in culture and are neurogenic after transplantation. Stem Cells 2006;24(4):1054-64.

126. Munoz-Elias G, Marcus AJ, Coyne TM, Woodbury D, Black IB. Adult bone marrow stromal cells in the embryonic brain: engraftment, migration, differentiation, and long-term survival. J Neurosci 2004;24(19):4585-95.

127. Neuhuber B, Timothy Himes B, Shumsky JS, Gallo G, Fischer I. Axon growth and recovery of function supported by human bone marrow stromal cells in the injured spinal cord exhibit donor variations. Brain Res 2005;1035(1):73-85.

128. Neuss S, Becher E, Woltje M, Tietze L, Jahnen-Dechent W. Functional expression of HGF and HGF receptor/c-met in adult human mesenchymal stem cells suggests a role in cell mobilization, tissue repair, and wound healing. Stem Cells 2004;22(3):405-14.

129. Chen Q, Long Y, Yuan X, Zou L, Sun J, Chen S, et al. Protective effects of bone marrow stromal cell transplantation in injured rodent brain: synthesis of neurotrophic factors. J Neurosci Res 2005;80(5):611-9.

130. Chen CJ, Ou YC, Liao SL, Chen WY, Chen SY, Wu CW, et al. Transplantation of bone marrow stromal cells for peripheral nerve repair. Exp Neurol 2007;204(1):443-53.

131. Sun Y, Jin K, Xie L, Childs J, Mao XO, Logvinova A, et al. VEGF-induced neuroprotection, neurogenesis, and angiogenesis after focal cerebral ischemia. J Clin Invest 2003;111(12):1843-51.

132. Docheva D, Popov C, Mutschler W, Schieker M. Human mesenchymal stem cells in contact with their environment: surface characteristics and the integrin system. J Cell Mol Med 2007;11(1):21-38.

133. Fibbe WE, Noort WA. Mesenchymal stem cells and hematopoietic stem cell transplantation. Ann N Y Acad Sci 2003;996:235-44.

134. Chen SL, Fang WW, Ye F, Liu YH, Qian J, Shan SJ, et al. Effect on left ventricular function of intracoronary transplantation of autologous bone marrow mesenchymal stem cell in patients with acute myocardial infarction. Am J Cardiol 2004;94(1):92-5.

135. Liang J, Zhang H, Hua B, Wang H, Wang J, Han Z, et al. Allogeneic mesenchymal stem cells transplantation in treatment of multiple sclerosis. Mult Scler 2009;15(5):644-6.

136. Crop MJ, Baan CC, Korevaar SS, Ijzermans JN, Alwayn IP, Weimar W, et al. Donor-derived mesenchymal stem cells suppress alloreactivity of kidney transplant patients. Transplantation 2009;87(6):896-906.

137. Maitra B, Szekely E, Gjini K, Laughlin MJ, Dennis J, Haynesworth SE, et al. Human mesenchymal stem cells support unrelated donor hematopoietic stem cells and suppress T-cell activation. Bone Marrow Transplant 2004;33(6):597-604.

138. Horwitz EM, Prockop DJ, Gordon PL, Koo WW, Fitzpatrick LA, Neel MD, et al. Clinical responses to bone marrow transplantation in children with severe osteogenesis imperfecta. Blood 2001;97(5):1227-31.

139. Korhonen M. Culture of human mesenchymal stem cells in serum-free conditions: no breakthroughs yet. Eur J Haematol 2007;78(2):167; author reply 168.

140. Lange C, Cakiroglu F, Spiess AN, Cappallo-Obermann H, Dierlamm J, Zander AR. Accelerated and safe expansion of human mesenchymal stromal cells in animal serum-free medium for transplantation and regenerative medicine. J Cell Physiol 2007;213(1):18-26.

141. Liu C, Wu M, Huang S. Optimization of serum free medium for cord blood mesenchymal stem cells. Biochemical Engineering Journal 2007;33:1-9.

142. Montzka K, Lassonczyk N, Tschoke B, Neuss S, Fuhrmann T, Franzen R, et al. Neural differentiation potential of human bone marrow-derived mesenchymal stromal cells: misleading marker gene expression. BMC Neurosci 2009;10:16.

143. Lennon DP, Haynesworth SE, Young RG, Dennis JE, Caplan AI. A chemically defined medium supports in vitro proliferation and maintains the osteochondral potential of rat marrow-derived mesenchymal stem cells. Exp Cell Res 1995;219(1):211-22.

144. Deans RJ, Moseley AB. Mesenchymal stem cells: biology and potential clinical uses. Exp Hematol 2000;28(8):875-84.

145. Scutt A, Bertram P. Basic fibroblast growth factor in the presence of dexamethasone stimulates colony formation, expansion, and osteoblastic differentiation by rat bone marrow stromal cells. Calcif Tissue Int 1999;64(1):69-77.

146. Meuleman N, Tondreau T, Delforge A, Dejeneffe M, Massy M, Libertalis M, et al. Human marrow mesenchymal stem cell culture: serum-free medium allows better expansion than classical alpha-MEM medium. Eur J Haematol 2006;76(4):309-16.

147. Dai W, Hale SL, Martin BJ, Kuang JQ, Dow JS, Wold LE, et al. Allogeneic mesenchymal stem cell transplantation in postinfarcted rat myocardium: short- and long-term effects. Circulation 2005;112(2):214-23.

148. Tang YL, Zhao Q, Qin X, Shen L, Cheng L, Ge J, et al. Paracrine action enhances the effects of autologous mesenchymal stem cell transplantation on vascular regeneration in rat model of myocardial infarction. Ann Thorac Surg 2005;80(1):229-36; discussion 236-7.

149. Silva GV, Litovsky S, Assad JA, Sousa AL, Martin BJ, Vela D, et al. Mesenchymal stem cells differentiate into an endothelial phenotype, enhance vascular density, and improve heart function in a canine chronic ischemia model. Circulation 2005;111(2):150-6.

150. Shake JG, Gruber PJ, Baumgartner WA, Senechal G, Meyers J, Redmond JM, et al. Mesenchymal stem cell implantation in a swine myocardial infarct model: engraftment and functional effects. Ann Thorac Surg 2002;73(6):1919-25; discussion 1926.

151. Amado LC, Saliaris AP, Schuleri KH, St John M, Xie JS, Cattaneo S, et al. Cardiac repair with intramyocardial injection of allogeneic mesenchymal stem cells after myocardial infarction. Proc Natl Acad Sci U S A 2005;102(32):11474-9.

152. Makino S, Fukuda K, Miyoshi S, Konishi F, Kodama H, Pan J, et al. Cardiomyocytes can be generated from marrow stromal cells in vitro. J Clin Invest 1999;103(5):697-705.

153. Toma C, Pittenger MF, Cahill KS, Byrne BJ, Kessler PD. Human mesenchymal stem cells differentiate to a cardiomyocyte phenotype in the adult murine heart. Circulation 2002;105(1):93-8.

154. Noiseux N, Gnecchi M, Lopez-Ilasaca M, Zhang L, Solomon SD, Deb A, et al. Mesenchymal stem cells overexpressing Akt dramatically repair infarcted myocardium and improve cardiac function despite infrequent cellular fusion or differentiation. Mol Ther 2006;14(6):840-50.

155. Rafei M, Birman E, Forner K, Galipeau J. Allogeneic mesenchymal stem cells for treatment of experimental autoimmune encephalomyelitis. Mol Ther 2009;17(10):1799-803.

156. Chamberlain G, Fox J, Ashton B, Middleton J. Concise review: mesenchymal stem cells: their phenotype, differentiation capacity, immunological features, and potential for homing. Stem Cells 2007;25(11):2739-49.

157. Ceradini DJ, Kulkarni AR, Callaghan MJ, Tepper OM, Bastidas N, Kleinman ME, et al. Progenitor cell trafficking is regulated by hypoxic gradients through HIF-1 induction of SDF-1. Nat Med 2004;10(8):858-64.

158. Hefti F. Nerve growth factor promotes survival of septal cholinergic neurons after fimbrial transections. J Neurosci 1986;6(8):2155-62.

159. Koliatsos VE, Clatterbuck RE, Winslow JW, Cayouette MH, Price DL. Evidence that brain-derived neurotrophic factor is a trophic factor for motor neurons in vivo. Neuron 1993;10(3):359-67.

160. Timmers L, Lim SK, Arslan F, Armstrong JS, Hoefer IE, Doevendans PA, et al. Reduction of myocardial infarct size by human mesenchymal stem cell conditioned medium. Stem Cell Res 2007;1(2):129-37.

161. Tomchuck SL, Zwezdaryk KJ, Coffelt SB, Waterman RS, Danka ES, Scandurro AB. Toll-like receptors on human mesenchymal stem cells drive their migration and immunomodulating responses. Stem Cells 2008;26(1):99-107.

162. Ohashi K, Burkart V, Flohe S, Kolb H. Cutting edge: heat shock protein 60 is a putative endogenous ligand of the toll-like receptor-4 complex. J Immunol 2000;164(2):558-61.

163. Li M, Carpio DF, Zheng Y, Bruzzo P, Singh V, Ouaaz F, et al. An essential role of the NF-kappa B/Toll-like receptor pathway in induction of inflammatory and tissue-repair gene expression by necrotic cells. J Immunol 2001;166(12):7128-35.

164. Asea A, Rehli M, Kabingu E, Boch JA, Bare O, Auron PE, et al. Novel signal transduction pathway utilized by extracellular HSP70: role of toll-like receptor (TLR) 2 and TLR4. J Biol Chem 2002;277(17):15028-34.

165. Termeer C, Benedix F, Sleeman J, Fieber C, Voith U, Ahrens T, et al. Oligosaccharides of Hyaluronan activate dendritic cells via toll-like receptor 4. J Exp Med 2002;195(1):99-111.

166. Montzka K, Fuhrmann T, Woltje M, Brook GA. Expansion of human bone marrow-derived mesenchymal stromal cells: serum-reduced medium is better than conventional medium. Cytotherapy 2010;12(5):587-92.

167. Muller-Ehmsen J, Peterson KL, Kedes L, Whittaker P, Dow JS, Long TI, et al. Rebuilding a damaged heart: long-term survival of transplanted neonatal rat cardiomyocytes after myocardial infarction and effect on cardiac function. Circulation 2002;105(14):1720-6.

168. Muller-Ehmsen J, Krausgrill B, Burst V, Schenk K, Neisen UC, Fries JW, et al. Effective engraftment but poor mid-term persistence of mononuclear and mesenchymal bone marrow cells in acute and chronic rat myocardial infarction. J Mol Cell Cardiol 2006;41(5):876-84.

169. Krausgrill B, Vantler M, Burst V, Raths M, Halbach M, Frank K, et al. Influence of cell treatment with PDGF-BB and reperfusion on cardiac persistence of mononuclear and mesenchymal bone marrow cells after transplantation into acute myocardial infarction in rats. Cell Transplant 2009;18(8):847-53.

170. Son BR, Marquez-Curtis LA, Kucia M, Wysoczynski M, Turner AR, Ratajczak J, et al. Migration of bone marrow and cord blood mesenchymal stem cells in vitro is regulated by stromal-derived factor-1-CXCR4 and hepatocyte growth factor-c-met axes and involves matrix metalloproteinases. Stem Cells 2006;24(5):1254-64.

171. Weil BR, Abarbanell AM, Herrmann JL, Wang Y, Meldrum DR. High glucose concentration in cell culture medium does not acutely affect human mesenchymal stem cell growth factor production or proliferation. Am J Physiol Regul Integr Comp Physiol 2009;296(6):R1735-43.

172. Crisostomo PR, Wang Y, Markel TA, Wang M, Lahm T, Meldrum DR. Human mesenchymal stem cells stimulated by TNF-alpha, LPS, or hypoxia produce growth factors by an NF kappa B- but not JNK-dependent mechanism. Am J Physiol Cell Physiol 2008;294(3):C675-82.

173. Okada-Ban M, Thiery JP, Jouanneau J. Fibroblast growth factor-2. Int J Biochem Cell Biol 2000;32(3):263-7.

174. Jiang ZS, Wen GB, Tang ZH, Srisakuldee W, Fandrich RR, Kardami E. High molecular weight FGF-2 promotes postconditioning-like cardioprotection linked to activation of the protein kinase C isoforms Akt and p70 S6 kinase. Can J Physiol Pharmacol 2009;87(10):798-804.

175. Stegmann TJ. New approaches to coronary heart disease: induction of neovascularisation by growth factors. BioDrugs 1999;11(5):301-8.

176. Ding S, Merkulova-Rainon T, Han ZC, Tobelem G. HGF receptor up-regulation contributes to the angiogenic phenotype of human endothelial cells and promotes angiogenesis in vitro. Blood 2003;101(12):4816-22.

177. Kitamura K, Iwanami A, Nakamura M, Yamane J, Watanabe K, Suzuki Y, et al. Hepatocyte growth factor promotes endogenous repair and functional recovery after spinal cord injury. J Neurosci Res 2007;85(11):2332-42.

178. Jung W, Castren E, Odenthal M, Vande Woude GF, Ishii T, Dienes HP, et al. Expression and functional interaction of hepatocyte growth factor-scatter factor and its receptor c-met in mammalian brain. J Cell Biol 1994;126(2):485-94.

179. Okano J, Shiota G, Kawasaki H. Expression of hepatocyte growth factor (HGF) and HGF receptor (c-met) proteins in liver diseases: an immunohistochemical study. Liver 1999;19(2):151-9.

180. Kmiecik TE, Keller JR, Rosen E, Vande Woude GF. Hepatocyte growth factor is a synergistic factor for the growth of hematopoietic progenitor cells. Blood 1992;80(10):2454-7.

181. Duan HF, Wu CT, Wu DL, Lu Y, Liu HJ, Ha XQ, et al. Treatment of myocardial ischemia with bone marrow-derived mesenchymal stem cells overexpressing hepatocyte growth factor. Mol Ther 2003;8(3):467-74.

182. Lessmann V, Gottmann K, Malcangio M. Neurotrophin secretion: current facts and future prospects. Prog Neurobiol 2003;69(5):341-74.

183. Caporali A, Sala-Newby GB, Meloni M, Graiani G, Pani E, Cristofaro B, et al. Identification of the prosurvival activity of nerve growth factor on cardiac myocytes. Cell Death Differ 2008;15(2):299-311.

184. Abe T, Morgan DA, Gutterman DD. Protective role of nerve growth factor against postischemic dysfunction of sympathetic coronary innervation. Circulation 1997;95(1):213-20.

185. Bleul CC, Fuhlbrigge RC, Casasnovas JM, Aiuti A, Springer TA. A highly efficacious lymphocyte chemoattractant, stromal cell-derived factor 1 (SDF-1). J Exp Med 1996;184(3):1101-9.

186. Zhang M, Mal N, Kiedrowski M, Chacko M, Askari AT, Popovic ZB, et al. SDF-1 expression by mesenchymal stem cells results in trophic support of cardiac myocytes after myocardial infarction. Faseb J 2007;21(12):3197-207.

187. Opatz J, Kury P, Schiwy N, Jarve A, Estrada V, Brazda N, et al. SDF-1 stimulates neurite growth on inhibitory CNS myelin. Mol Cell Neurosci 2009;40(2):293-300.

188. Bonner JF, Blesch A, Neuhuber B, Fischer I. Promoting directional axon growth from neural progenitors grafted into the injured spinal cord. J Neurosci Res 2009.

189. Sasaki M, Radtke C, Tan AM, Zhao P, Hamada H, Houkin K, et al. BDNF-hypersecreting human mesenchymal stem cells promote functional recovery, axonal sprouting, and protection of corticospinal neurons after spinal cord injury. J Neurosci 2009;29(47):14932-41.

190. McAllister AK. Bdnf. Curr Biol 2002;12(9):R310.

191. Kermani P, Rafii D, Jin DK, Whitlock P, Schaffer W, Chiang A, et al. Neurotrophins promote revascularization by local recruitment of TrkB+ endothelial cells and systemic mobilization of hematopoietic progenitors. J Clin Invest 2005;115(3):653-63.

192. Kermani P, Hempstead B. Brain-derived neurotrophic factor: a newly described mediator of angiogenesis. Trends Cardiovasc Med 2007;17(4):140-3.

193. Herbst RS. Review of epidermal growth factor receptor biology. Int J Radiat Oncol Biol Phys 2004;59(2 Suppl):21-6.

194. Reichardt LF. Neurotrophin-regulated signalling pathways. Philos Trans R Soc Lond B Biol Sci 2006;361(1473):1545-64.

195. Priestley JV, Ramer MS, King VR, McMahon SB, Brown RA. Stimulating regeneration in the damaged spinal cord. J Physiol Paris 2002;96(1-2):123-33.

196. Tessarollo L, Tsoulfas P, Donovan MJ, Palko ME, Blair-Flynn J, Hempstead BL, et al. Targeted deletion of all isoforms of the trkC gene suggests the use of alternate receptors by its ligand neurotrophin-3 in neuronal development and implicates trkC in normal cardiogenesis. Proc Natl Acad Sci U S A 1997;94(26):14776-81.

197. Story GM, Dicarlo SE, Rodenbaugh DW, Dluzen DE, Kucera J, Maron MB, et al. Inactivation of one copy of the mouse neurotrophin-3 gene induces cardiac sympathetic deficits. Physiol Genomics 2000;2(3):129-36.

198. Breen EC. VEGF in biological control. J Cell Biochem 2007;102(6):1358-67.

199. Goncalves GA, Vassallo PF, Dos Santos L, Schettert IT, Nakamuta JS, Becker C, et al. Intramyocardial transplantation of fibroblasts expressing vascular endothelial growth factor attenuates cardiac dysfunction. Gene Ther 2009.

200. Tang J, Wang J, Kong X, Yang J, Guo L, Zheng F, et al. Vascular endothelial growth factor promotes cardiac stem cell migration via the PI3K/Akt pathway. Exp Cell Res 2009;315(20):3521-31.

201. Liu Y, Figley S, Spratt SK, Lee G, Ando D, Surosky R, et al. An engineered transcription factor which activates VEGF-A enhances recovery after spinal cord injury. Neurobiol Dis 2009.

202. Kim HM, Hwang DH, Lee JE, Kim SU, Kim BG. Ex vivo VEGF delivery by neural stem cells enhances proliferation of glial progenitors, angiogenesis, and tissue sparing after spinal cord injury. PLoS One 2009;4(3):e4987.

203. Yao Y, Zhang F, Wang L, Zhang G, Wang Z, Chen J, et al. Lipopolysaccharide preconditioning enhances the efficacy of mesenchymal stem cells transplantation in a rat model of acute myocardial infarction. J Biomed Sci 2009;16:74.

204. Chung R, Foster BK, Zannettino AC, Xian CJ. Potential roles of growth factor PDGF-BB in the bony repair of injured growth plate. Bone 2009;44(5):878-85.

205. Ozaki Y, Nishimura M, Sekiya K, Suehiro F, Kanawa M, Nikawa H, et al. Comprehensive analysis of chemotactic factors for bone marrow mesenchymal stem cells. Stem Cells Dev 2007;16(1):119-29.

206. Schnell L, Fearn S, Klassen H, Schwab ME, Perry VH. Acute inflammatory responses to mechanical lesions in the CNS: differences between brain and spinal cord. Eur J Neurosci 1999;11(10):3648-58.

207. Schnell L, Fearn S, Schwab ME, Perry VH, Anthony DC. Cytokine-induced acute inflammation in the brain and spinal cord. J Neuropathol Exp Neurol 1999;58(3):245-54.

208. Xu XM, Chen A, Guenard V, Kleitman N, Bunge MB. Bridging Schwann cell transplants promote axonal regeneration from both the rostral and caudal stumps of transected adult rat spinal cord. J Neurocytol 1997;26(1):1-16.

209. Pfeifer K, Vroemen M, Blesch A, Weidner N. Adult neural progenitor cells provide a permissive guiding substrate for corticospinal axon growth following spinal cord injury. Eur J Neurosci 2004;20(7):1695-704.

210. Fuhrmann T, Montzka K, Hillen LM, Hodde D, Dreier A, Bozkurt A, et al. Axon growth promoting properties of human bone marrow mesenchymal stromal cells. Neurosci Lett 2010;474(1):37-41.

211. Montzka K, Fuhrmann T, Muller-Ehmsen J, Woltje M, Brook GA. Growth factor and cytokine expression of human mesenchymal stromal cells is not altered in an in vitro model of tissue damage. Cytotherapy 2010;12(7):870-80.

212. Fuhrmann T, Hillen LM, Montzka K, Woltje M, Brook GA. Cell-cell interactions of human neural progenitor-derived astrocytes within a microstructured 3D-scaffold. Biomaterials 2010;31(30):7705-15.

213. Hamers FP, Koopmans GC, Joosten EA. CatWalk-assisted gait analysis in the assessment of spinal cord injury. J Neurotrauma 2006;23(3-4):537-48.

214. Hamers FP, Lankhorst AJ, van Laar TJ, Veldhuis WB, Gispen WH. Automated quantitative gait analysis during overground locomotion in the rat: its application to spinal cord contusion and transection injuries. J Neurotrauma 2001;18(2):187-201.

215. Koopmans GC, Deumens R, Honig WM, Hamers FP, Steinbusch HW, Joosten EA. The assessment of locomotor function in spinal cord injured rats: the importance of objective analysis of coordination. J Neurotrauma 2005;22(2):214-25.

216. Chaplan SR, Bach FW, Pogrel JW, Chung JM, Yaksh TL. Quantitative assessment of tactile allodynia in the rat paw. J Neurosci Methods 1994;53(1):55-63.

217. Pedersen EB, Zimmer J, Finsen B. Triple immunosuppression protects murine intracerebral, hippocampal xenografts in adult rat hosts: effects on cellular infiltration, major histocompatibility complex antigen induction and blood-brain barrier leakage. Neuroscience 1997;78(3):685-701.

218. Silver J, Miller JH. Regeneration beyond the glial scar. Nat Rev Neurosci 2004;5(2):146-56.

219. Properzi F, Asher RA, Fawcett JW. Chondroitin sulphate proteoglycans in the central nervous system: changes and synthesis after injury. Biochem Soc Trans 2003;31(2):335-6.

220. Hejcl A, Sedy J, Kapcalova M, Toro DA, Amemori T, Lesny P, et al. HPMA-RGD hydrogels seeded with mesenchymal stem cells improve functional outcome in chronic spinal cord injury. Stem Cells Dev;19(10):1535-46.

221. Liang H, Liang P, Xu Y, Wu J, Liang T, Xu X. DHAM-BMSC matrix promotes axonal regeneration and functional recovery after spinal cord injury in adult rats. J Neurotrauma 2009;26(10):1745-57.

222. Di Nicola M, Carlo-Stella C, Magni M, Milanesi M, Longoni PD, Matteucci P, et al. Human bone marrow stromal cells suppress T-lymphocyte proliferation induced by cellular or nonspecific mitogenic stimuli. Blood 2002;99(10):3838-43.

223. Bartholomew A, Sturgeon C, Siatskas M, Ferrer K, McIntosh K, Patil S, et al. Mesenchymal stem cells suppress lymphocyte proliferation in vitro and prolong skin graft survival in vivo. Exp Hematol 2002;30(1):42-8.

224. Jiang XX, Zhang Y, Liu B, Zhang SX, Wu Y, Yu XD, et al. Human mesenchymal stem cells inhibit differentiation and function of monocyte-derived dendritic cells. Blood 2005;105(10):4120-6.

225. Corcione A, Benvenuto F, Ferretti E, Giunti D, Cappiello V, Cazzanti F, et al. Human mesenchymal stem cells modulate B-cell functions. Blood 2006;107(1):367-72.

226. Abrams MB, Dominguez C, Pernold K, Reger R, Wiesenfeld-Hallin Z, Olson L, et al. Multipotent mesenchymal stromal cells attenuate chronic inflammation and injury-induced sensitivity to mechanical stimuli in experimental spinal cord injury. Restor Neurol Neurosci 2009;27(4):307-21.

227. Bundesen LQ, Scheel TA, Bregman BS, Kromer LF. Ephrin-B2 and EphB2 regulation of astrocyte-meningeal fibroblast interactions in response to spinal cord lesions in adult rats. J Neurosci 2003;23(21):7789-800.

228. Zeng X, Zeng YS, Ma YH, Lu LY, Du BL, Zhang W, et al. Bone Marrow Mesenchymal Stem Cells in a Three Dimensional Gelatin Sponge Scaffold Attenuate Inflammation, Promote Angiogenesis and Reduce Cavity Formation in Experimental Spinal Cord Injury. Cell Transplant 2011.

229. McKeon RJ, Schreiber RC, Rudge JS, Silver J. Reduction of neurite outgrowth in a model of glial scarring following CNS injury is correlated with the expression of inhibitory molecules on reactive astrocytes. J Neurosci 1991;11(11):3398-411.

230. Niederost BP, Zimmermann DR, Schwab ME, Bandtlow CE. Bovine CNS myelin contains neurite growth-inhibitory activity associated with chondroitin sulfate proteoglycans. J Neurosci 1999;19(20):8979-89.

231. Bradbury EJ, Moon LD, Popat RJ, King VR, Bennett GS, Patel PN, et al. Chondroitinase ABC promotes functional recovery after spinal cord injury. Nature 2002;416(6881):636-40.

232. Rolls A, Shechter R, London A, Segev Y, Jacob-Hirsch J, Amariglio N, et al. Two faces of chondroitin sulfate proteoglycan in spinal cord repair: a role in microglia/macrophage activation. PLoS Med 2008;5(8):e171.

233. Noble LJ, Donovan F, Igarashi T, Goussev S, Werb Z. Matrix metalloproteinases limit functional recovery after spinal cord injury by modulation of early vascular events. J Neurosci 2002;22(17):7526-35.

234. Popovich PG, Guan Z, McGaughy V, Fisher L, Hickey WF, Basso DM. The neuropathological and behavioral consequences of intraspinal microglial/macrophage activation. J Neuropathol Exp Neurol 2002;61(7):623-33.

235. Davies SJ, Shih CH, Noble M, Mayer-Proschel M, Davies JE, Proschel C. Transplantation of specific human astrocytes promotes functional recovery after spinal cord injury. PLoS One;6(3):e17328.

236. McKerracher L, David S, Jackson DL, Kottis V, Dunn RJ, Braun PE. Identification of myelin-associated glycoprotein as a major myelin-derived inhibitor of neurite growth. Neuron 1994;13(4):805-11.

237. Chen MS, Huber AB, van der Haar ME, Frank M, Schnell L, Spillmann AA, et al. Nogo-A is a myelin-associated neurite outgrowth inhibitor and an antigen for monoclonal antibody IN-1. Nature 2000;403(6768):434-9.

238. Ousman SS, David S. MIP-1alpha, MCP-1, GM-CSF, and TNF-alpha control the immune cell response that mediates rapid phagocytosis of myelin from the adult mouse spinal cord. J Neurosci 2001;21(13):4649-56.

239. DeKosky ST, Goss JR, Miller PD, Styren SD, Kochanek PM, Marion D. Upregulation of nerve growth factor following cortical trauma. Exp Neurol 1994;130(2):173-7.

240. Ho A, Blum M. Regulation of astroglial-derived dopaminergic neurotrophic factors by interleukin-1 beta in the striatum of young and middle-aged mice. Exp Neurol 1997;148(1):348-59.

241. Lu P, Blesch A, Tuszynski MH. Induction of bone marrow stromal cells to neurons: differentiation, transdifferentiation, or artifact? J Neurosci Res 2004;77(2):174-91.

242. Uccelli A, Pistoia V, Moretta L. Mesenchymal stem cells: a new strategy for immunosuppression? Trends Immunol 2007;28(5):219-26.

243. Macias MI, Grande J, Moreno A, Dominguez I, Bornstein R, Flores AI. Isolation and characterization of true mesenchymal stem cells derived from human term decidua capable of multilineage differentiation into all 3 embryonic layers. Am J Obstet Gynecol;203(5):495 e9-495 e23.

244. Zhang HT, Chen H, Zhao H, Dai YW, Xu RX. Neural stem cells differentiation ability of human umbilical cord mesenchymal stromal cells is not altered by cryopreservation. Neurosci Lett 2011;487(1):118-22.

245. Mimura S, Kimura N, Hirata M, Tateyama D, Hayashida M, Umezawa A, et al. Growth factor-defined culture medium for human mesenchymal stem cells. Int J Dev Biol 2011;55(2):181-187.

246. Chase LG, Lakshmipathy U, Solchaga LA, Rao MS, Vemuri MC. A novel serum-free medium for the expansion of human mesenchymal stem cells. Stem Cell Res Ther 2010;1(1):8.

247. Furue MK, Na J, Jackson JP, Okamoto T, Jones M, Baker D, et al. Heparin promotes the growth of human embryonic stem cells in a defined serum-free medium. Proc Natl Acad Sci U S A 2008;105(36):13409-14.

248. Phinney DG, Prockop DJ. Concise review: mesenchymal stem/multipotent stromal cells: the state of transdifferentiation and modes of tissue repair--current views. Stem Cells 2007;25(11):2896-902.

249. Nicaise C, Mitrecic D, Pochet R. Brain and spinal cord affected by amyotrophic lateral sclerosis induce differential growth factors expression in rat mesenchymal and neural stem cells. Neuropathol Appl Neurobiol;37(2):179-88.

250. Paul C, Samdani AF, Betz RR, Fischer I, Neuhuber B. Grafting of human bone marrow stromal cells into spinal cord injury: a comparison of delivery methods. Spine (Phila Pa 1976) 2009;34(4):328-34.

251. Basso DM, Beattie MS, Bresnahan JC. A sensitive and reliable locomotor rating scale for open field testing in rats. J Neurotrauma 1995;12(1):1-21.

252. Fuhrmann T, Montzka K, Hillen LM, Hodde D, Dreier A, Bozkurt A, et al. Axon growth-promoting properties of human bone marrow mesenchymal stromal cells. Neurosci Lett 2010;474(1):37-41.

253. Ryan JM, Barry FP, Murphy JM, Mahon BP. Mesenchymal stem cells avoid allogeneic rejection. J Inflamm (Lond) 2005;2:8.

10. Abbreviations

3D	three dimensional
ASCL1	achaete-scute complex homolog 1
AT cells	autoimmune T cells
BDNF	brain-derived neurotrophic factor
bFGF	basic fibroblast growth factor
BL	baseline
BOS	base of support
BSA	bovine serum albumin
CNS	central nervous system
CNTF	ciliary neurotrophic factor
CSPG	chondroitin sulfate proteoglycans
DAPI	4,6-diamidino-2-phenylindole dihydrochlorid
DMEM	Dulbecco's Modified Eagle Medium
DMSO	dimethylsulfoxide
DRD2	dopamine receptor D2
EDTA	ethylene diamine tetra acedic acid
EGF	epidermal growth factor
ESC	embryonic stem cell
FACS	fluorescent activated cell sorting
FBS	foetal bovine serum
GAPDH	glyceraldehyde-3-phosphate dehydrogenase
GDNF	glial-derived neurotrophic factor
GFAP	glial fibrillary acidic protein
GFP	green fluorescent protein
hFbl	human fibroblasts
HGF	hepatocyte growth factor
hMSC	human mesenchymal stromal cells
hNuclei	human nuclei
Iba1	ionized calcium binding adaptor molecule 1
IL	interleukin
LPS	lipopolysaccharide
MAP1b	microtubule-associated protein 1b
MAPT	microtubule-associated protein tau
MBP	myelin basic protein
MSC	mesenchymal stromal cell

NEUROD6	neurogenic differentiation 6
NF200	neurofilament 200 kDa
NFH	neurofilament heavy
NFL	neurofilament medium
NFL	neurofilament light
NGF	nerve growth factor
NSE	neuron-specific enolase
NT	neurotrophin
OEC	olfactory ensheathing cell
PBS	phosphate-buffered saline
PDGF (-BB)	platelet-derived growth factor (BB)
PFA	paraformaldehyde
PGK	phosphoglycerate kinase
RAU	random arbitrary units
SCI	spinal cord injury
SDF	stromal-derived factor
SYP	synaptophysin
TH	tyrosine hydroxylase
TLR	toll-like receptor
VEGF	vascular endothelial growth factor

11. List of figures and tables

PAGE

12. Publications

K. Montzka, N. Lassonczyk, B. Tschöke, S. Neuss, T. Führmann, R. Franzen, R. Smeets, G. Brook, M. Wöltje. Neural differentiation potential of human bone marrow derived mesenchymal stromal cells: misleading marker gene expression. BMC Neuroscience 2009 Mar 3;10(1):16

K. Montzka and A. Heidenreich. Application of mesenchymal stromal cells in urological diseases. BJU Int. 2010 Feb;105(3):309-12

T. Führmann, **K. Montzka**, L. Hillen, D. Hodde, A. Dreier, A. Bozkurt, M. Wöltje, G. Brook. Axon growth promoting properties of human bone marrow mesenchymal stromal cells. Neurosci Lett. 2010 Apr 19;474(1):37-41

K. Montzka, T. Führmann, M. Wöltje, G. Brook. Expansion of human bone marrow-derived mesenchymal stromal cells: serum-reduced medium is better than conventional medium. Cytotherapy 2010 Sep;12(5):587-92

T. Führmann, L. Hillen, **K. Montzka**, M. Wöltje, G. Brook. Cell-cell interactions of human neural progenitor-derived astrocytes within a microstructured 3D-scaffold. Biomaterials 2010 Oct;31(30):7705-15

K. Montzka, T. Führmann, J. Müller-Ehmsen, M. Wöltje, G. Brook. Growth factor and cytokine expression of human mesenchymal stromal cells is not altered in an *in vitro* model of tissue damage. Cytotherapy 2010 Nov;12(7):870-80

K. Montzka and A. Heidenreich. Castration-resistant prostate cancer: definition, biology and novel therapeutic intervention strategies. The Annals of Urology 2010: Vol I Issue 1

K. Montzka, T. Läufer, C. Becker, J. Grosse, A. Heidenreich. Microstructure and cytocompatibility of collagen matrices for urological tissue engineering. BJU Int. 2011 Jun;107(12):1974-81

13. Acknowledgements

I would like to take the opportunity to express my gratitude to PD Dr. Gary Brook for providing the challenging topic, the helpful discussions and even more importantly, for steady support whenever needed.

Additionally, I would like to thank Prof. Dr. Hermann Wagner for his interest in this work and for the official encouragement of my thesis.

I would like to thank Dr. Michael Wöltje for introducing me into the field of MSC, the helpful discussions and especially for his steady support in generating new studies.

Many thanks to Tobias Führmann (my understanding fellow sufferer) for his help during the last years and especially for his encouragement during frustrating times. We finally made it!

Special thanks to Dr. Ronald Deumens for the establishment of the behavioural analysis and his tuition in animal handling.

Thanks to all the people of the IZKF, Neuropathology and Urology for their steady support during my thesis, the great working atmosphere and for their friendship.

Finally, I would like to thank Tobias and my family for their understanding and support during this work.